ABSTRACT

Title of Dissertation:	SPATIO-TEMPORAL ANALYSIS OF PHOTOTROPISM IN ARABIDOPSIS SEEDLINGS
	Candace Amy Pritchard, Doctor of Philosophy, 2019
Dissertation directed by:	Dr. Angus Murphy, Plant Science and Landscape Architecture

Optimization of light capture during seedling development is a major determinant of plant fitness. As seedlings emerge from the soil, the processes of photomorphogenesis and phototropism optimize deployment of structures that capture light for photosynthesis. Photomorphogenesis produces hypocotyl thickening, cotyledon expansion, and chloroplast maturation. Concurrent phototropic responses initiated by blue light position the expanding cotyledons to maximize photosynthesis. The mechanisms underlying both processes have been explored for more than 140 years, but are still not fully understood. This dissertation seeks to provide a better understanding of phototropism by exploring the timing and localization of the constituent mechanisms downstream of the well-characterized perception of blue light by the PHOTOTROPIN photoreceptors. The experiments described herein characterize temporally and spatially distinct processes involved in asymmetric auxin

accumulations that lead to differential hypocotyl elongation. To better identify the link between early perception and later auxin transport and elongation events, an open-air system was used to remove seedling hindrance and provide better spatio-temporal resolution. These experiments confirmed the more rapid bending conferred by loss of the ATP Binding Cassette class B (ABCB) 19 auxin efflux transporter and loss of differential elongation in the mid hypocotyl elongation zone in higher order *pinformed* mutants. However, apart from the enhancement of phototropic bending observed in *abcb19* and *pin4* mutants, no auxin transport mutants tested showed alterations in early phototropic responses, and no mutant exhibited a delay in the onset of phototropic bending. Recently identified CBC1 and CBC2 (CONVERGENCE OF BLUE LIGHT (BL) AND CO_2 1/2) have been shown to act in downstream signaling during phot1-mediated regulation of stomatal conductance. Similarly, during phototropism *cbc1cbc2* double mutants show early defects in phot1-mediated phototropism. Further, CBC1 and CBC2 have been shown to regulate S-type anion channels. Analysis of S-type anion channel mutants also reveals defects in early bending responses. These results point to blue light-dependent regulation of anion channel activity having an important role during the earliest stages of phototropism

SPATIO-TEMPORAL ANALYSIS OF PHOTOTROPISM IN ARABIDOPSIS SEEDLINGS

by

Candace Amy Pritchard

Dissertation submitted to the Faculty of the Graduate School of the
University of Maryland, College Park, in partial fulfillment
of the requirements for the degree of
Doctor of Philosophy
2019

Advisory Committee:
Professor Angus Murphy, Chair
Dr. Caren Chang
Dr. Gary Coleman
Dr. Zhongchi Liu
Dr. Wendy Peer

Contributions to this dissertation

Chapter 2: Phototropic bending assays following excision and auxin depletion were performed by Jinshan Lin. pHusion assays were conducted by Guojie Ma.

Chapter 4: Auxin quantitations were performed by Dr. Reuben Tayengwa. Apical hook maintenance assays for *ABCB* mutants were conducted by Gabrielle Bate and Dr. Mark Jenness.

Table of Contents

List of Figures

List of Abbreviations

ABC ATP-binding cassette

ACC 1-aminocyclopropane-1-carboxylic acid

BL blue light

CLSM confocal laser scanning microscopy

CPD 1-cyclopropyl propane dione

IAA indole-3-acetic acid

NPA 1-naphthylphthalamic acid

NPPB 5-nitro-2-(3-phenylpropyl amino)-benzoic acid

PAT polar auxin transport

phot1 PHOTOTROPIN1 (holoprotein)

PIN PIN-FORMED

RL red light

WL white light

Chapter 1: General Introduction

Discovery of Phototropism

Phototropism, or the bending of plants towards a unilateral light source, is crucial for optimization of light capture. This is especially important during seedling establishment to improve success of directly seeded crops and competition with weeds. The earliest systematic studies of photropism in grass coleoptiles showed that signal perception occurs at the shoot apex and that a diffusible signal likely initiated bending in a lower elongation zone (Darwin & Darwin, 1880). From this research they made three important conclusions. First, there appeared to be a diffusible element responsible for bending. Second, there is a spatial and temporal separation between perception and bending. Third, the response appeared to be a modification of circumnutation. Later experiments reproduced in dicots suggested a universal mode of action for monocots and dicots (Zimmerman & Briggs, 1963; Babourina *et al.*, 2004; Volkov *et al.*, 2005). The discovery of the identity of this diffusible compound (auxin, indole-3-acetic acid) by Went and Thimann led to the Cholodny-Went hypothesis that illumination results in apical lateral auxin redirection followed by transport down the unlit side to stimulate elongation at a lower point (Went & Thimann, 1937).

Polar Auxin Transport

The chemiosmotic model of auxin transport describes how auxin moves through the plant in a cell-to-cell manner (Rubery & Sheldrake, 1974; Raven, 1975) (**Fig. 1.1**). The apoplast that surrounds cells is acidic, approximately pH 5.5, thus the

majority of auxin is present in a protonated/uncharged (IAAH) form that can freely diffuse across the plasma membrane. However, the cytosol has a more neutral pH of approximately 7. Thus, IAAH is de-protonated to IAA- and is unable to freely diffuse out of the cell and must be exported via specialized carriers and transporters. Polar auxin transport is achieved via highly regulated expression of auxin uptake and efflux proteins that results in establishment of cell-type specific auxin transport streams that are capable of moving auxin over long distances.

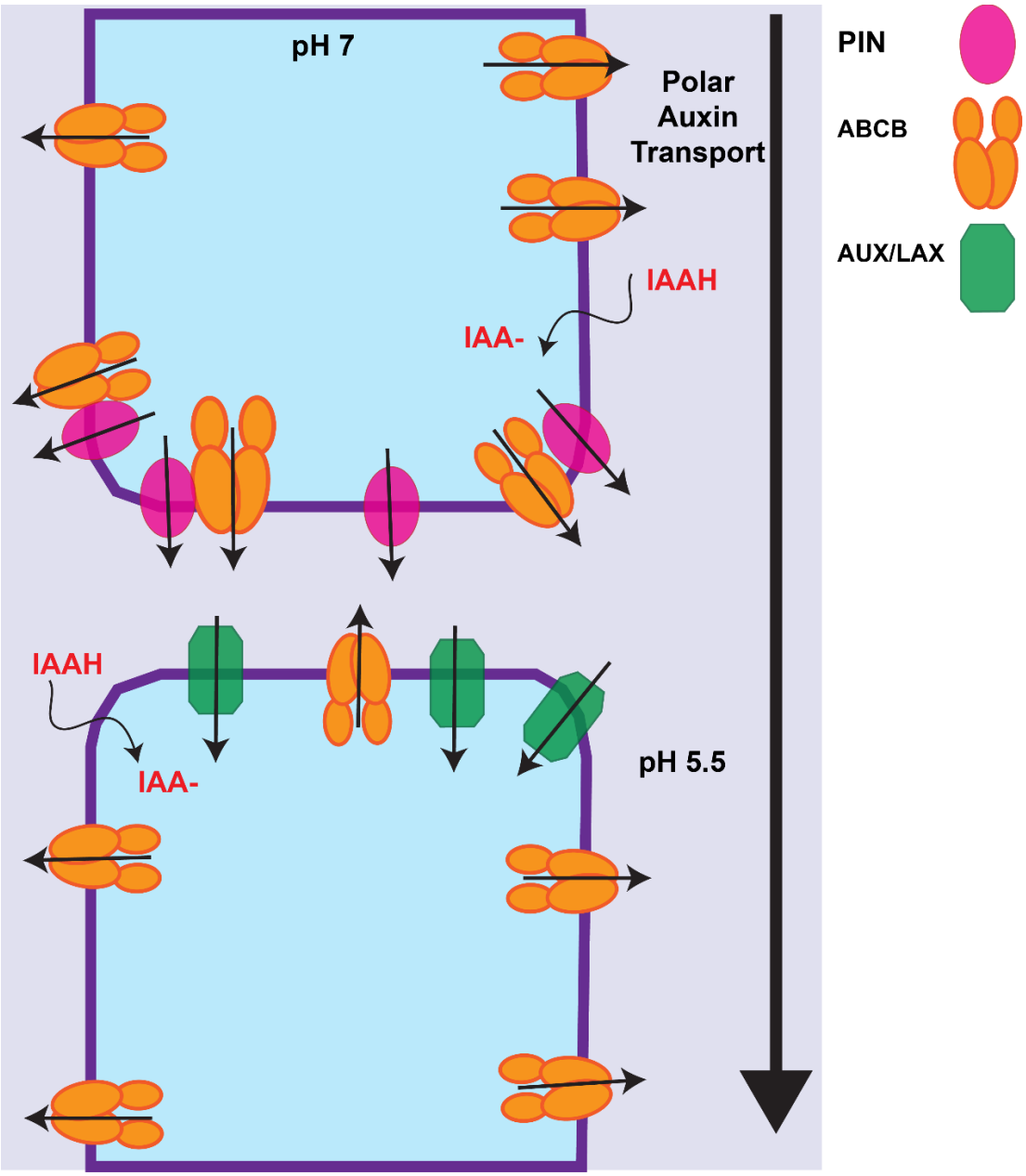

Figure 1.1 Chemiosmotic model of polar auxin transport. Indole-3-Acetic Acid (IAA) is protonated (IAAH) in the pH 5.5 of the apoplast and can diffuse into the cell or be transported into the cell via AUX/LAX permeases. Once inside the pH 7 cytosol, IAAH is deprotonated (IAA-) and must be transported out of the cell via the PINs and ABCBs. Polar coordination of PIN and AUX/LAX expression establishes directional auxin fluxes to drive polar auxin transport in seedlings.

Although ~15% of IAA can freely enter into cells by lipophilic diffusion, at apoplastic pH roughly 85% of auxin is present as IAA- and must be transported into the cell (reviewed in Zazímalová et al., 2010). Uptake of IAA is achieved via the AUXIN1/LIKE-AUXIN1 (AUX1/LAX) family of permeases. Members of this family exhibit defects in lateral root formation, gravitropism, and vascular development (Swarup & Péret, 2012). While AUX1/LAX proteins appear to contribute to auxin movement during phototropism, bending rate and angle are only slightly decreased, suggesting a minimal role (Stone *et al.*, 2008b; Christie *et al.*, 2011).

The PIN-FORMED (PIN) family of auxin efflux carriers are responsible for auxin transport and determination of directional auxin fluxes that are required for apical-basal determination, plant patterning, organogenesis, and embryogenesis (Krecek *et al.*, 2009; Adamowski & Friml, 2015). The founding member of the PIN family is PIN1, which is named for the pin-formed inflorescence phenotype (**Fig. 1.2**) (Gälweiler, 1998). *Pin1* mutants have the most severe phenotypes observed in that family and have severe defects in leaf morphology, phyllotaxy, and organ formation. Members of this family can be separated into two categories based on the size of the hydrophilic loop: long PINs (PIN1, PIN2, PIN3, PIN4, and PIN7) and short PINs (PIN5, PIN6, PIN8) (reviewed in Krecek *et al.*, 2009). Short PINs are primarily found on the ER membrane and are proposed to be involved in intercellular auxin homeostasis, with the exception of PIN6, which has been sometimes found on the plasma membrane (Krecek *et al.*, 2009; Simon *et al.*, 2016). PIN localization and activity are regulated via phosphorylation by several members of the AGCVIII

kinases family, including PINOID (PID)/WAG and DOMAIN6 PROTEIN KINASE (D6PK) (Zourelidou *et al.*, 2009; Huang *et al.*, 2010; Dhonukshe *et al.*, 2010). PID and WAG function to direct polar PIN localization, and thus establish directionality of auxin transport streams (Zhang *et al.*, 2009; Dhonukshe *et al.*, 2010; Barbosa & Schwechheimer, 2014). Alternatively, D6PK does not appear to alter polar localization of PINs, but is required for activation of PIN-mediated auxin efflux (Zourelidou *et al.*, 2009; Willige *et al.*, 2013; Barbosa & Schwechheimer, 2014).

A subset of ATP-BINDING CASSETTE subfamily B (ABCB) transporters participate in long distance polar auxin movement by excluding auxin from the plasma membrane and preventing re-uptake into the cell (Yang & Murphy, 2009; Bailly *et al.*, 2011; Jenness & Murphy, 2014). The best-characterized of these are ABCB1 and ABCB19. Loss of ABCB1 and ABCB19 in seedlings results in 60-75% decrease in basipetal auxin transport (Noh *et al.*, 2001; Blakeslee *et al.*, 2007). TWISTED DWARF1 (TWD1), an immunophilin-like FKBP42 (FK506-binding protein), is predicted facilitate proper folding of ABCBs. It has been demonstrated that TWD1 interacts with ABCB4, ABCB1, and ABCB19 and mediates their trafficking to and functionality at the plasma membrane (Wu *et al.*, 2010b). ABCB activity on the plasma membrane appears to be additionally regulated by phosphorylation, as PID has been shown to regulate ABCB1 activity, and ABCB19 is phosphorylated and inactivated by the photoreceptor PHOTOTROPIN1 (Christie *et al.*, 2011; Henrichs *et al.*, 2012; Wang *et al.*, 2012). Additionally, ABCB19 and PIN1 have synergistic activities that appear to amplify auxin flux in tissues where they are expressed (Blakeslee *et al.*, 2007; Titapiwatanakun *et al.*, 2009). While the

contributions of ABCBs to polar auxin transport are significant, the mechanisms that regulate ABCB activity remain poorly understood.

Major Classes of Plant Photoreceptors

Plant growth is highly regulated via detection of red/far-red, blue, and UV light. The PHYTOCHROME (PHY) family of photoreceptors are red and far-red light sensing proteins that are found in not only plants, but are also present in bacteria and fungi (Montgomery & Lagarias, 2002) (**Fig. 1.2A**). Members of this family regulate nearly every stage of plant development and are particularly crucial in seedlings for induction of germination and photomorphogenesis (Quail *et al.*, 1995; Chen & Chory, 2011). These proteins have a covalently bound bilin chromophore, phytochromobilin (PφB), that functions in red and far-red light sensing (Kohchi *et al.*, 2001). Phytochromes are found in plants as dimers of either the red absorbing inactive form (Pr) or far-red absorbing active form (Pfr). Upon perception of red light (RL), the inactive Pr form is converted to active the Pfr. Active Pfr is transported to the nucleus where it participates in direct protein-protein interactions resulting in repression or de-repression of downstream genes (Chen & Chory, 2011). Active Pfr can revert back to inactive Pr rapidly following far-red irradiation, spontaneously but slowly upon removal of red light, or may be sent to the 26S proteasome for degradation (Kim *et al.*, 2005; Franklin & Quail, 2010; Jang *et al.*, 2010; Chen & Chory, 2011; Zhu *et al.*, 2016).

Blue light absorbing CHRYPTOCHOME (CRY) proteins (**Fig. 1.2B**) consist of an N-terminal photolyase-related domain (PHR) that binds both the flavin adenine

dinucleotide (FAD) and the pterin 5,10-methyltetrahydrofolate (MTHF) (Ahmad, 2016). Blue light (BL) absorption by the chromophores results in a conformational change of the Cryptochrome C-terminal domain (CCT), enabling signaling. Following activation, the protein is transported to the nucleus where is involved in protein-protein interactions that affect downstream signaling, resulting in physiological changes such as anthocyanin accumulation, initiation of photomorphogenesis, and circadian rhythms (Goyal *et al.*, 2016).

The blue light and UV-A sensing PHOTOTROPIN (PHOT) family consists of two members: phot1 and phot2, which respond to low fluence (0.1-1 μmol m^{-2} s^{-1}) and high fluence (≥1 μmol m^{-2} s^{-1}) blue light, respectively. These proteins consist of two domains: an N-terminal photosensory domain and a C-terminal output domain. The N-terminal domain contains two light-oxygen-voltage (LOV) domains that each have a bound flavin mononucleotide (FMN) chromophore. The C-terminus contains a Serine/Threonine kinase domain (STK), while a helix Jα region joins the N-terminal and C-terminal domains (**Fig. 1.2C**) (Christie, 2007). Sensing of blue light by the LOV domains results in autophosphorylation and a dramatic conformational change that exposes the kinase domain (Christie *et al.*, 2002). Direct phosphorylation of target proteins via the kinase domain results in physiological and morphological changes such as stomatal opening, chloroplast relocalization, leaf positioning, and phototropism (Liscum & Briggs, 1995; Sakamoto, 2002; Harada *et al.*, 2003; Cho *et al.*, 2007; Christie *et al.*, 2011).

The ULTRAVIOLET RESISTANCE LOCUS 8 (UVR8) protein is responsible for the perception of UV-B. Inactive UVR8 is a cytosolic dimer consisting of two monomers joined by salt bridges and consisting of a series of tryptophan residues at the interaction surface (**Fig. 1.2D**). It is these tryptophan residues, specifically Trp233/Trp285, that sense UV-B, resulting in interruption of the salt bridges that connect the dimer, producing two active monomers (Rizzini *et al.*, 2011). Active UVR8 monomers are transported to the nucleus where they participate in protein-protein interactions that result in downstream regulation of UV-B responsive genes (Tilbrook *et al.*, 2013; Heijde & Ulm, 2013).

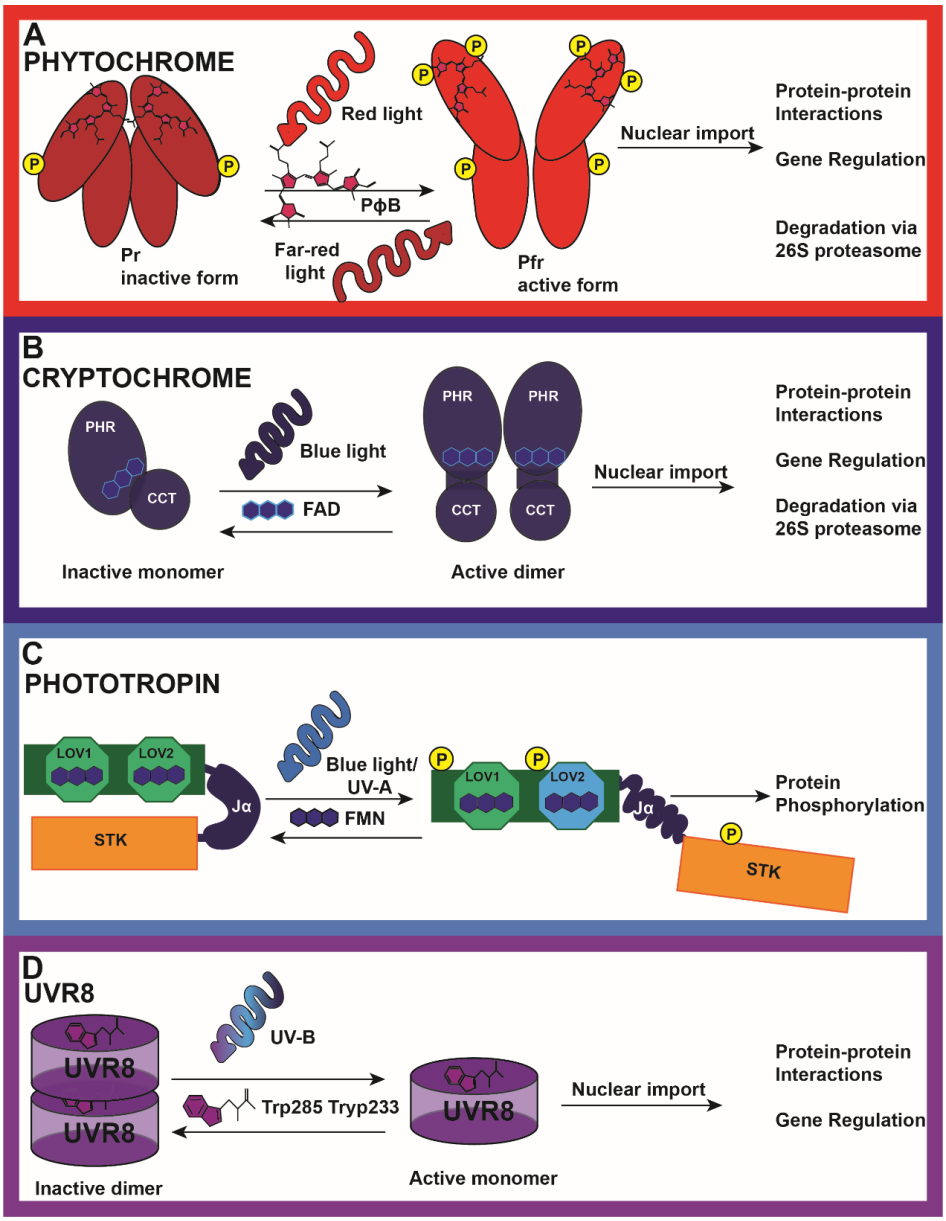

Figure 1.2 Overview of photoreceptor families in *Arabidopsis*. (**A**) The PHYTOCHROME family of photoreceptors perceive red and far-red light via a covalently bound phytochromobilin (PφB) chromophore. It is present as red-absorbing inactive (Pr) or far-red absorbing active (Pfr). Upon perception of red light, the Pr is converted to active Pfr and imported to the nucleus. Reversion from Pfr to inactive Pr occurs rapidly upon red light irradiation or, in the absence of red light,

over time spontaneously. (**B**) CRYPTOCHOME proteins sense blue light via absorption by flavin adenine dinucleotide (FAD) and the pterin 5,10-methyltetrahydrofolate (MTHF) in the N-terminal photolyase-related domain (PHR). A conformational change of the cryptochrome C-terminal domain (CCT) results, resulting in an active dimer, enabling signaling. (**C**) PHOTOTROPIN proteins sense blue and UV-A light. The N-terminal photosensory domain consists of two light-oxygen-voltage (LOV) domains that each have a bound flavin mononucleotide (FMN) chromophore. A helix Jα region joins the N-terminal domain and C-terminal Serine/Threonine kinase domain (STK). Light sensing via LOV results in autophosphorylation (P) conformational change, which exposes the kinase domain for direct protein-protein interaction and phosphorylation of targets. (**D**) UV-B is perceived via ULTRAVIOLET RESISTANCE LOCUS 8 (UVR8). The inactive UVR8 homodimer is joined by salt bridges consisting of a series of tryptophan (Trp) residues at the interaction surface. Two Trp residues, Trp285 and Trp233, disrupting the salt bridges, resulting in active monomers.

phot1-Mediated Phototropic Signaling in Arabidopsis

Phototropic responses in Arabidopsis are induced by blue and UV light (Liscum & Briggs, 1995; Kasahara *et al.*, 2002). First positive, or pulse-induced, phototropism results from a transient irradiation, while second positive, or continuous light phototropism, results from continuous unilateral irradiation (Janoudi & Poff, 1990). In etiolated seedlings phot1 is plasma-membrane associated (Sakamoto, 2002). However, upon blue light treatment, phot1 is internalized on the order of roughly twenty minutes (Wan *et al.*, 2008). It has been hypothesized that this internalization may play an important role in downstream events in phototropism (Christie & Murphy, 2013; Goyal *et al.*, 2013; Liscum, 2016). However, more recently, it has been demonstrated that dissociation from the membrane is not required for proper phototropic bending (Preuten *et al.*, 2015). Proteins that have been shown to directly interact with phot1 include members of the NPH3/RPT2-LIKE (NRL), and PROTIEN KINASE SUBSTRATE (PKS) and ABCB families. In particular, NPH3, NPH4/ARF7, PKS4, and ABCB19 contribute to phot1-dependent phototropism (Motchoulski, 1999; Christie *et al.*, 2011; Demarsy *et al.*, 2012). Upon BL perception NPH3 is rapidly de-phosphorylated in a phot1-dependent manner and has been proposed to regulate asymmetric auxin distributions during phototropism, though its role in phototropism is still not known (Motchoulski, 1999; Furutani *et al.*, 2011; Sullivan *et al.*, 2016b, 2019). Upon blue light perception ABCB19 is phosphorylated and inactivated, resulting in accumulations of the plant phytohormone indole-3-acetic acid (IAA) in the upper hypocotyl (Christie *et al.*, 2011).

Red-light pre-treatment has been shown to result in enhancement of phototropic curvature in a phytochrome-dependent manner (Parks *et al.*, 1996). Specifically, it has been determined that this mainly due to phyA and phyB activity (Parks *et al.*, 1996; Sullivan *et al.*, 2016a; Goyal *et al.*, 2016). PHY-mediated enhancement of phototropic bending appears to be indirect, as red light treatment has been shown to increase expression of members of the AGCVII kinase family, such as PINOID (PID). Additionally, red light has been shown to results in up-regulate auxin biosynthetic genes and overall auxin levels (Furutani *et al.*, 2014). UV-B dependent phototropism via activation of the UVR8 photoreceptor has been observed (Tilbrook *et al.*, 2013; Vandenbussche *et al.*, 2014). However, this response is observed in *phot1phot2* mutants, indicating a mechanism separate from PHOT-mediated phototropic bending (Vandenbussche *et al.*, 2014).

For the purpose of this dissertation the scope was restricted to phot1-mediated phototropism events. In order to identify specific mechanisms involved in phototropism it was determined that a single receptor-mediated response would allow for a more direct interpretation of results.

phot1-mediated Phototropism Events Downstream of Initial Perception

All subsequent experimental evidence suggests that phototropism occurs in a series of temporally and spatially distinct processes. Events downstream of initial perception of blue light and signaling components include reduction in ABCB19-mediated rootward auxin transport, microtubule reorientation, plasmodesmal gating, differential auxin accumulations at the elongation zone, and acidification-driven cell

expansion (Benková *et al.*, 2003; Christie *et al.*, 2011; Lindeboom *et al.*, 2013; Willige *et al.*, 2013; Hohm *et al.*, 2014; Han *et al.*, 2014; Ren *et al.*, 2018). Temporally, these events can be separated into rapidly observable responses and late-stage phototropic responses. However, the mechanisms that link certain early and late events, such as differential auxin accumulation, are not well understood.

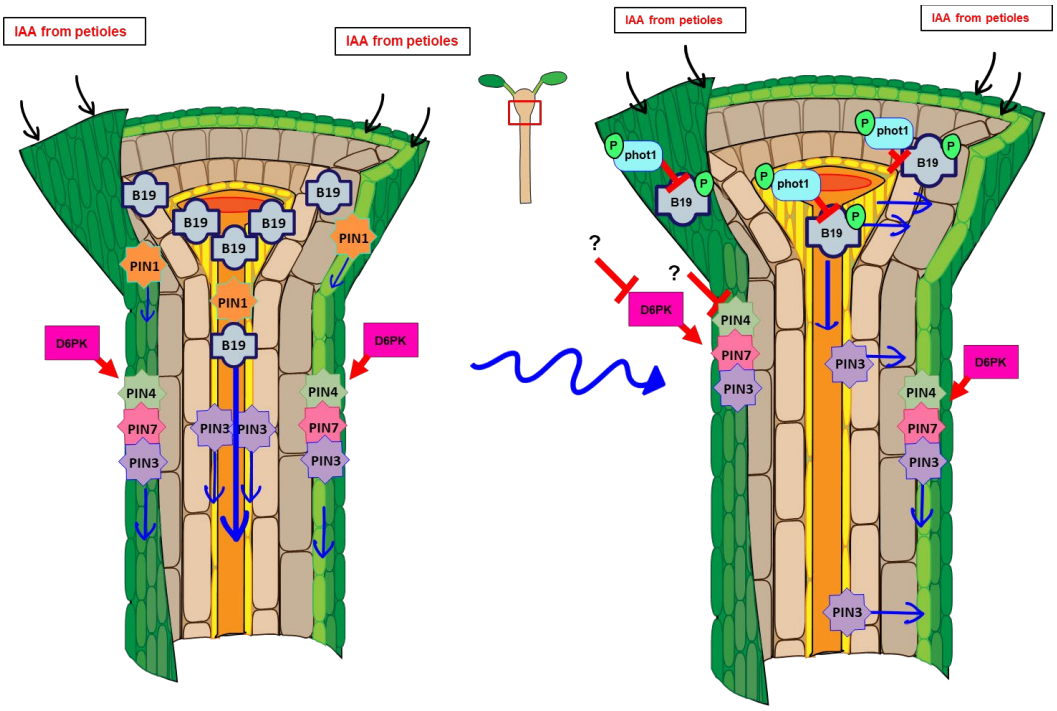

Figure 1.2 Schematic of auxin movement during phototropism in *Arabidopsis*. Auxin transport streams during hypocotyl elongation are indicated by straight blue arrows. ABCB19, PIN3 and, to a lesser extent, PIN1, restrict auxin to the vasculature in the upper hypocotyl. PIN3, PIN4, and PIN7 appear to transport auxin in the epidermis, which requires activation via D6PK. Upon BL perception (wavy blue arrow) phot1 is autophosphorylated and directly interacts with and inhibits ABCB19 via phosphorylation, resulting in a decrease in rootward transport. Asymmetric auxin accumulations are observed and an increase in auxin promotes cell expansion on the shaded side of the hypocotyl. It has been proposed that asymmetric accumulation is PIN-mediated due to directional lateral transport via PIN3, differential rootward transport down the epidermis by redundant PINs, or deactivation of D6PK resulting in a halt in PIN-mediated auxin efflux on the lit side of the hypocotyl. However, the events that link perception and asymmetric auxin accumulations are still unclear.

Rapidly observable responses include phot1 inhibition of ABCB19 and microtubule reorientation (**Fig. 1.3**). *In vivo* and *in vitro* experiments have demonstrated direct interactions of phot1 with ABCB19 and that blue light irradiation results in phot1 phosphorylation and inactivation of ABCB19. This results in an increase in upper hypocotyl auxin and a decrease in downward auxin transport (Christie *et al.*, 2011). ABCB19 was first discovered as a blue-light activated anion channel that was blocked upon 5-nitro-2-(3-phenylpropyl amino)-benzoic acid (NPPB) treatment (Cho & Spalding, 1996; Noh *et al.*, 2001). However, *abcb19* seedlings show enhancements in phototropism, so a role in activation of phototropism is unlikely (Noh *et al.*, 2003; Christie *et al.*, 2011).

Microtubule orientation has been shown to establish cell polarity and directional growth in seedlings (Bisgrove, 2008; Yang, 2008; Ma *et al.*, 2018). During phototropism microtubules have been shown to reorient from transverse to longitudinal on the order of minutes via KATANIN (KTN1)-mediated microtubule severing (Lindeboom *et al.*, 2013). In *phot1phot2* reorientation fails to occur, indicating the process is phot-mediated. However, *ktn1* seedlings still bend, indicating other underlying mechanisms may drive curvature. It has been proposed microtubule reorientation may function coordinately with other mechanisms during bending, as KTN1 has been shown to interact with the microtubule protein KINESIN-LIKE 14-A (KIN-14A) involved in chloroplast reorientation (Suetsugu *et al.*, 2010; Luptovčiak *et al.*, 2017).

Late stages of phototropism involve cell expansion at the elongation zone, presumably via auxin mediated acid-growth. It has been demonstrated that phosphorylation and activation of plasma membrane (PM) H+-ATPases occurs within minutes of IAA treatment (Takahashi *et al.*, 2012). This process involves activation of PM H+-ATPases (AHA) via SMALL AUXIN-UP RNA (SAUR) proteins and PROTEIN PHOSPHATASE 2C (PP2C) (Spartz *et al.*, 2012; Hohm *et al.*, 2014; Ren & Gray, 2015; Ren *et al.*, 2018). PKS5 has also been shown to inhibit AHA2, a PM H+ -ATPase with partially overlapping functions with AHA1 (Fuglsang *et al.*, 2007; Haruta *et al.*, 2010). AHA2 has been shown to be activated by phosphorylation and subsequent binding of a member of the 14-3-3 regulatory protein family, which are involved in signal transduction (DeWitt *et al.*, 1996; Kinoshita & Shimazaki, 1999; DeLille *et al.*, 2001). It has been proposed that SAUR19 and members of PP2C/PP2D families are important for proper phototropic bending (DeWitt *et al.*, 1996; Ren *et al.*, 2018).

The best studied late stage events are differential accumulations of auxin and auxin transport via the PINs. Evidence supporting auxin accumulation on the shaded side of hypocotyls has been documented (Friml *et al.*, 2002a; Christie *et al.*, 2011; Han *et al.*, 2014; Fankhauser & Christie, 2015a), but the mechanism by which this occurs and the connection to phot1 are unknown. It has been proposed that PIN3 and PIN7 mediate differential auxin transport during phototropism due to the decreased bending response observed in *pin3pin7* and *pin3pin4pin7* mutants (Friml *et al.*, 2002b; Zourelidou *et al.*, 2009; Ding *et al.*, 2011; Preuten *et al.*, 2013; Kami *et al.*, 2014). It has been suggested that PIN3 shows lateral relocalization during

phototropism and differential auxin transport to the shaded side of the hypocotyl is PIN3-mediated (**Fig. 1.3**) (Ding *et al.*, 2011). However, assays conducted under stringent low-fluence blue light conditions suggest that PIN3 lateral relocalization is not observed during continuous light phototropism (Haga & Sakai, 2012). While it has been demonstrated that PIN-mediated auxin transport during phototropism requires activation by D6PK, no differential activation has been observed (Zourelidou *et al.*, 2009; Willige *et al.*, 2013; Haga *et al.*, 2018). Additionally, it is still unknown how defects in phototropism observed in PIN and D6PK mutants could be blue light regulated.

Goals of this dissertation

Despite over a hundred years of study, the mechanisms that link phototropic perception and asymmetric auxin accumulation that drive phototropic bending are still not fully understood. It has been established that there is perception of a blue light phototropic stimulus by phot1, and phot1 then participates in signaling and directly interacts with and phosphorylates the auxin transporter ABCB19. Later events in phototropic bending involve asymmetric auxin accumulations on the lit and shaded side of the hypocotyl, presumably via PIN-mediated polar auxin transport. However, it is still unclear how perception on the illuminated side of the hypocotyl results in asymmetric auxin accumulations and elongation of the unilluminated side of the hypocotyl.

The objective of this dissertation was to elucidate the roles of known mechanisms involved in phototropism using a multi-system approach and, further, to

use this approach to identify the roles of yet-untested mechanisms. In using this approach overlapping mechanisms could be evaluated and placed into a spatio-temporal framework. Specifically, my goals were to 1) determine the path of auxin during phototropism in the hypocotyl and assign known mechanisms within discrete timeframes, 2) to identify down-stream targets of phot1 perception involved during the initiation of phototropic bending responses and establishment of asymmetric auxin fluxes, and 3) to further elucidate the role of ABCB19 in mediating apical hook maintenance.

Chapter 2: Spatio-temporal Analysis Suggests a Role for Auxin-dependent Elongation During Late-stage Phototropism

Abstract

Auxin is required for a variety of processes during plant growth, development, and tropic responses. Although phototropism, or the process of plant growth toward a unilateral light source, is the physiological response that led to the discovery of auxin, this response is still not fully understood. It is clear that the initial event is perception of blue light by PHOTOTROPIN1 and that later events involve asymmetric auxin accumulations that result in differential growth. However, the specific mechanisms linking these spatially and temporally separated events are largely unknown. To better study this link an open-air system provides better resolution. In this system phototropic bending can be visualized within 60 minutes of blue light treatment and is complete within approximately 3 hours. Further linking kinetics with spatially discrete areas of bending responsiveness allows for correlation of time and place to untangle overlapping events during phototropic bending.

Introduction

Seedling phototropism is initiated by perception of an asymmetric blue light stimulus and involves differential accumulation of the plant phytohormone auxin to achieve bending toward light. Early physiological studies of phototropism utilized grass coleoptiles and pea stems, as these systems exhibit highly reproducible responses and are highly amenable to physical manipulation (Darwin & Darwin,

1880; Zimmerman & Briggs, 1963; Kang & Burg, 1974). For the past twenty five years, the model plant *Arabidopsis thaliana* (L.) Heynh., with its sequenced genome, readily available site-specific mutations, tools to visualize cell-specific gene expression, hormone reporters, and translational fusions to multiple fluorescent proteins, has become the primary system for fundamental phototropism studies (reviewed in Fankhauser & Christie, 2015; Haga & Kimura, 2019).

It has been proposed that the process of phototropism occurs in stages, with both rapid/early events and those that occur during latter stages of bending. The first, and best studied, step in this process is the perception of blue light (BL). This signal is perceived by the PHOTOTROPIN photoreceptors, phot1 and phot2, which are active under low fluence (<1 μmol m^{-2} s^{-1}) or higher fluence (>1 μmol m^{-2} s^{-1}) blue light, respectively (Liscum & Briggs, 1995; Hu, 1997; Briggs *et al.*, 2001). Following this, phot1 directly interacts with and inactivates a member of the ATP-BINDING CASSETTE Subclass B family, ABCB19, which is involved in long-distance auxin transport (Noh *et al.*, 2001; Blakeslee *et al.*, 2007; Christie *et al.*, 2011). This results in an inhibition of downward auxin transport, which may prime later stages of bending (Christie *et al.*, 2011). These later stages of bending include differential accumulation of auxin on the shaded side of the hypocotyl, possibly via transport of auxin by members of the PIN-FORMED (PIN) auxin efflux carrier family (Ding *et al.*, 2011; Christie *et al.*, 2011; Haga & Sakai, 2012). This accumulation of auxin results in differential elongation and bending toward the light source (Li *et al.*, 1991; Friml, 2003; Han *et al.*, 2014). However, the events driving differential auxin movement and linking early and late stages of bending are still not fully understood.

Reported methodologies used to study phototropism in Arabidopsis vary considerably with experimental objectives, such as study of perception events, auxin transport events, or events that modulate phototropic bending. One of the most common and reproducible approaches employed is the analysis of skotomorphogenic/etiolated seedlings grown on vertical semi-solid media with directional blue or white light administered at low fluences (Liscum & Briggs, 1995; Christie *et al.*, 1998; Sakai *et al.*, 2001). Etiolated seedlings are characterized by unexpanded cotyledons, little or no chlorophyll, and an apical hook that protects the aerial tissues during emergence from the soil (Gendreau *et al.*, 1997). However, the presence of the apical hook and associated asymmetric auxin /auxin transporter distributions in the upper hypocotyl of etiolated seedlings that are accentuated in some mutants can obscure observations of phototropic changes (Haga & Sakai, 2013; Kami *et al.*, 2014). Asymmetric distributions are highest on the concave side of the apical hook and the cells immediately below and, to a lesser degree, in the epidermal cells in the convex side of the hook (Friml *et al.*, 2003; Zádníková *et al.*, 2010). Integration of photomorphogenic hook opening, gravitropic responses associated with the downward-oriented cotyledons, and phototropic bending mechanisms complicates measurements of bending dynamics, auxin movement, and visualization of fluorescent fusions to auxin transporter proteins that function in both apical hook maintenance and phototropism, (Friml *et al.*, 2002b; Rakusová *et al.*, 2011; Kami *et al.*, 2014). Although now clearly distinguished, the hook-associated asymmetries observed in etiolated seedlings were initially mistaken for mechanisms mediating phototropic bending (Peer *et al.*, 2004; Kami *et al.*, 2014).

Assays of post-photomorphogenic (also referred to as de-etiolated or dark-acclimated) seedlings eliminate confusion of hook opening and phototropic mechanisms (Christie *et al.*, 2011). In post-photomorphogenic seedlings auxin accumulates in the cotyledonary node, upper vasculature, and upper portion of the epidermis and is more or less symmetrically distributed (Christie *et al.*, 2011). However, as noted in the earliest documented phototropism experiments (Darwin & Darwin, 1880), the mass of cotyledons in post-photomorphogenic seedlings contributes to more erratic bending pattern, as does cell wall lignification (Neff & Van Volkenburgh, 1994; Gendreau *et al.*, 1997). Autofluorescence associated with chlorophyll and other compounds present in post-photomorphogenic seedlings also limits the discernment of fluorescently-tagged proteins in microscopic imaging (Sakai, 2019), and more extensive cuticular wax deposition can also reduce the efficacy of pharmacological agents (Gendreau *et al.*, 1997; Bessire *et al.*, 2011; Jacq *et al.*, 2017). As with etiolated seedlings, some of the variability and other limitations observed with post-photomorphogenic seedlings can be overcome by varying the growth conditions and the timing of assays (Christie *et al.*, 2011; Preuten *et al.*, 2013). However, such changes in experimental conditions also alter the location and extent of phototropic bending (Sullivan *et al.*, 2019). A number of reports have sought to compare results from etiolated and post-photomorphogenic seedlings to develop a consensus understanding (Christie and Murphy, 2013; Fankhauser and Christie, 2015). Decapitation and kinetic analyses show that the uppermost portion of the hypocotyl is required for proper phototropic responses despite other differential

responses observed between the two systems, such as differences in timing and location of elongation zone (Preuten *et al.*, 2013; Sullivan *et al.*, 2019).

Here, I provide an analysis of hypocotyl characteristics of etiolated and dark-acclimated post-photomorphogenic seedlings illuminated with unilateral blue light over time to test the relationship of phototropism, circumnutation and hypocotyl elongation. The kinetic analysis revealed that there are discrete stages that are apparent during phototropic bending. First, there is an initial lag in response, followed by initiation of bending within 60 minutes that occurs at a linear rate. Later events include achievement of bending at 3 hours, which is followed by phototropic elongation toward the light source and, at approximately 12 hours, a resumption of circumnutation. These data were correlated with regions of auxin maxima, which suggest auxin-dependent elongation during the later stages of phototropic bending, allowing placement of auxin transport and epidermal elongation into an overall timeframe and spatial context.

Results

Phototropism in an Open-Air System Allows for an Unconstrained Bending Response

In observing open air bending seedlings were observed to bend along a circular arc throughout the response (**Fig. 2.1A**). While the position and direction of the hypocotyl apex changed during the response, a circular arc was present during early and later stages of bending. However, it is evident that the length of the arc, as well as the ratio of the arc length to overall hypocotyl length, did change over time

(**Fig. 2.1A**). By focusing on only the curved section of the hypocotyl, the central angle can be extrapolated from the arc length and area of the circle that fits into the arc (**Fig. 2.1A**). The central angle measurement is comparable to the widely used deviation from vertical measurement (**Fig. S2.1A-C**), but also provides spatial information about the location of the elongation zone along the hypocotyl over time (**Fig. 2.1A**). Isolation of the dynamic elongation zone responses allowed for a simple geometric comparison of bending differences, even between morphologically varied seedlings (**Fig. 2.2A**). This is especially useful for mutants that show hypocotyl elongation differences, since there is no anchoring of the angle measurement to any assumed fixed hypocotyl point not part of the visible bending arc area. Instead the rotation of the seedlings about its own elongation zone can be exploited to isolate the bending curve apart from elongation. Additionally, assuming all seedlings are selected for a uniform height, arc length to overall hypocotyl length ratio can be used along with observations to describe the scope and position of bending along the hypocotyl. The extent to which this elongation zone migrates down the length of the hypocotyl can be quantitated as the ratio of bending zone to overall hypocotyl length (Bending Position) (**Fig. 2.1C,D**). This method of quantitation yielded two simple measurements that provided information about the extent of curvature and the scope of the elongation zone relative to overall hypocotyl length.

Phototropic bending is commonly studied using either endpoint or kinetic measurements. While endpoint assays are ideal for high throughput mutant analysis and study of spatial differences in protein or reporter distribution, differences identified using end point assays may depend largely on the irradiation end-point time

chosen for the experiment. However, measurements needed to relate kinetics to spatial differences can be used to quantitate responses. Kinetic assays provide greater temporal resolution, but the number of timepoints, thus the number of measurements required to be made to quantitate responses can be exceedingly time consuming. The majority of assays have been conducted on vertical agar plates (Ding *et al.*, 2011; Christie *et al.*, 2011; Preuten *et al.*, 2013; Willige *et al.*, 2013), however, the media affects hypocotyl bending in this system (**Fig. 2.1A-C**). One method to overcome this media interaction is use of an open-air system. A closer look revealed that phototropic bending on agar can produce a falsely acute bending angle compared to bending in open air (**Fig. 2.1B**). On agar, seedlings appeared to have an increased bending ratio compared to open air and the ratio of arc length to overall hypocotyl length was much larger, indicating an expansion of the elongation zone (**Fig. 2.1D**). As the topmost portion of the seedling bends and interacts with the media, elongation caused torsion of the hypocotyl that produced an exaggerated angle, and this was never observed during unconstrainted bending. This exaggerated angle resulted in seedlings that also appeared to have bent at a lower position along the hypocotyl, whereas open-air bending results indicated that the site of auxin action was restricted to a much more discrete area (**Fig. 2.1D**). Combined with the observed delay in bending on media, this suggests an open-air system may provide valuable information about exactly when and where phototropic events take place. Comparison of these two systems indicates that, though the same processes occur in each system, there are slight differences in real-time analysis. First, initiation of bending response was observed

slightly earlier in open air (**Fig. 2.1C**). Second, the relationship among elongation, circumnutation, and phototropism can be observed due to lack of media constraint.

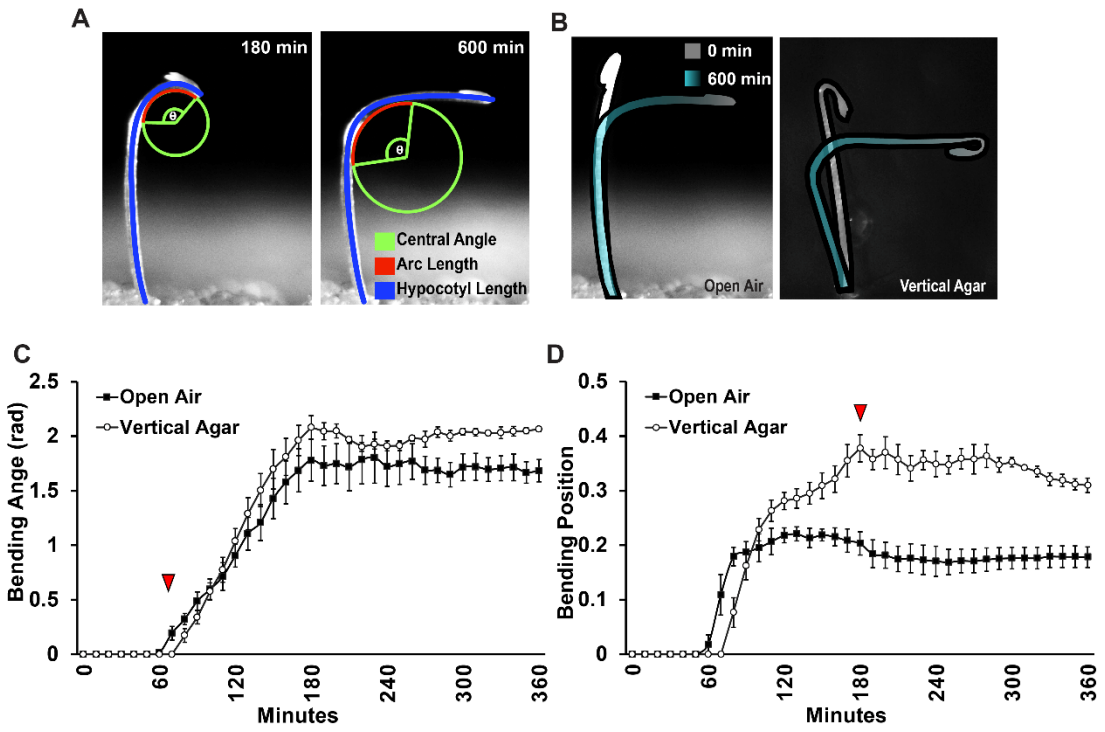

Figure 2.1. Media interactions distort phototropic curvature. (**A**) Seedlings were measured by fitting a circle and arc to the bending area. From these two measurements the central angle was determined. Arc length to hypocotyl length ratio can provide information about the bending angle location even after elongation has continued past original bending angle. (**B**) Etiolated seedlings irradiated with unilateral BL 6 hours show distorted bending angle on vertical agar compared to open air. (**C**) Etiolated bending on vertical agar results in a slight delay in earliest detectable bending, indicated by a red arrow (**D**) and a lower bending position compared to open air during later stages of phototropic bending, indicated by red arrow. Data shown are means ±SE. Data are representative of 2 independent experiments of n>10 seedlings for each treatment.

Hypocotyl Circumnutation is Suspended During Phototropic Bending

It was originally proposed by Charles and Francis Darwin that phototropism is a modification of circumnutation (Darwin & Darwin, 1880). Etiolated and post-photomorphogenic seedlings demonstrated circumnutation during hypocotyl elongation (**Movie S2.1, S2.2**), though the mechanisms underlying circumnutation are not fully understood (Stolarz, 2009). To determine the contribution of circumnutation to phototropic bending, an open-air system was used to observe unrestricted hypocotyl responses (**Fig 2.1.A, Movie S2.3**). Upon unilateral BL illumination there was a brief halt in elongation (**Fig. S2.2, Movie S2.3**). However, elongation resumed after approximately 30 minutes (**Fig. S2.2**). A resumption of elongation occurred just prior to observable bending and continued at a linear rate. While circumnutation does appear to be a component of normal hypocotyl elongation, there was no observable nutation during the first 8 hours of phototropic bending (**Movie S2.3**). However, after 8 hours of illumination, the upper hypocotyl was positioned so that the blue light incident on the seedling was similar to an overhead light source. After 8 hours, nutational elongation of the upper hypocotyl resumed. This absence of circumnutation during initial unilateral blue light illumination suggests that, as previously proposed, phototropism is a suspension or near halt in circumnutation, rather than modification or re-purposing of the mechanism (Orbović & Poff, 1997).

Phototropic Responses of Etiolated and Post-photomorphogenic Seedlings

Besides the most obvious feature of the apical hook in etiolated seedlings and green, expanded cotyledons of light-treated seedlings, there are key physiological factors that may explain that result in differences in bending observed (**Fig. 2.2D**).

While upper hypocotyl cell morphology in etiolated seedlings reflected longitudinal elongation, light-treated hypocotyls were thicker with wider cells cortical and epidermal cells (**Fig. 2.3A**), which is a reflection of previously observed photomorphogenic increases in hypocotyl thickness (Gendreau *et al.*, 1997). The upper-most region of both etiolated and light-treated hypocotyls contained cells that were more compact, while the lower hypocotyl contained cells at or near maximum elongation (**Fig. 2.3A**) (Gendreau *et al.*, 1997). One of the most notable differences between etiolated and post-photomorphogenic seedlings was the pattern of auxin distribution in the upper hypocotyl. Fluorescence signals from the auxin reporter DR5:RFP indicated that the distribution of auxin in post-photomorphogenic seedlings was more restricted to the uppermost area of the hypocotyl, cotyledons, and cotyledonary node (**Fig. 2.3B**). In contrast, etiolated seedlings contained abundant DR5 signals in the cells not only in the concave side of the hook, but also signal in the cells below the concave side of the hook (Friml *et al.*, 2003; Vandenbussche *et al.*, 2010; Abbas *et al.*, 2013) (**Fig. 2.3B**). This indicates there may be available auxin throughout the upper hypocotyl.

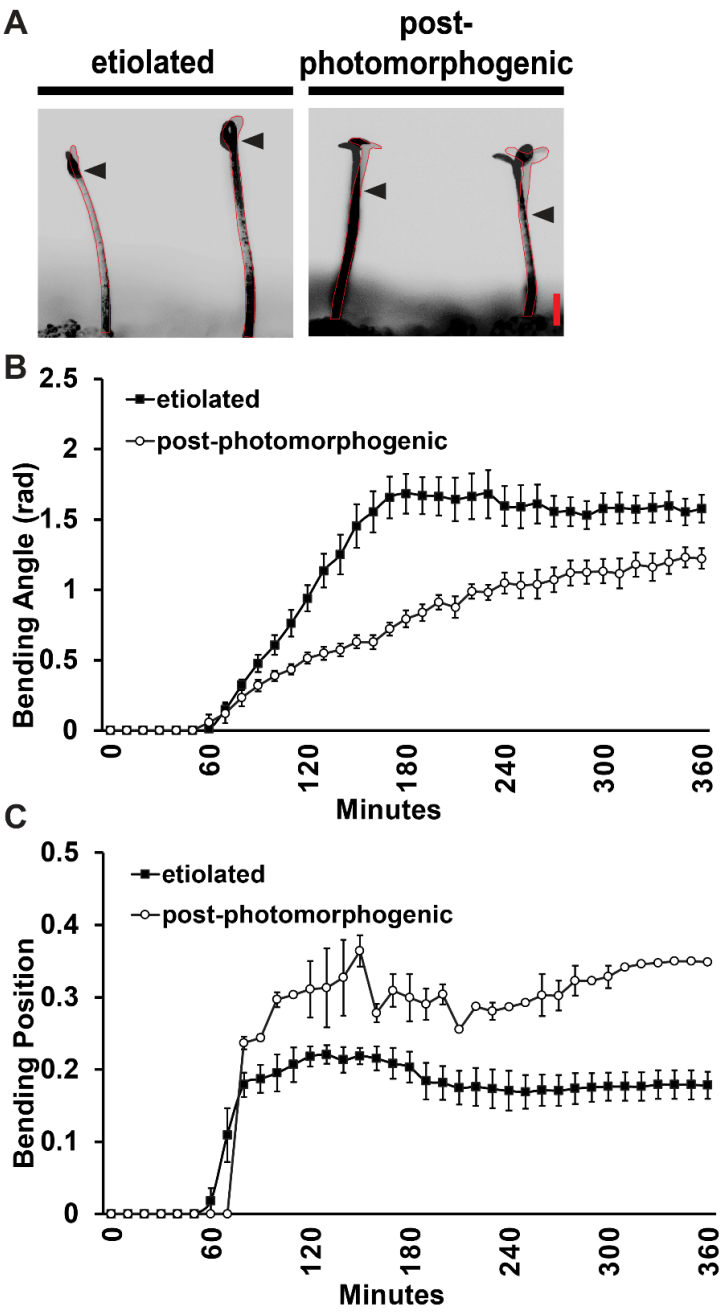

Figure 2.2. Comparison of BL phototropism kinetics for etiolated and dark-acclimated post-photomorphogenic seedlings. (**A)** Etiolated and light-treated seedlings bend at different positions along the hypocotyl. Seedlings are shown at 0 min BL illumination and the red outline overlay demonstrates response at 90 min. Phototropic bending kinetics (**B**) indicated that light-treated seedlings showed a

slower bending rate overall compared to etiolated and that peak phototropic bending was observed in etiolated seedlings within approximately 3 hours of unilateral blue light illumination. (**C**) Etiolated seedlings initiated bending near the very top of the hypocotyl, whereas light-treated seedlings bent at a lower position along the hypocotyl. Data shown are means ±SE. Data are representative of 2 independent experiments of n>5 seedlings for each treatment.

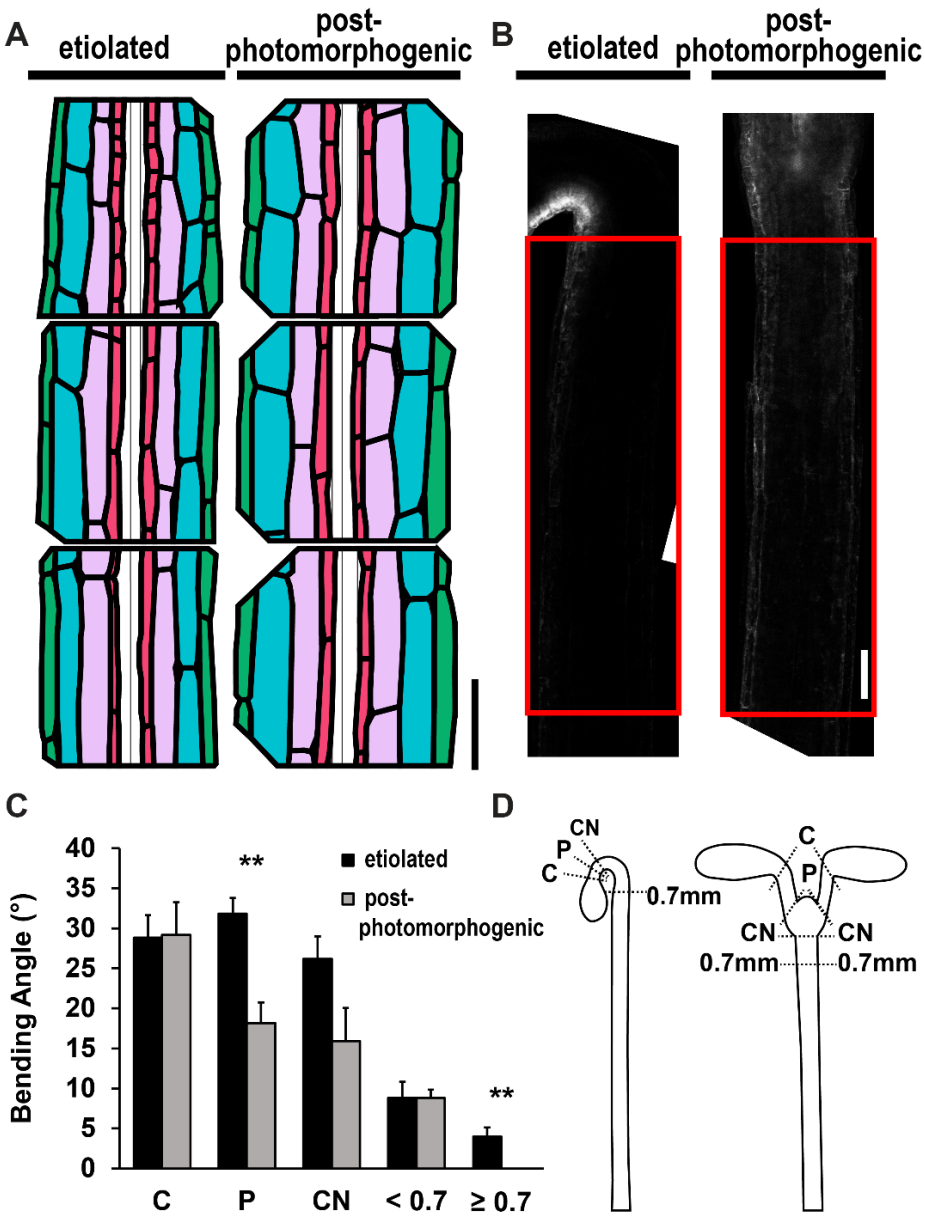

Figure 2.3. Etiolated and post-photomorphogenic seedlings show differences in morphology and auxin distributions. (**A**) Upper hypocotyl cell outlines of etiolated and post-photomorphogenic seedlings. Scale bars represent 0.1 mm. (**B**) The auxin reporter DR5:RFP in 3 day etiolated and post-photomorphogenic seedlings. The area within the red box correlates roughly to the cells outlined in (**A**). (**C**) Phototropic bending of etiolated and post-photomorphogenic seedlings following excision and 8h

unilateral BL treatment. Areas excised are grouped into sections: cotyledons (C), petioles (P), cotyledonary node (CN), <0.7mm, or ≥0.7mm of the hypocotyl. Data shown are means ± SE, n≥10 for each treatment. ** indicates $P \leq 0.01$ (**D**) Schematic demonstrating location of excision areas etiolated and post-photomorphogenic seedlings for **(C)**.

Epidermal Elongation and Auxin Distributions Indicate a Role for Auxin-Induced Elongation During Late Phototropic Bending

Previously, upper hypocotyl excision experiments have demonstrated that excision of large regions of the hypocotyl results in decreases in bending responses (Preuten *et al.*, 2013). As larger areas of the upper hypocotyl were excised there was a gradient decrease in bending response in both etiolated and post-photomorphogenic seedlings (**Fig. 2.3C,D**). Specifically, excision of the auxin-containing epidermal areas specific to etiolated or post-photomorphogenic seedlings decreased bending. This correlated with reductions in both available dynamic cells, or cells in the uppermost hypocotyl that have been previously demonstrated to be involved in hypocotyl elongation (Gendreau *et al.*, 1997; Han *et al.*, 2014) (**Fig. 2.3A**), and areas of available auxin supply (**Fig. 2.3B**). Accordingly, excision of the cotyledonary node and cells just below it resulted in large decreases in the bending response in post-photomorphogenic, but not etiolated seedlings (**Fig. 2.3C,D**). This correlates with increased auxin in the apical hook, which extends down past the cotyledonary node in etiolated, but not in post-photomorphogenic seedlings. A concern in performing these experiments is the possibility of wound-induced auxin production at the site of excision. To address this concern seedlings were excised and kept in the dark for 2 or 4 hours prior to BL illumination to allow any wound-induced auxin to be depleted from the excision site. However, auxin depletion experiments showed that auxin levels, as well as phototropic bending, decreased as the time from excision increased (**Fig. S2.2**). Since it has been demonstrated that phot1-mediated signaling events occur throughout the length of the hypocotyl (Sullivan *et al.*, 2016b), these results suggest that a sufficient upper hypocotyl-derived auxin source may be required for

late stage bending and that the different bending responses seen between etiolated and post-photomorphogenic seedlings may be due to both auxin source and cell size differences.

To explore this further cell size and auxin distribution changes were determined during early stages of phototropism when the bending response is in the linear range. This can present difficulty, as the hypocotyl epidermis consists of two distinct cell profiles (Gendreau *et al.*, 1997; Kono *et al.*, 2007). One cell type is the vertically short, but laterally non-protruding that are capable of giving rise to the meristemoid mother cell (MMC) and, eventually, to guard cells (**Fig. 2.4A**) (Nadeau & Sack, 2002; Kono *et al.*, 2007). In contrast, non-MMC-producing cell profiles are approximately 3 times longer (**Fig. 2.4E**). These cells also appear to bulge at vertical cell-cell attachment sites, though overall width is not significantly different (Gendreau *et al.*, 1997). To determine contributions to early phototropic bending, each type was measured separately for width and length over time and separated spatially on the illuminated or dark side of the hypocotyl (**Fig. 2.4B-E**). Interestingly, no cell width or length changes were detected over the first two hours of blue light illumination, even though at that time linear phototropic bending was observed (**Fig 2.1B**). It was not until approximately three hours after blue light illumination that cell length increased in both MMC-producing and non-MMC producing cells alike, though cell size of the latter was not able to be determined definitively at this timepoint due to the length and twisting nature of the hypocotyl epidermis.

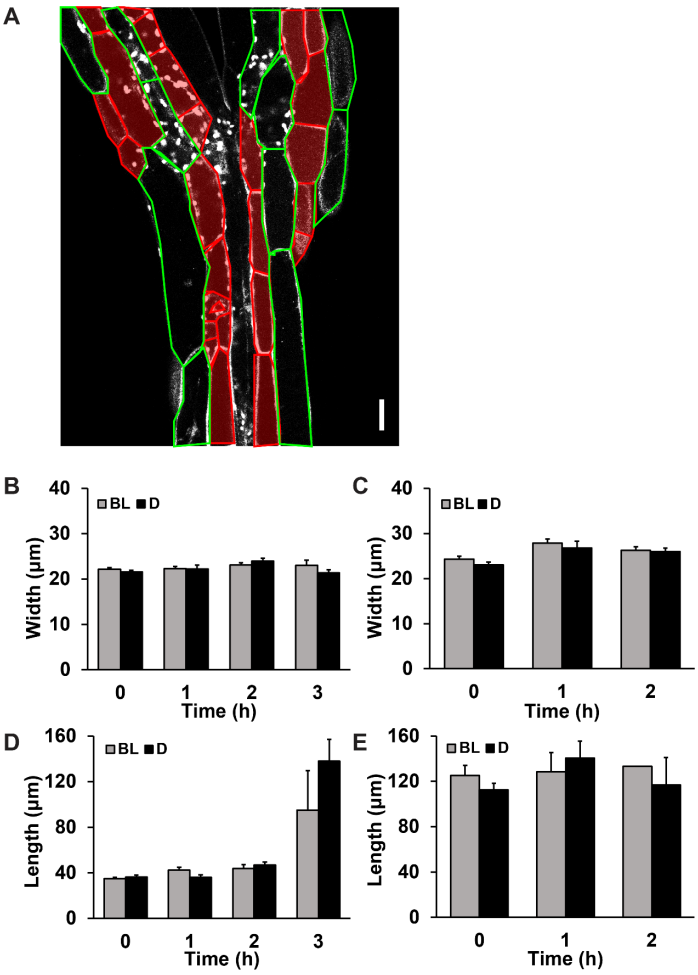

Figure 2.4. Upper hypocotyl cell size quantitations indicate epidermal elongation occurs during late stages of phototropism. (**A**) Hypocotyl epidermal cells consist of two morphologically distinct types of cell profiles: MMC-producing (green) and non-MMC producing (red). Arrow indicates site of guard cell divisions within the MMC-producing cell profile. (**B,C**) Upper hypocotyl epidermal cell width and (**D,E**) length quantitated separately on the blue-light illuminated (BL) or unilluminated (D) side of the hypocotyl over time in light-treated seedlings. (A,C) represent cell size of MMC-producing cells, while (**B,D)** represent non-MMC producing cells. Data shown are means ±SE. Data are representative of 3 independent experiments of n ≥ 3 seedlings for each timepoint. Scale bar represents 20 µm.

Previously, it has been proposed that rapid redirection of auxin to the unilluminated side of the hypocotyl drives the bending response observed (Ding *et al.*, 2011; Christie *et al.*, 2011; Christie & Murphy, 2013; Fankhauser & Christie, 2015a) . It has already been well documented that the auxin responsive reporter DR5 indicates that at 4 hours and beyond auxin accumulations are observed on the shaded side of the hypocotyl (Friml *et al.*, 2002b; Ding *et al.*, 2011; Christie *et al.*, 2011; Han *et al.*, 2014). This is in agreement with the timing of cell elongation observed at 3 hours of BL illumination and beyond (**Fig 2.4D**). To determine if early auxin redistribution precedes this elongation both DII-VENUS and DR5:RFP auxin responsive reporters were used (Marin *et al.*, 2010; Brunoud *et al.*, 2012). DII-VENUS relies on degradation of signal that can be observed in as little as 15 minutes, while DR5 expression relies on protein synthesis, which has been shown to require approximately 45 minutes (Ulmasov *et al.*, 1997; Brunoud *et al.*, 2012). Use of a rapid reporter such as DII-VENUS could help to track initial, rapid dynamic auxin fluxes during phototropism. However, as previously published, DII-VENUS proved too difficult to use in these tissues due to low nuclear signal and variability in expression among seedlings (Han *et al.*, 2014; Sakai, 2019). The presence of high VENUS nuclear signal in the guard cells can also confound analysis (**Fig. S2.3A,B**). It was observed that DII-VENUS signals did not appear to differentially change during the first hour of unilateral BL illumination (**Fig. S2.3C**). However, the apical hook-dependent auxin asymmetry that is normally observed in DR5:RFP seedlings was not measurable in DII-VENUS seedlings (**Fig. S2.3C,D**) (Friml *et al.*, 2003; Benková *et al.*, 2003; Zádníková *et al.*, 2010; Hohm *et al.*, 2014; Han *et al.*, 2014;

Sakai, 2019). DR5:RFP was used instead due to the relatively high autofluorescence and low DR5:GFP fluorescence observed during confocal laser scanning microscopy etiolated and post-photomorphogenic seedlings (**Fig. S2.3E-H**). DR5:RFP has been used extensively, including during phototropism assays, and has demonstrated similar expression patterns to DR5:GFP (Marin *et al.*, 2010; Bielach *et al.*, 2012; Han *et al.*, 2014; Feraru *et al.*, 2019). However, no measurable difference in asymmetric auxin distributions were observed over the first two hours of phototropism in the areas of the hypocotyl in which bending was observed to take place (**Fig. 2.5A**). While a trend of increasing overall signal on the dark side was observed, during this timeframe it was not statistically significant when hook positioning was taken into account (**Fig. S2.3D**). One pattern that was consistent among all treatments was that the DR5:RFP signal was below the apical hook region, regardless of BL illumination sidedness (**Fig. 2.5B, Fig. S2.4**). Further, this pattern persists even in post-photomorphogenic seedlings that no longer have an apical hook. The apical hook location/orientation was noted prior to photomorphogenesis, and following 12-24 hours of dark acclimation, the DR5:RFP distribution was nonetheless apical hook position-dependent. Therefore, in measuring sided fluorescence following BL illumination, care was taken to measure seedlings with equivalent hook positions/orientations. With this factor taken into account, no significant changes in DR5:RFP sidedness were observed during early phototropic bending.

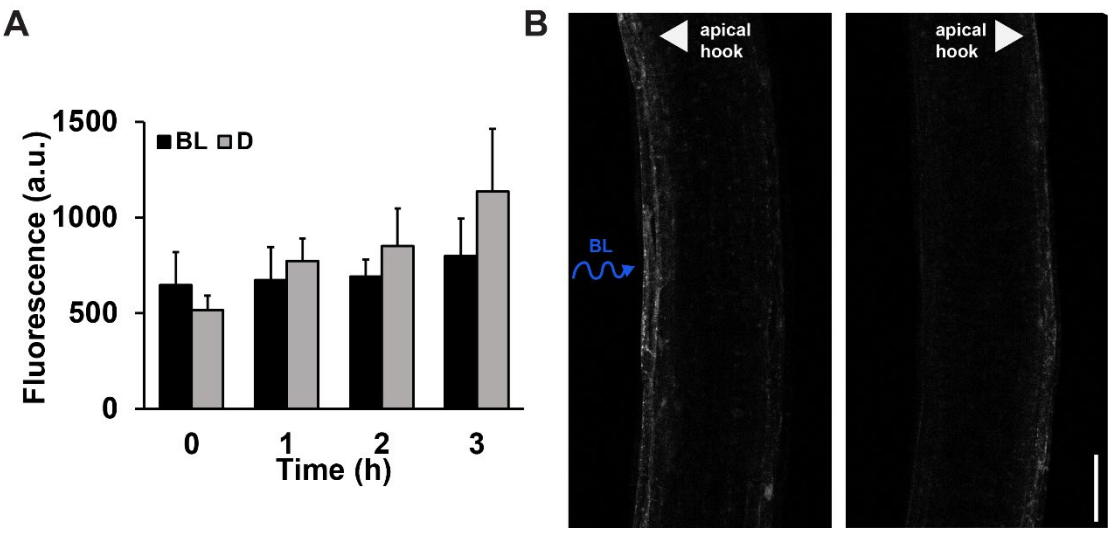

Figure 2.5. DR5:RFP auxin responsive reporter expression over time during phototropism. (**A**) DR5:RFP auxin reporter fluorescence measured at 1 hour timepoints in etiolated seedlings. (**B)** DR5:RFP signal after 3 hours of BL illumination in post-photomorphogenic seedlings. Arrows indicate direction of the apical hook prior to photomorphogenesis. Data presented are means ±SE, n ≥ 5 seedlings. Scale bar represents 100 μm.

Discussion

Results presented here support previously proposed stages of phototropic bending and allow for assignation of defects or enhancements to discrete stages of the bending response (Christie & Murphy, 2013; Hohm *et al.*, 2013). Using the open-air system and method of quantitation presented here, small changes in bending can be determined and direct comparisons can be made among morphologically distinct growth conditions. From the data presented here, four spatially and temporally distinct stages to phototropism can be proposed (**Fig. 2.6**). It is clear that there is an initial lag in response, including a halt in elongation, as has been previously reported (Noh *et al.*, 2003; Sullivan *et al.*, 2016b, 2019). This phase likely correlates to perception of blue light by phot1, including interaction with and inactivation of ABCB19 (Christie *et al.*, 2011). Phototropic bending appears to initiate within one hour after blue light treatment, following which there is linear bending during the next hour. Maximum bending is achieved within 3 hours of initial blue light treatment, though the rate decreases as this maximum angle is achieved. This bending maximum appears to be the end of phototropic bending, with a decline in bending rate and angle following. This decline phase, possibly an attenuation of bending and/or integration of gravitropism, consists of a slight bending rate decrease and a slight decrease in curvature lasting roughly an hour, though the bending angle remains mostly stable. Lastly, a pattern that can be described as phototropic elongation occurs and appears to be distinct from the initial phototropic bending response. These four stages of phototropic bending can be used to determine spatial and temporal contributions of discrete mechanisms to phototropism.

Since phototropic bending initiates within an hour and is complete within the following two hours, this would suggest that mechanisms that occur after this timeframe are post-phototropic. Results presented here show no change in differential cell elongation and no difference in auxin distribution within the first three hours of bending in etiolated or post-photomorphogenic seedlings. This may suggest that auxin accumulation-dependent elongation is responsible for achievement of later stages of bending. However, the contribution and location of auxin during early stages of bending remain to be determined due to limitations of available methods. The rapidity with which bending is initiated and relatively slow nature of long-distance auxin transport indicates that there may be auxin-dependent and auxin-independent events during phototropism. Early auxin-independent responses that have been identified are microtubule reorientation, acidification, and membrane depolarization events (Spalding, 2000; Lindeboom *et al.*, 2013; Hohm *et al.*, 2014). However, these responses have not been observed to be asymmetric. This suggests that these events do occur during phototropism, but that the specific mechanisms involved in initiation of phototropic bending are still not known.

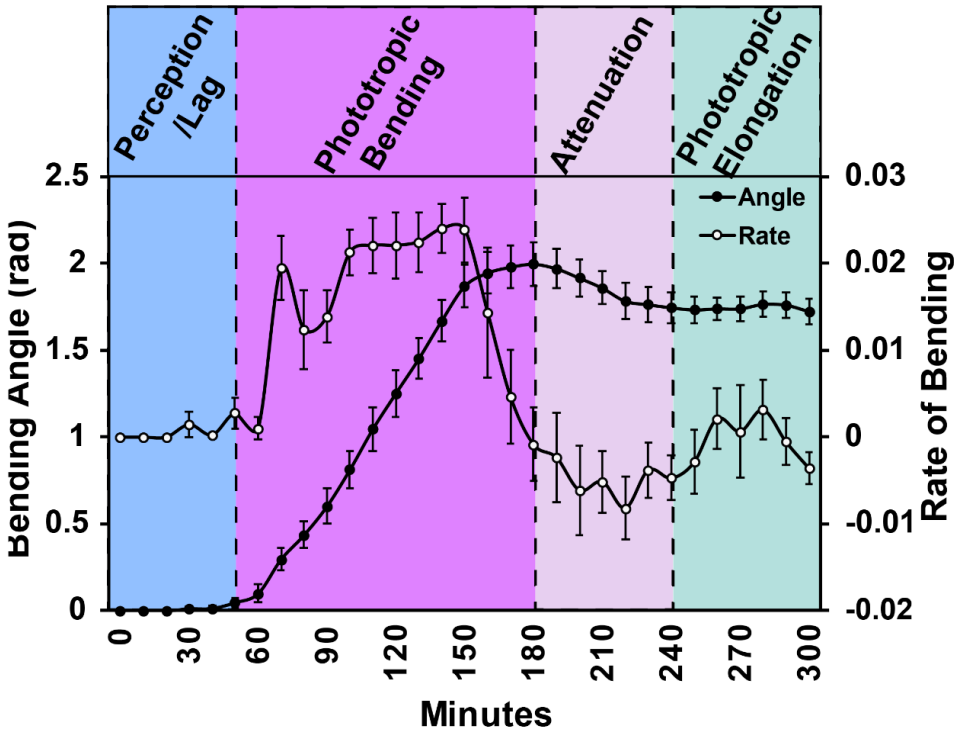

Figure 2.6. Stages of etiolated open-air blue light phototropism related to bending rate. Phototropic bending can be described as containing stages, including: lag/perception, bending, attenuation, and phototropic elongation. Phototropic bending takes place over approximately 2 hours at a constant linear rate. Once bending has reached a maximum there is a dramatic decrease in bending rate and slight decrease in bending angle. Finally, elongation continues at a steady rate as the bending angle remains stable. Data shown are means ± SE (n>5).

Materials and Methods

Plant Material and Growth Conditions. Throughout the study the Col-0 ecotype was used. Lines used include p*DR5:mRFP1er* (Marin *et al.*, 2010), *pPIN3::PIN3:GFP*, and *pPIN4::PIN4:GFP* (Friml *et al.*, 2003; Blilou *et al.*, 2005). Except where otherwise stated seeds were surface sterilized and sown on vertically oriented ¼ MS (pH 5.6; Caisson Labs, Smithfield, UT, USA), 0.5% sucrose, and 0.8% agar (RPI Corp, Mt Prospect, IL, USA) plates. All seeds were stratified at 4 °C for 2-4 days and placed in 80 µmol m^{-2} s^{-1} light (Philips f32t8/tl741; Philips, Andover, MA, USA) at 22°C light for 12 hours to induce germination. For etiolated growth assays, seedlings were removed from light and placed in the dark for 3 days at 22˚C until hypocotyls reached 7-8mm in height. Post-photomorphogenic seedlings were removed from light, placed in dark until the hypocotyls were 3-4 mm in height, then returned to 80 µmol m^{-2} s^{-1} light at 22°C for 8 hours, then returned to dark at least 12 hours, until the hypocotyls were 7-8 mm in height.

Phototropism Assays. Three-day old etiolated seedlings were transferred in dark vertical plates to 60 mm petri dishes filled with silicon dioxide (Sigma, St. Louis, MO; Cat #274739) and water. After a 30-minute acclimation, seedlings were exposed to 0.8 -0.4 µmol m^{-2} s^{-1} unilateral LED blue light illumination for 8 hours (Rothner Laser Technic). For all assays steps performed in dark were carried out under green safe light (Roscolux #2004 Storaro Green, Rosco, Stamford, CT, USA). Images were captured every 10 minutes with a USB3 uEYE CP camera (IDS Imaging Development Systems, Woburn, MA, USA) and processed for clarity (brightness, contrast, and exposure adjusted) with Photoshop (Adobe Systems Inc., Cupertino

CA). For excision experiments seedlings were grown on ¼ MS, 0.5% sucrose, 1% phytagel vertically oriented media, according to standard bending assay conditions as described above. Immediately prior to blue light treatment, the tops of the seedlings were excised under a green safe light using a #9 scalpel blade. Areas excised are grouped into sections: cotyledons, petioles, cotyledonary node, <0.7mm, or ≥0.7mm of the hypocotyl. Seedlings were immediately placed in unilateral blue light (BL) treatment for 8 hours, then imaged using a Zeiss Stemi 200-C dissecting microscope (Carl Zeiss, Oberkochen, Germany) equipped with Infinity Capture software (Lumenera Corporation. Ottowa, Ontario, Canada). For excision and auxin depletion experiments, sections were excised as described and placed in the dark for 2 hours prior to BL illumination. For all excision experiments, seedlings were exposed to 0.8 -0.4 μmol m^{-2} s^{-1} unilateral LED blue light illumination for 8 hours. All phototropic bending and hypocotyl elongation measurements were analyzed using FIJI software (Schindelin *et al.*, 2012; Schneider *et al.*, 2012).

Confocal Microscopy. Confocal Laser Scanning Microscopy (CLSM) images were collected using a Zeiss 710 Laser Spectral Scanning Microscope (Carl Zeiss, Oberkochen, Germany). For all imaging of seedling hypocotyls, the 10x objective was used, except where otherwise stated. The detector gain was set to below 800 and pinhole was set to 3.8 μm. DR5:RFP excitation was set at 594-nm with 15% laser strength and emission collected between 599-662-nm. DR5:RFP fluorescence intensity quantitations were carried out using Zeiss Zen 2012 by recording the average intensity of equivalent regions of interest on the lit and shaded sides of the hypocotyl. DII-VENUS excitation was set at 514-nm with 20% laser strength and

emission restricted between 515-562-nm to reduce autofluorescence. Overall fluorescence was quantitated from z-stack images using FIJI. Equivalent regions of interest were placed on the lit and shaded sides of the hypocotyl and average intensity measured as described above. DR5:GFP excitation was set at 488 nm with 20% laser strength and emission collected between 495-558-nm. All images were processed to increase brightness and exposure equally for all treatments using Photoshop and Illustrator for ease of visualization in in figures (Adobe Systems Inc., Cupertino, CA, USA). The Arabidopsis line pHusion has been described previously (Gjetting *et al.*, 2012). Seedlings were grown according to the standard phototropism assay conditions. Then live plant images were acquired using a Zeiss LSM 710 confocal laser-scanning microscope with a 40x water immersion objective (1.2 numerical aperture, C-Apochromatic) and argon laser (Christie et al., 2011, Gjetting et al., 2012). The excitation for EGFP (track2) was fixed at 488 nm, the meta detector was 499-550 nm emission, laser intensity was 12% and master gain was set to 670. The excitation for mRFP1 (track1) was fixed 594 nm, the meta detector was 600-630 nm emission, laser intensity was 30% and mater gain was set to 805-835 (depending on the auto-fluorescence). Pinhole size for both tracks was 203 μm. For our experiment, the area directly underneath the cotyledonary node was imaged and analyzed.

Cell Size Quantitations. Cell size was determined from CLSM images obtained using the *pPIN3::*PIN3-GFP and *pPIN4::*PIN4-GFP marker lines. Since these proteins show plasma membrane localization, cell outlines were clearly visible and measurements could be easily obtained. Seedlings were grown according to standard post-photomorphogenic seedlings growth conditions as described above. Post-

photomorphogenic seedlings were used here due to the inherent cell size asymmetry present in etiolated seedlings (Gendreau *et al.*, 1997; Zádníková *et al.*, 2010). Cell length and width were quantitated using Zeiss Zen 2012.

Statistical Analysis. All Student's *t*-tests were carried out in JMP PRO 14.

Supplementary Figures

Movie S2.1 Etiolated Elongation 16h.avi

Movie S2.1. Elongation and Circumnutation of etiolated seedlings. Etiolated seedling elongation in open air is accompanied by circumnutation in the upper hypocotyl over a 16 hour time-lapse

Movie S.2.2 LightTreated Elongat

Movie S2.2. Elongation and Circumnutation of light-treated seedlings. Light-treated seedling elongation in open air is accompanied by circumnutation in the upper hypocotyl over a 16 hour time-lapse.

Movie S2.3.Circumnutation

Movie S2.3. Elongation and Circumnutation are interrupted following unilateral blue light illumination. Elongation and circumnutation of light-treated seedlings can

be seen for 3 hours previous to blue light illumination. After 3 hours a unilateral blue light source was added, denoted by the blue arrow. Elongation and nutation are briefly interrupted before bending is observed.

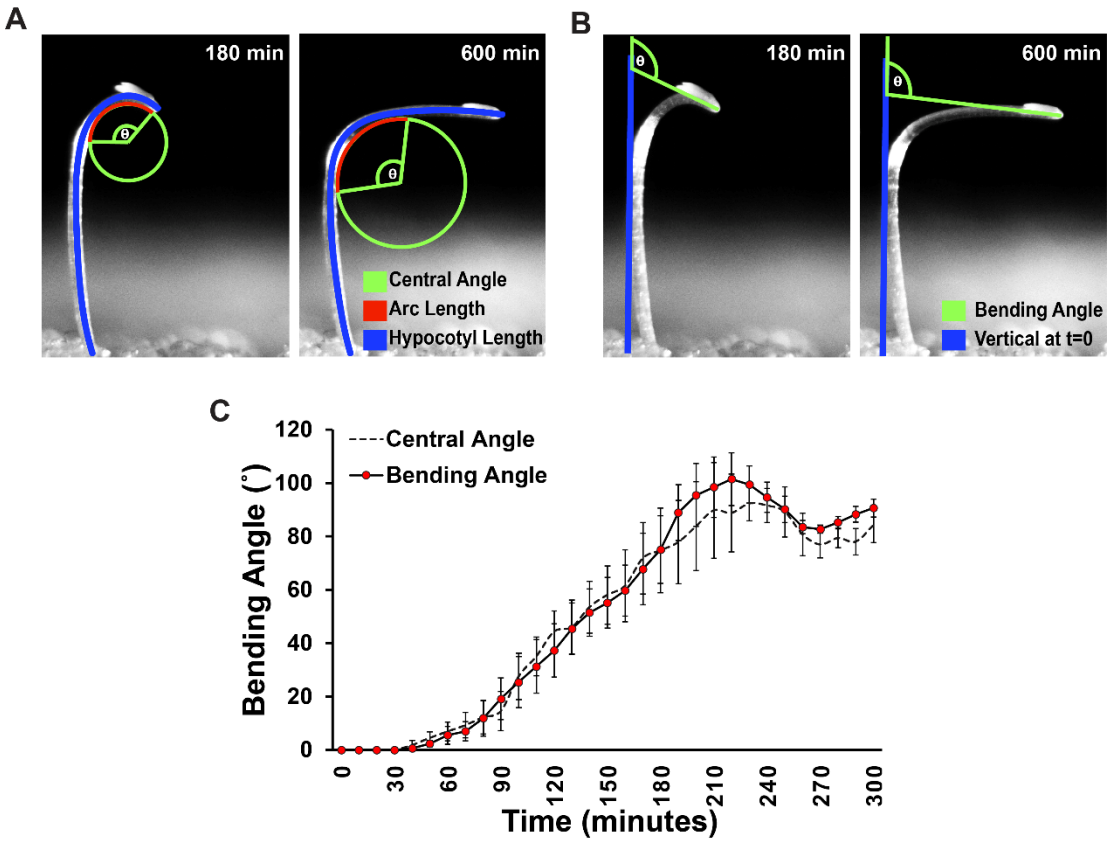

Figure S2.1. Comparison of BL phototropism kinetics measurement. Central angle measurement by fitting a circle and arc to the bending area (**A**). Arc length to hypocotyl length ratio can provide information about the bending angle location. Bending angle measurement of deviation from vertical (**B**). Comparison of both methods demonstrates that the bending angle measured is not significantly different (**C**) between the two methods. Data shown are means ±SE. Data are representative of 2 independent experiments of n>5 seedlings for each treatment.

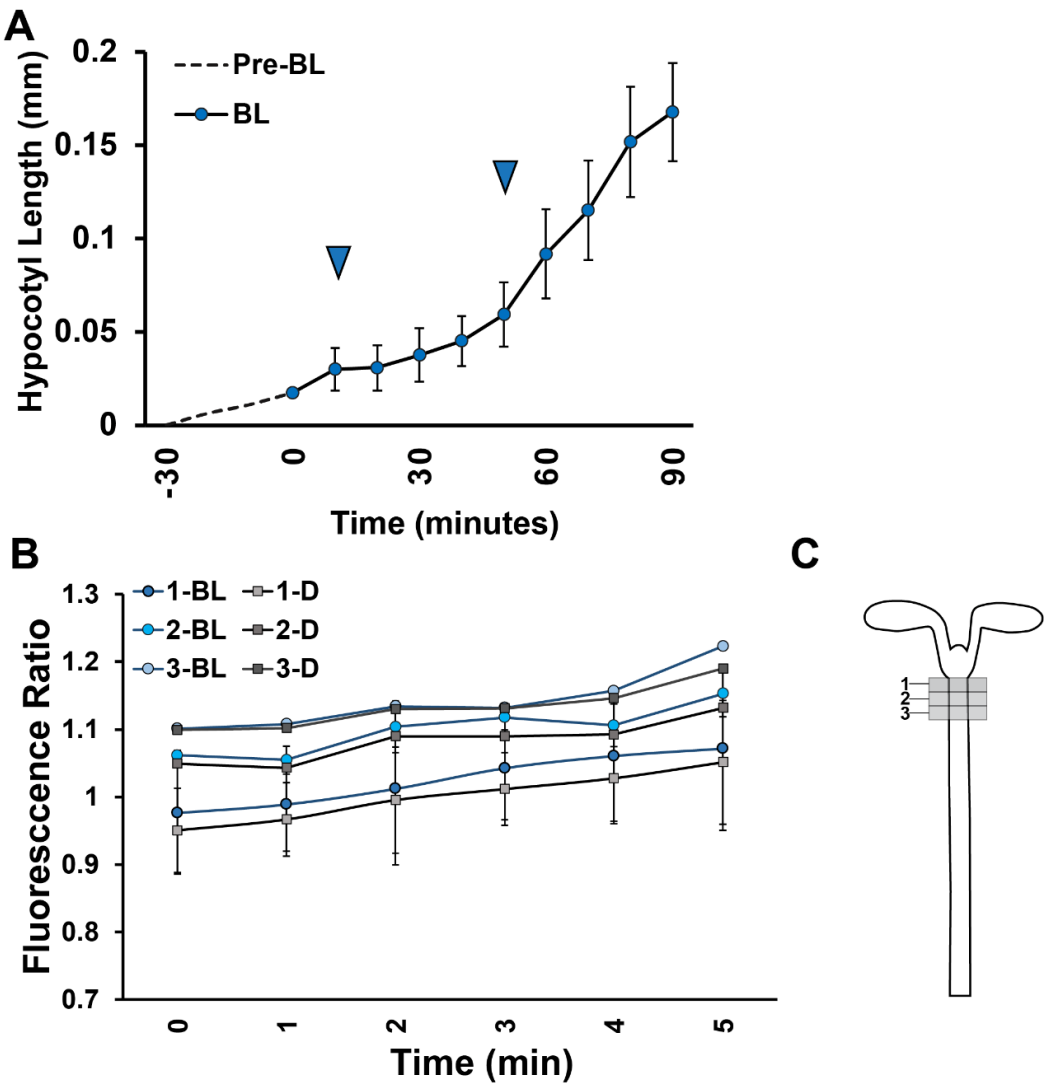

Figure S2.2. Hypocotyl elongation during unilateral blue light illumination. (**A**) Measurement of elongation change of etiolated hypocotyls measured starting at 30 minutes prior to < 0.8 -0.4 µmol m^{-2} s^{-1} unilateral LED blue light illumination. Blue arrows indicate rate changes. Within roughly ten minutes the elongation rate briefly decreases. At roughly 60 minutes the rate of elongation sharply increases. (**B**) pHusion data collected from upper hypocotyl on blue light illuminated (BL) vs dark (D) side of the hypocotyl. (**C**) Schematic of location of cell layer 1, 2, and 3 in the hypocotyl.

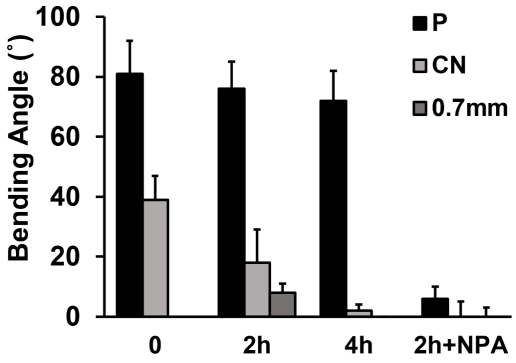

Figure S2.2. Phototropic bending following excision and auxin depletion.

Bending responses of post-photomorphogenic seedlings excised at petioles (P), cotyledonary node (CN), or 0.7mm of the hypocotyl. Following excision seedlings were left in dark for 0 hours, 2 hours, 2 hours with 5 μM NPA, or 4 hours. Phototropic curvature was measured following 8 hours of 0.8 -0.4 μmol m^{-2} s^{-1} unilateral LED blue light illumination. Data shown are means ± SE, 3 replicates, n=10 for each treatment.

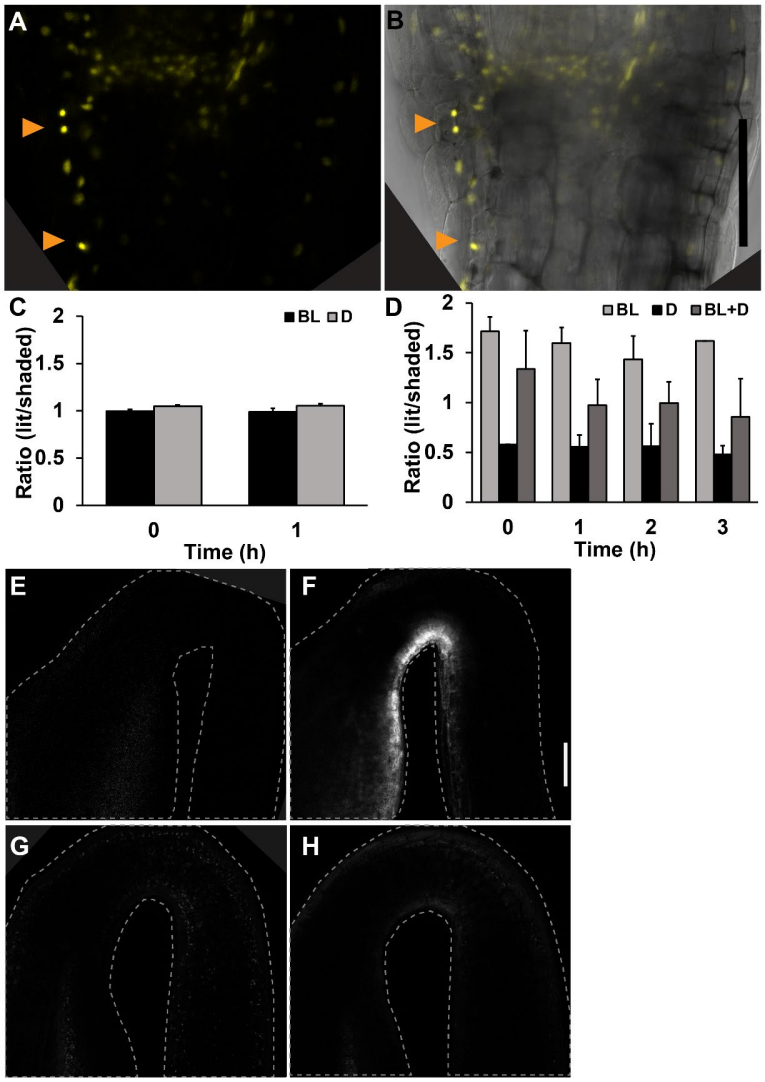

Figure S2.3. Auxin reporter distribution in etiolated seedlings. (A,B) DII-VENUS quantitation in the upper hypocotyl of light-treated seedlings is complicated by presence of guard cells, which show very bright nuclear signal. (**B**) A look at the bright field merged image shows the presence of paired cells at locations that contain paired, bright, spherical VENUS signal. (**C**) Quantitation of sided VENUS signal in etiolated seedlings shows a lack of well-established apical hook-associated asymmetric auxin distribution. (**D**) This asymmetry is observed in all DR5:RFP seedlings and is maintained through early phototropic bending. Scale represents

0.1mm. For all fluorescence quantitations (**B,C**) n≥5. For auxin distribution visualization DR5:RFP was chosen due to (**E**) very low autofluorescence observed. (**F**) DR5:RFP fluorescence in the hypocotyl demonstrated expression patterns similar to those previously published (Friml *et al.*, 2003; Zádníková *et al.*, 2010; Han *et al.*, 2014). (**G**) Relatively high autofluorescence was observed using DR5:GFP compared to DR5:RFP (**E**). (**H**) Additionally, lower DR5:GFP signal was observed compared to DR5:RFP (**F**).

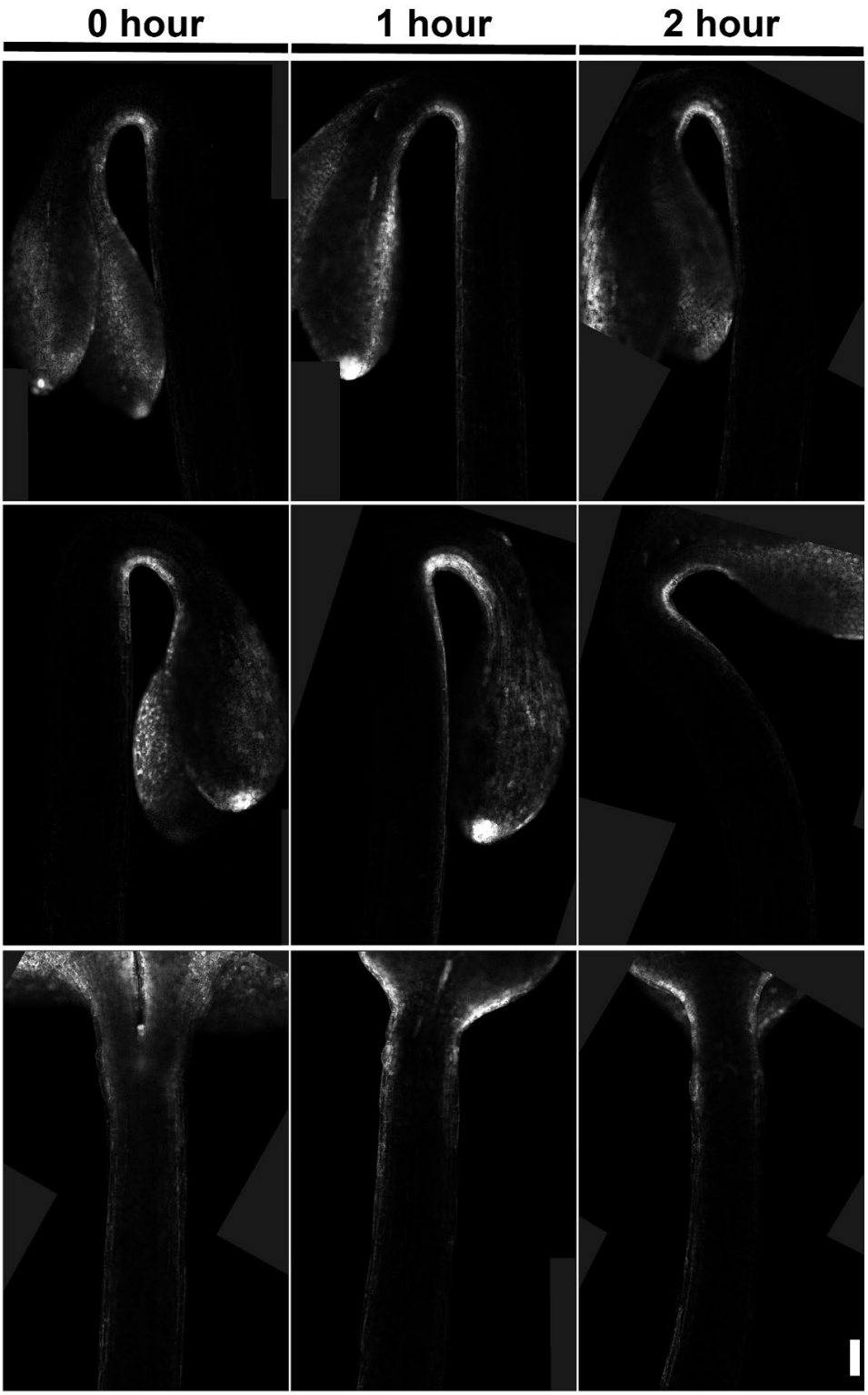

Figure S2.4. Auxin distribution does not appear to change during early stages of phototropism. DR5:RFP auxin reporter imaging does not suggest auxin distributions

change during the first 3 hours of phototropism. Etiolated seedlings were irradiated with unilateral blue light either with the hook facing (**A**) or away from the light source (**B**). Auxin distribution is asymmetric dependent on hook position, but does not increase in the non-illuminated side of the hypocotyl within a 3 hour timeframe. Additionally, light-treated seedlings (**C**) show no increase in asymmetric auxin distribution during the initial 3 hour timeframe during which phototropic bending is observed. Scale represents 0.1mm.

Chapter 3: Spatio and Temporal Placement of Auxin Transport Events During Phototropism

Manuscript in preparation: Pritchard, *et al*. 2019.

Abstract

Phototropism occurs in a series of discrete stages. First, there is initial perception of the asymmetric blue light signal by phot1, which leads to rapid signaling events and direct interaction with the auxin transporter ABCB19. Following this, there is rapid linear phototropic bending. As bending is achieved and the seedling is oriented to the light source the rate of bending decreases and hypocotyl elongation resumes. However, the events that link initial phot1 perception and initial curvatures toward the light are not known. Two components recently identified in guard cell regulation, CBC1 and CBC2, also appear to be involved in early phototropic bending. Further, mutant analysis of several members of the slow anion channel family show delays in initiation of bending, indicating a role in early stages of phototropism that precede elongation. Further analysis of these mechanisms may provide clues to determining the relationship between early phot1 signaling events and downstream bending responses during phototropism.

Introduction

Phototropic curvature in Arabidopsis seedlings is initiated by perception of blue light by the PHOTOTROPIN (phot) AGC kinases and is mechanically realized by differential auxin distribution leading to asymmetric cellular elongation in the hypocotyl (Liscum & Briggs, 1995; reviewed in Haga & Kimura, 2019). Blue light

excitation of flavin co-factors associated with phot light-oxygen-voltage (LOV) domains results in autophosphorylation and conformational change to activate the serine/threonine kinase activity of the phot receptor. PHOTOTROPIN2 (phot2) is active under high light conditions (≥1 μmol m^{-2} s^{-1}), while PHOTOTROPIN1 (phot1) is active under low light conditions (0.1-1 μmol m^{-2} s^{-1}) (Briggs & Christie, 2002). Upon activation, phot1 dissociates from the plasma membrane within 20 minutes (Sakamoto, 2002; Kaiserli *et al.*, 2009), but this dissociation does not appear to be required for initiation of phototropic processes, as seedlings expressing a non-internalized lipid-anchored phot1 did not display defects in phototropic bending (Preuten *et al.*, 2015). Downstream phototropic intermediaries include members of the NRL family including NONPHOTOTROPIC HYPOCOTYL3 (NPH3), which directly interacts with phot1 and is required for bending under low fluence unilateral blue light (Motchoulski, 1999; Sullivan *et al.*, 2009, 2016b; Wan *et al.*, 2012) as well as the Auxin Response Factor ARF7/NPH4, (Stone *et al.*, 2008a; Petrásek & Friml, 2009). Another early step in phototropic responses is the direct blue light-dependent phosphorylation of the ATP-Binding Cassette Subclass B member 19 (ABCB19) transporter by phot1 (Christie *et al.*, 2011). This interaction represses ABCB19 auxin transport activity, halts rootward auxin transport in the upper hypocotyl in early stages of the response, but does not contribute to lateral redistribution of auxin, as *abcb19* mutants bend faster than wild type (Noh *et al.*, 2003; Christie *et al.*, 2011).

The primary transporters that direct polarized auxin streams through the hypocotyl are members of the AUXIN1/LIKE AUXIN1 (AUX1/LAX), PIN-FORMED (PIN), and ABCB families. AUX1/LAX proteins are responsible for

uptake and transport of auxin into the cell, and are important for events during seedling growth, such as formation of lateral roots and apical hook maintenance (Ugartechea-Chirino *et al.*, 2010; Vandenbussche *et al.*, 2010). PIN proteins are efflux carriers that direct polar auxin fluxes and are essential to organogenesis and plastic directional plant growth responses (Vanneste & Friml, 2009; Peer *et al.*, 2011). PIN3, PIN4 and PIN7 have all been implicated as having roles in various stages of the phototropic response, including lateral transport of auxin to the shaded side of the hypocotyl and transport down to the elongation zone (Blilou *et al.*, 2005; Christie *et al.*, 2011). PIN3, and to some extent PIN7, are involved in translocation of auxin to the elongation zone, resulting in bending of the hypocotyl towards the light source (Friml *et al.*, 2002b; Ding *et al.*, 2011; Christie *et al.*, 2011). However, no combination of PIN mutants tested to date shows a complete lack of bending (Christie *et al.*, 2011; Preuten *et al.*, 2013; Willige *et al.*, 2013) and reported PIN asymmetries appears to amplify, but not play a causal role in phototropic bending, as all PIN mutants tested respond phototropically (Haga & Sakai, 2012). Instead, activation of PINs by the AGCVIII kinase D6PK may actuate lateral/differential auxin streams in phototropic seedlings (Willige *et al.*, 2013; Barbosa & Schwechheimer, 2014). D6PK mutants, show only slight phototropic bending in the upper hypocotyl (Zourelidou *et al.*, 2009; Willige *et al.*, 2013) consistent with primary PIN function in directing rootward streams to the elongation zone after lateral auxin re-localization. The persistence of residual bending in both *d6pk* and *pin3pin4pin7* mutants indicates a yet unknown mechanism responsible for the initial lateral movement of auxin.

ABCB proteins function in auxin efflux at the plasma membrane efflux and prevent reuptake, and rootward auxin transport is mediated primarily by ABCB19 supplemented by activity of ABCB1 and ABCB21 (Noh *et al.*, 2001; Geisler *et al.*, 2005; Blakeslee *et al.*, 2007; Jenness *et al.*, 2019). In etiolated seedlings, ABCB19 has been reported to be ubiquitous throughout the hypocotyl and shows an increased expression on the concave side of the apical hook (Noh *et al.*, 2003; Wu *et al.*, 2010a). In post-photomorphogenic seedlings, ABCB19 is localized ubiquitously in the upper hypocotyl, though in the mid and lower hypocotyl is largely restricted to the bundle sheath cells (Blakeslee *et al.*, 2007).

Later stages of phototropism involve acidification to aid cell expansion in the elongation zone and it has been proposed that early events in phototropism may be differential regulation of H^+-ATPase maintenance of proton gradients. It has been demonstrated that members of the AHA H^+-ATPase family co-immunoprecipitate with phot1 in dark and after BL exposure (Christie *et al.*, 2011) and *in silico* models support a role for gradient formation driving lateral auxin fluxes (Hohm *et al.*, 2014). Interestingly, some evidence has linked the localization of AHAs and ABCBs, specifically ABCB19 and AHA2 (Titapiwatanakun *et al.*, 2009). It is evident that AHAs play a role in phototropism, though it is still unclear the extent to which they affect the phototropic response and if there is a differential proton gradient formed during initiation of phototropism.

Microtubules (MTs) have previously been implicated in tropisms, and *spiral* and *lefty* mutants have oblique microtubule patterning in roots that results in helical

plant growth (Furutani et al., 2000; Thitamadee et al., 2002; Lloyd, 2002; Nakajima et al., 2004; Ishida et al., 2007). Microtubules are also involved in regulation of cell polarity and expansion via differential patterns of microtubule orientation that controls cell elongation (Lloyd, 2002; Yang, 2008; Bisgrove, 2008). *phot1phot2* mutants have been shown to regulate microtubule severing, branching, and reorientation during the earliest stages of phototropism via KATANIN, a microtubule severing protein (Lindeboom *et al.*, 2013). Seedlings lacking katanin show decreased phototropic response and reduced microtubule reorientation, while *phot1phot2* mutants show defects in this microtubule reorientation (Lindeboom *et al.*, 2013). Moreover, it was shown that the reorganization is very rapid, with microtubule severing and transverse to longitudinal reorientation occurring on the BL illuminated side of the hypocotyl within 15 minutes (Lindeboom *et al.*, 2013). These results suggest that microtubule reorientation may contribute to the earliest steps of phototropic bending.

Other rapid events that have been proposed to play a role in phototropism include ion channel activity, calcium signaling, and plasmodesmal gating (Cho & Spalding, 1996; Harada *et al.*, 2003; Babourina *et al.*, 2004; Han *et al.*, 2014). Ion channel activity is among the earliest events detectable upon BL irradiation and has been demonstrated to be important during phototropic bending in both oat and soybean (Cho & Spalding, 1996; Babourina *et al.*, 2004; Volkov *et al.*, 2005). Interestingly, a BL-dependent anion channel activity screen identified the auxin transporter ABCB19 (Cho & Spalding, 1996; Noh *et al.*, 2001). However, the extent to which anion channel activity is important during phototropism is still unclear.

Rapid increases in cytosolic Ca^{2+} have also been observed following BL irradiation under phot1 conditions (Folta *et al.*, 2003). However, this is likely as part of signaling, and not a direct mediator of initial relocalization of auxin fluxes. BL-dependent callose formation has been demonstrated during phototropic bending, potentially to restrict auxin to sites of elongation (Han *et al.*, 2014). However, increases in callose deposition are only seen during very late stages of phototropism, so it is unlikely that plasmodesmal gating drives initial auxin fluxes.

Here we test the contributions of auxin transporters, microtubules, plasmodesmata, pH, and anion channels during the four stages of phototropic bending. The results suggest that PIN-mediated auxin transport, H^+-ATPase activity, plasmodesmal gating, and MT reorientation are all involved during later stages of phototropism. These mechanisms appear to be important after phototropic bending is complete and may function during attenuation and phototropic elongation. Recently identified phot1 interactors *CONVERGENCE OF BL AND CO_2 1* and *2* (*CBC1* and *CBC2*), which have been shown to regulate anion channels, were found to exhibit defects in initiation of phototropic bending. Analysis of slow anion channels that act downstream of CBC1/2 revealed delays in initiation of phototropic bending. While the contributions of channel activity are a promising area of research the exact mechanism by which these channels are involved in bending need to be further investigated.

Results

Kinetic analysis of auxin transport mutants during phototropism in non-restrictive conditions.

Role of PINs

It has been reported that PIN-mediated auxin transport is important for proper phototropic bending, with most action attributed to PIN3 in particular (Friml et al., 2002b; Ding et al., 2011; Kami et al., 2013). Additionally, higher order *PIN* mutants show moderate to severe phototropism defects (Friml *et al.*, 2002b; Ding *et al.*, 2011; Christie *et al.*, 2011; Kami *et al.*, 2013; Willige *et al.*, 2013). However, no observable bending angle defects were observed in any plasma membrane *PIN* single mutants during phototropic bending in an unconstrained open-air system, (**Fig. 3.1A**), except a slight enhancement of bending angle that was observed in *pin4*. However, all *pin* single mutants showed a trend of slight loss of bending angle and slightly higher bending position along the hypocotyl (**Fig. 3.1B**), as has been reported previously (Christie *et al.*, 2011; Kami *et al.*, 2013; Preuten *et al.*, 2013). The higher order *pin3pin7* and *pin3pin4pin7* mutants showed increasingly dramatic defects in curvature response (**Fig. 3.1C**). *pin3pin7* mutants bent at a slower rate and maximum bending angle is decreased slightly. Additionally, bending angle position was higher along the hypocotyl compared to Col-0. (**Fig. 3.1D**). Since no initial phototropic delay was observed, these results suggest a role for PIN-mediated auxin efflux during later stages of bending. This is additionally supported by the presence of a higher elongation zone location along the hypocotyl. The lack of an early phototropic defect suggests that differential auxin accumulations occur even in the absence of PINs,

while the higher bending position indicates a defect in rootward transport to the elongation zone.

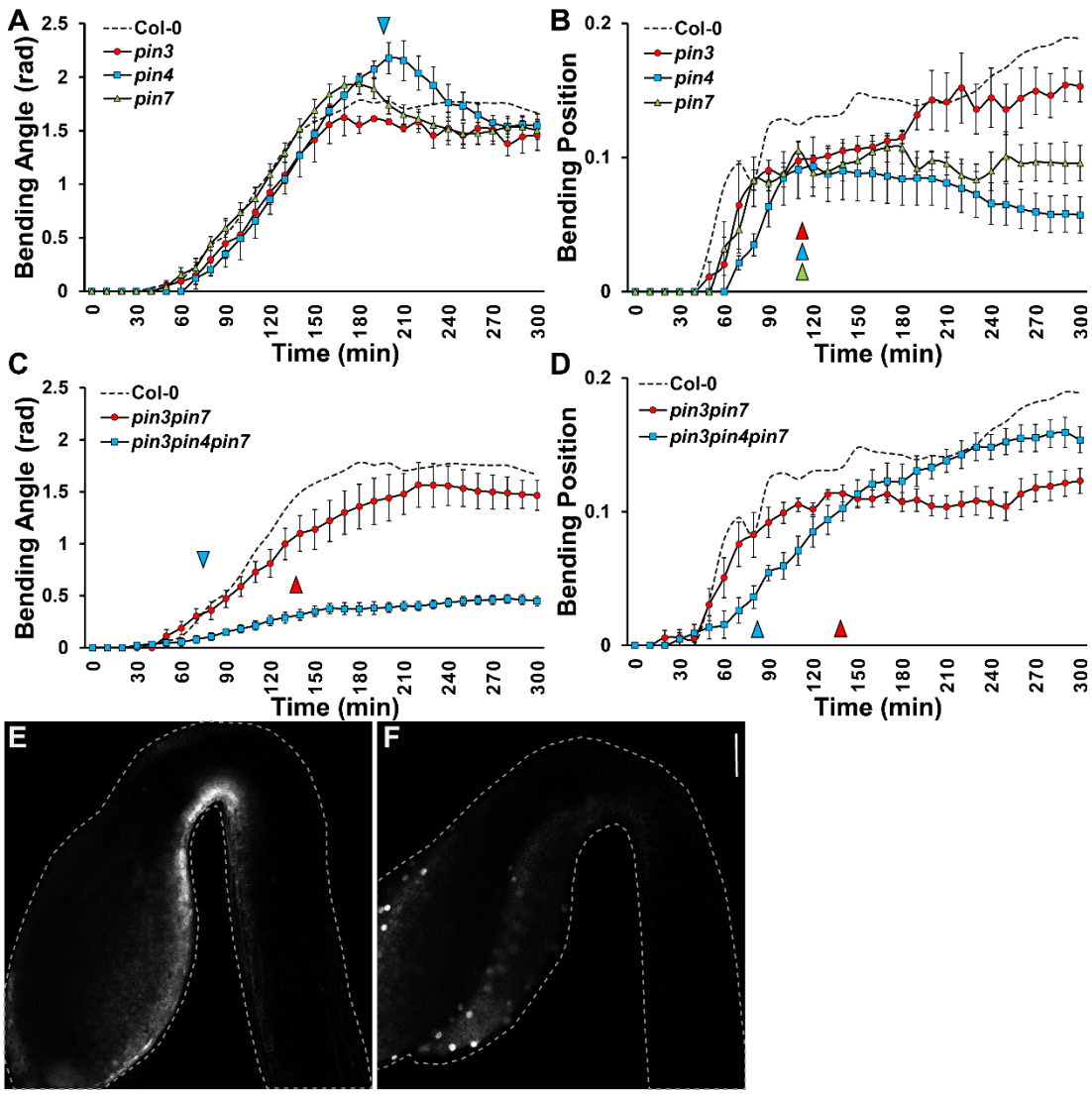

Figure 3.1. Bending kinetics of *pin* mutants and auxin distribution in *pin3* indicate a role in later stages of phototropic bending. (**A**) Phototropic bending and (**B**) bending position of *pin* single mutants *pin3*, *pin4*, and *pin7* over time compared to Col-0. (**C**) Phototropic bending and (**D**) bending position of *pin* double and triple mutants, *pin3pin7* and *pin3pin4pin7* over time compared to Col-0. Data presented are means ±SE, n ≥ 5 seedlings. The DR5:RFP auxin reporter fluorescence in 3-day (**C**) Col-0 and (**D**) the *pin3* backgrounds. Scale bar represents 100 μm.

In etiolated seedlings, plasma membrane localized PINs have all been shown to exhibit differential expression in the concave and convex sides of the apical hook and the upper hypocotyl directly below the hook (Benková *et al.*, 2003; Vieten *et al.*, 2005; Zádníková *et al.*, 2010; Haga & Sakai, 2013). However, in post-photomorphogenic seedlings PIN3-GFP signals showed a decrease in vascular signal and a more apolar epidermal signal in the upper hypocotyl epidermis compared to etiolated seedlings (**Fig. 3.2A-C**).

When PIN3-GFP signals were observed during continuous, unidirectional blue light treatment in post-photomorphogenic seedlings, no observable differential epidermal PIN3-GFP signal was observed at 3 hours (**Fig. 3.2E**), as is consistent with results previously reported (Haga & Sakai, 2012). While differential PIN3 expression has been previously observed at 6 hours (Ding *et al.*, 2011), this is well after the kinetics of phototropism demonstrate that bending is complete, consistent with a role for PIN3 during late stages phototropism, or following establishment of phototropic curvatures. Interestingly, during later stages of phototropism, a global reduction of PIN4-GFP signal was observed in the upper hypocotyl and an asymmetric reduction in outer cortical expression was occasionally observed (**Fig. 3.3A**). The phototropism kinetics of *PIN* mutants support a role for PIN function downstream of initial phototropic events, as no mutants tested demonstrated defects in initial bending response. Additionally, dynamic changes observed in *PIN*s were evident after phototropic bending was complete (at ~4 hours), further supporting a role in attenuation or phototropic elongation.

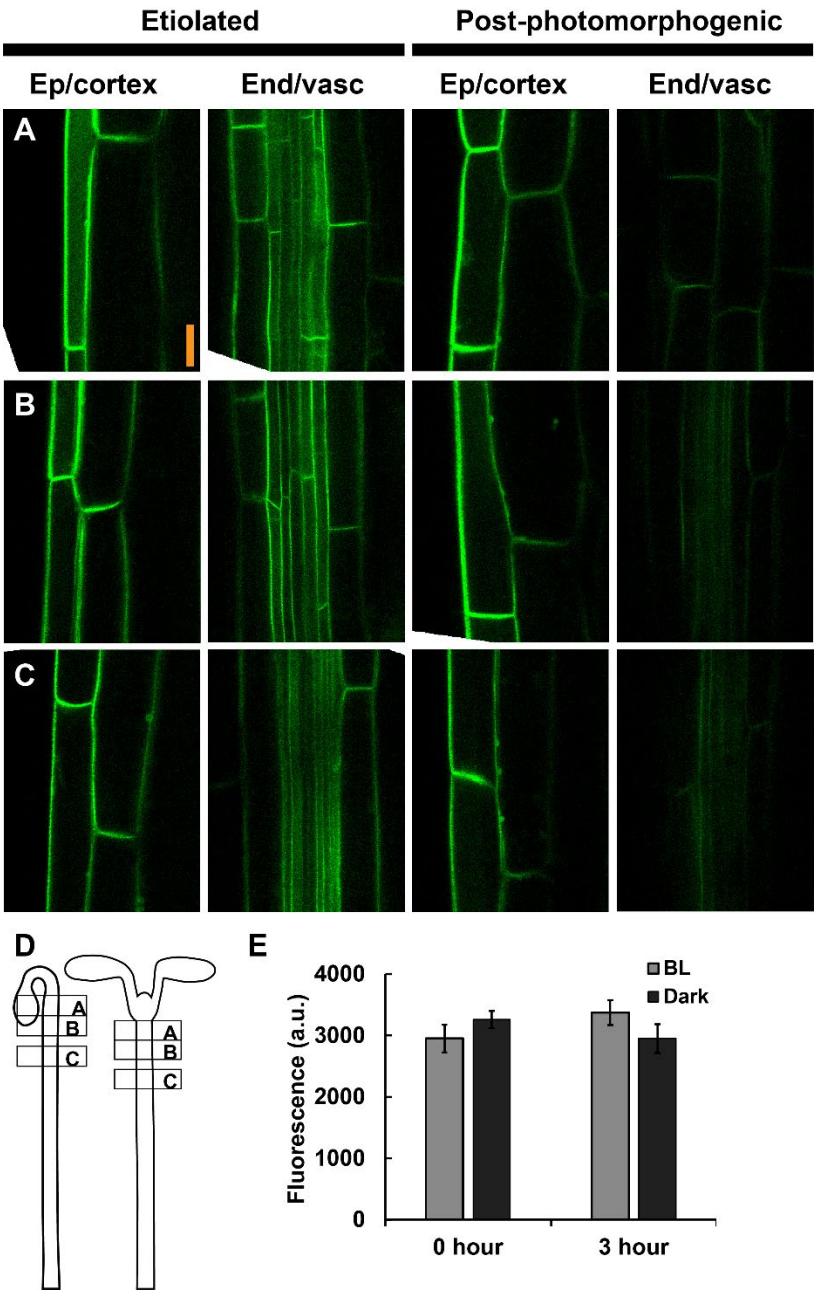

Figure 3.2. Localization pattern of PIN3-GFP in the upper hypocotyl of etiolated and post-photomorphogenic seedlings. Localization of PIN3-GFP in etiolated and post-photomorphogenic seedlings shows a reduction in PIN3 signal in the vasculature of post-photomorphogenic seedlings. (**A**) Images were obtained from the upper hypocotyl just below the cotyledonary node, (**B**) immediately below zone **A**, or (**C**)

just below the area where initial phototropic curvatures have been observed to initiate. (**D**) The seedlings schematic represents the sampling areas for A-C in etiolated and post-photomorphogenic seedlings. (**E**) Due to asymmetric apical hook-dependent PIN3-GFP signals differential expression following unilateral BL illumination was quantitated in post-photomorphogenic seedlings at zone (**B**) where phototropic bending is first observed. Data presented are means ±SE, $n \geq 5$ seedlings. Scale bar represents 20 μm.

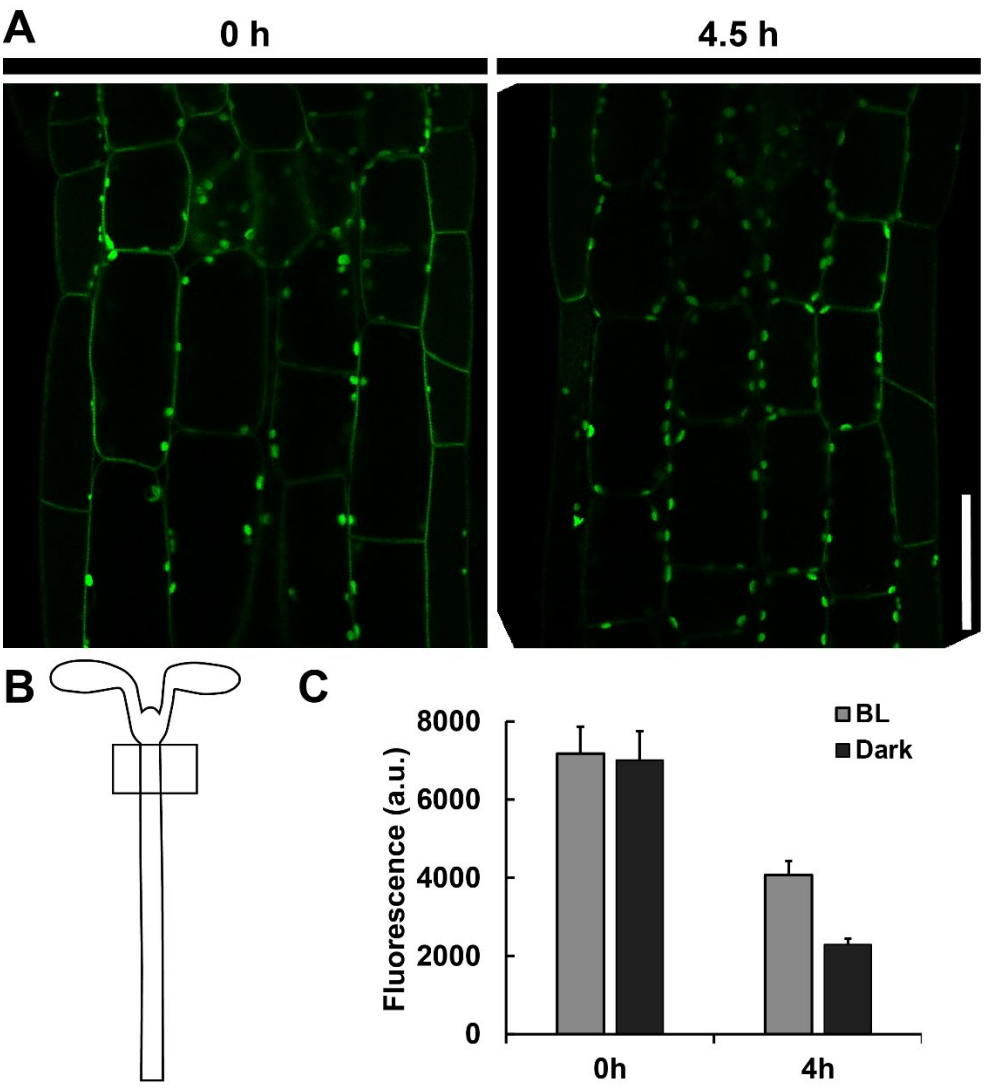

Figure 3.3. Localization of PIN4-GFP in the upper hypocotyl of post-photomorphogenic seedlings. (**A**) Localization pattern of PIN4-GFP in post-photomorphogenic hypocotyls at 0 hour and (**B**) after 4 hours of unilateral BL irradiation. (**C**) Schematic demonstrating the area of the hypocotyl sampled for imaging. (**D**) Fluorescence intensity of PIN4-GFP on BL-illuminated and dark sides of the hypocotyl at 0h and 4h. Data presented are means ±SE, n ≥ 5 seedlings. Scale bar represents 20 μm.

Role of ABCB19

Previously it was shown that phot1 directly interacts with and phosphorylates ABCB19 (Christie *et al.*, 2011). This results in a halt in downward auxin transport and is observable as a more rapid initiation of phototropic bending (**Fig. 3.2A**). Open-air kinetic bending results observed agree with previously published results (Christie *et al.*, 2011). *abcb19* seedlings initiate bending faster, slightly more overall, and overshoots slightly (**Fig. 3.1A**). *abcb19* mutants show defects in inhibition of hypocotyl elongation with BL (Folta *et al.*, 2003), whereas wild type seedlings demonstrate an initial halt in elongation prior to bending that lasts approximately 30 minutes (**Fig. 2.S2**). Bending is observed approximately 20 minutes faster in the *abcb19* mutant compared to wild type, although the rate of bending and overall bending angle are not changed (**Fig. 3.2A**).

In later stages, *ABCB19* mutants show a higher bending position compared to wild type (**Fig. 3.4.B**). This appears to be due to overall elongation increases observed in *abcb19*, since after initial phototropic bending is achieved, elongation is observed in the uppermost region of the hypocotyl above the area of phototropic curvature. Alternatively, it has been noted that *abcb19* seedlings have higher baseline levels of auxin, which could also contribute to the faster bending response observed (Christie *et al.*, 2011). Visualization using the DR5:RFP auxin reporter supports elevated auxin levels over a more diffuse area of the hypocotyl in *abcb19* compared to wild type (**Fig. 3.4C,D**). This suggests ABCB19 may contribute to auxin distribution during seedling growth prior to initiation of phototropism.

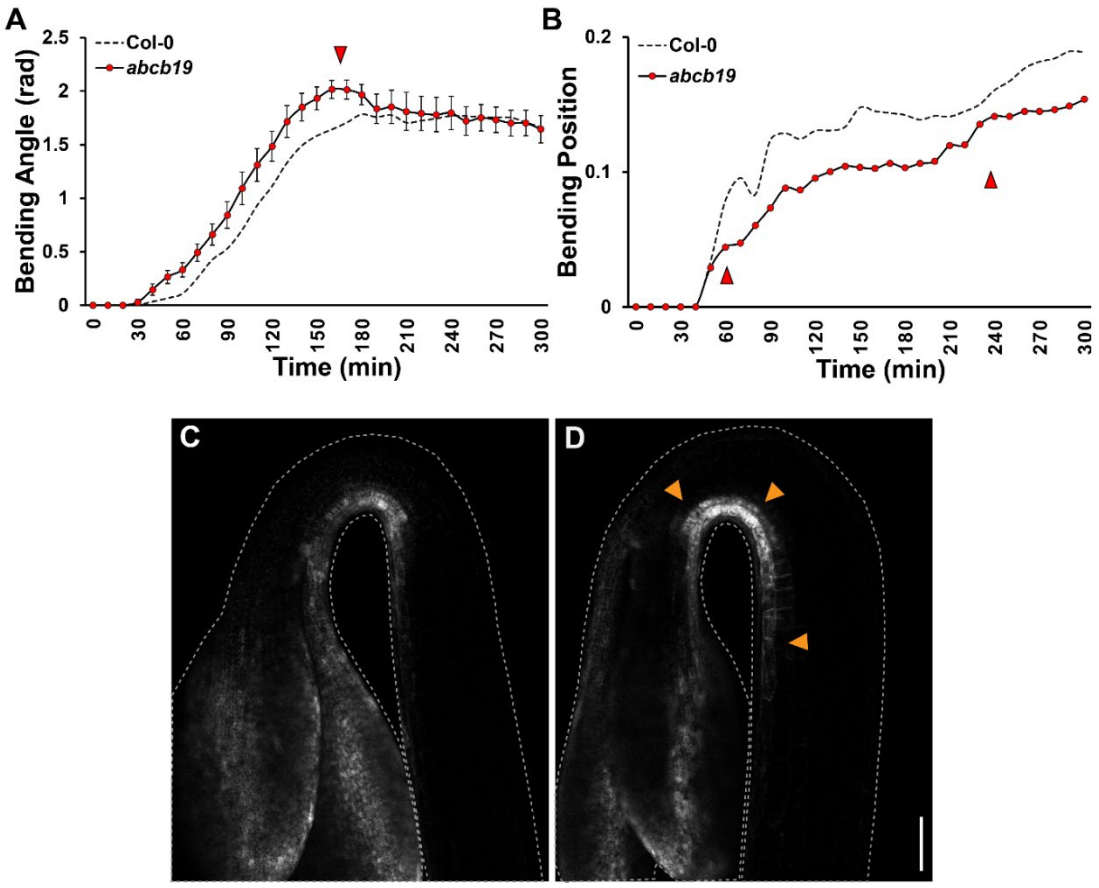

Figure 3.4. Faster initial bending in and expanded area of auxin distribution in *abcb19*. (**A**) Phototropic bending and (**B**) bending position of Col-0 and *abcb19* seedlings over time. Data presented are means ±SE, n ≥ 5 seedlings. The DR5:RFP auxin reporter fluorescence in 3 day (**C**) Col-0 and (**D**) the *abcb19* backgrounds. Orange arrows indicate expanded area of fluorescence on the concave side of the hook present in *abcb19*. Scale bar represents 100 μm.

Kinetic analysis of other modulators during phototropism in non-restrictive conditions.

Role of plasmodesmata

Many processes have been proposed to be involved in lateral relocalization of auxin, including plasmodesmal gating, microtubule reorientation, calcium signaling, proton gradient formation, and anion channel activity (Cho & Spalding, 1996; Lindeboom *et al.*, 2013; Hohm *et al.*, 2014; Han *et al.*, 2014). To determine if the plasmodesmata are involved in early or late stages of the phototropic response, the plasmodesmal closure protein mutant *pdlp5* was tested in post-photomorphogenic seedlings. *pdlp5* mutants had defects in overall bending angle and showed a somewhat higher bending position along the hypocotyl (**Fig. S3.1A-C**)**.** To visualize callose deposition during phototropic bending, post-photomorphogenic Col-0 seedlings were stained with aniline blue over a time series with unilateral blue light. After approximately 4 hours, callose deposition could be observed. After 8 hours BL treatment, a bright signal in the region of the elongation zone at the parenchyma was detected in wild type seedlings (**Fig. S3.1E**), but not in the untreated control (**Fig. S3.1D**). To determine if the aniline blue signal was indeed due to callose deposition seedlings were treated with 5μM NAA, which is known to increase callose deposition in etiolated seedlings (Lee *et al.*, 2011). Seedlings treated with NAA showed enhanced callose deposition compared to untreated seedlings or those treated with BL alone (**Fig. S3.1F**). These defects in bending and observation of callose deposition after 4 hours suggest that plasmodesmal gating may be important for maintenance of phototropic curvature and downstream of auxin response.

Role of microtubules

Blue light-induced (10 μmol m^{-2} s^{-1}) microtubule reorientation from transverse to longitudinal has been demonstrated to be phot1phot2 dependent (Lindeboom *et al.*, 2013). However, the *ktn1-1* microtubule severing mutant responds to blue light long-term and bends prototropically (Lindeboom *et al.*, 2013). To determine if microtubule reorientation is differential during unilateral illumination, β-tubulin-GFP seedlings were imaged. Microtubules showed transverse orientation and this did not change over the first 30 minutes of unilateral blue light illumination (**Fig. S3.2A**). To further look at the early effects of microtubule reorientation on phototropic bending, seedlings were treated with various microtubule inhibitors prior to blue light illumination. Treatment with the microtubule-depolymerizing drug oryzalin or the microtubule-stabilizing drug Taxol also showed no defects in bending response at 4 hours (**Fig. S3.2B**). Treatment with 1-aminocyclopropane-1-carboxylic acid (ACC) was shown to result in a reorientation of microtubules from transverse to longitudinal in etiolated seedlings (Le *et al.*, 2005; Ma *et al.*, 2016). Interestingly, treatment with ACC resulted in reduced early-stage (~ 2 hour) phototropic bending, though no differences were measured at later timepoints (**Fig. S3.2C**). These results suggest that microtubule reorientation may occur under phot2-mediated conditions, but that longitudinal microtubule orientation may inhibit phototropic bending.

Role of acidification

Differential acidification has been proposed as a driving factor in very earliest stages of phototropism. To further investigate this the H^+-ATPase loss-of-function mutants *aha1* and *aha2* were tested (**Fig. 3.6A,B**). AHA1 and AHA2 are plasma membrane H^+-ATPases that are functionally redundant, demonstrate overlapping expression patterns, and *aha1aha2* mutants are embryo lethal, making mutant analysis difficult (Haruta *et al.*, 2010). Neither single mutant demonstrated initial defects in phototropic bending, though *aha1* did show an enhancement in rate of bending (**Fig. 3.6A**). Most strikingly, the bending position in both mutants were both much higher up along the hypocotyl and the elongation zone was much more compact compared to Col-0 (**Fig. 3.6B**). These results are consistent with acidification required for cell expansion and elongation during achievement of bending and post-bending phototropic elongation. Additionally, imaging with the pHusion pH sensor (Gjetting *et al.*, 2012) showed no sided changes in apoplastic pH upon unilateral blue light illumination (**Fig. 2.S2B**). Vertical differences in apoplastic pH in the uppermost hypocotyl were observed, which is consistent with elongation zone in etiolated hypocotyl (Gendreau *et al.*, 1997). Additionally, localized transient pH fluxes have been reported during hypocotyl elongation (Stolarz, 2009). Together, these results suggest a role for H^+-ATPase activity during etiolated hypocotyl elongation and late stage phototropic elongation.

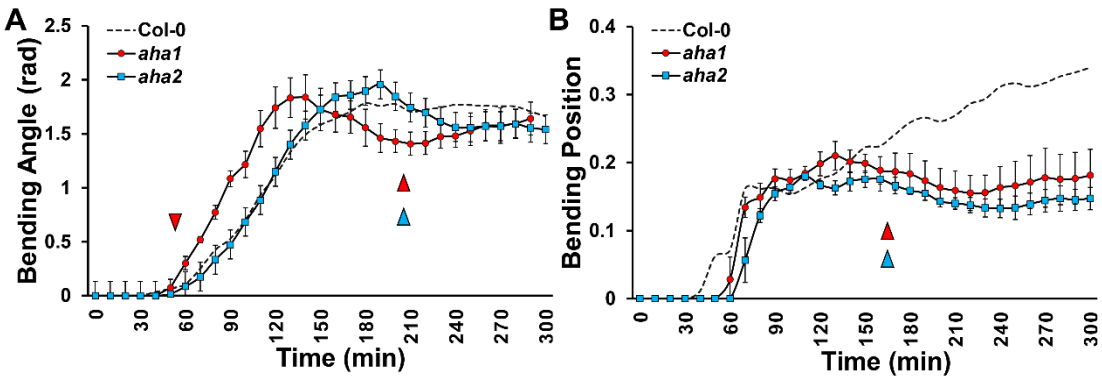

Figure 3.6. Bending kinetics of H^+-ATPase mutants. (**A**) Bending angle of *aha1* and *aha2* mutants over time indicates no defects at early or late stages. (**B**) Bending position suggests a smaller, more restricted elongation zone compared to Col-0. Data presented are means ±SE, n ≥ 5 seedlings.

Role of anion channels

Recently, two new components involved in blue light-mediated regulation of guard cell aperture were identified, *CONVERGENCE OF BL AND CO_2 1* and *2* (*CBC1* and *CBC2*) (Hiyama *et al.*, 2017). It has been proposed that a CBC1/CBC2 complex acts to negatively regulate anion cell channels to inhibit guard cell closing. Since it has been shown to directly interact with and be phosphorylated by phot1, the *cbc1cbc2* double mutant was tested for phototropism phenotypes (**Fig. 3.7A,B**). Mutants exhibited a slight reduction in overall bending angle (**Fig. 3.7A**), but no defects in elongation zone position (**Fig. 3.7B**) compared to wild type. Most interestingly, *cbc1cbc2* showed an initial delay in phototropic response and a slower bending rate than Col-0 during the first 120 minutes of linear bending, indicating a role for them during the initiation of phototropic bending (**Fig. 3.7A**). Downstream interactors of CBC1/CBC2 in the hypocotyl are unknown, although interaction with anion channels has been demonstrated in guard cells (Hiyama *et al.*, 2017).

To investigate whether anion channel activity is important for initiation of phototropism, mutants of several members of the slow anion channel family were tested for phototropic defects. The nitrate-specific *slac-like2* (*slah2*) mutant exhibited no defects in phototropic bending angle, rate, or elongation zone position (**Fig. 3.7C,D**). However, the chloride-specific mutants *slac1* and *slah1slah3* both show defects in initiation of phototropic bending (**Fig. 3.7C**). Additionally, *slac1* mutants bend at a slower rate overall, resulting in an approximately 90 minutes delay in reaching the maximum bending angle, significantly longer than wild type (**Fig. 3.7C**). While *slah1slah3* showed a significant delay in initiation of bending compared to

wild type, the maximum bending angle defect is not significantly different from wild type (**Fig. 3.7C**). However, the elongation zone in *slah1slah3* appeared to be expanded during maximum bending compared to wild type (**Fig. 3.6D**). Phenotypically this appears to be an overshoot of phototropic bending, similar to what is observed in *abcb19*, although the bending angle does not reflect this. These results indicate that chloride channel activity may play a role in initiation of bending, as well as achievement of maximum bending angle, possibly in a CBC-regulated manner.

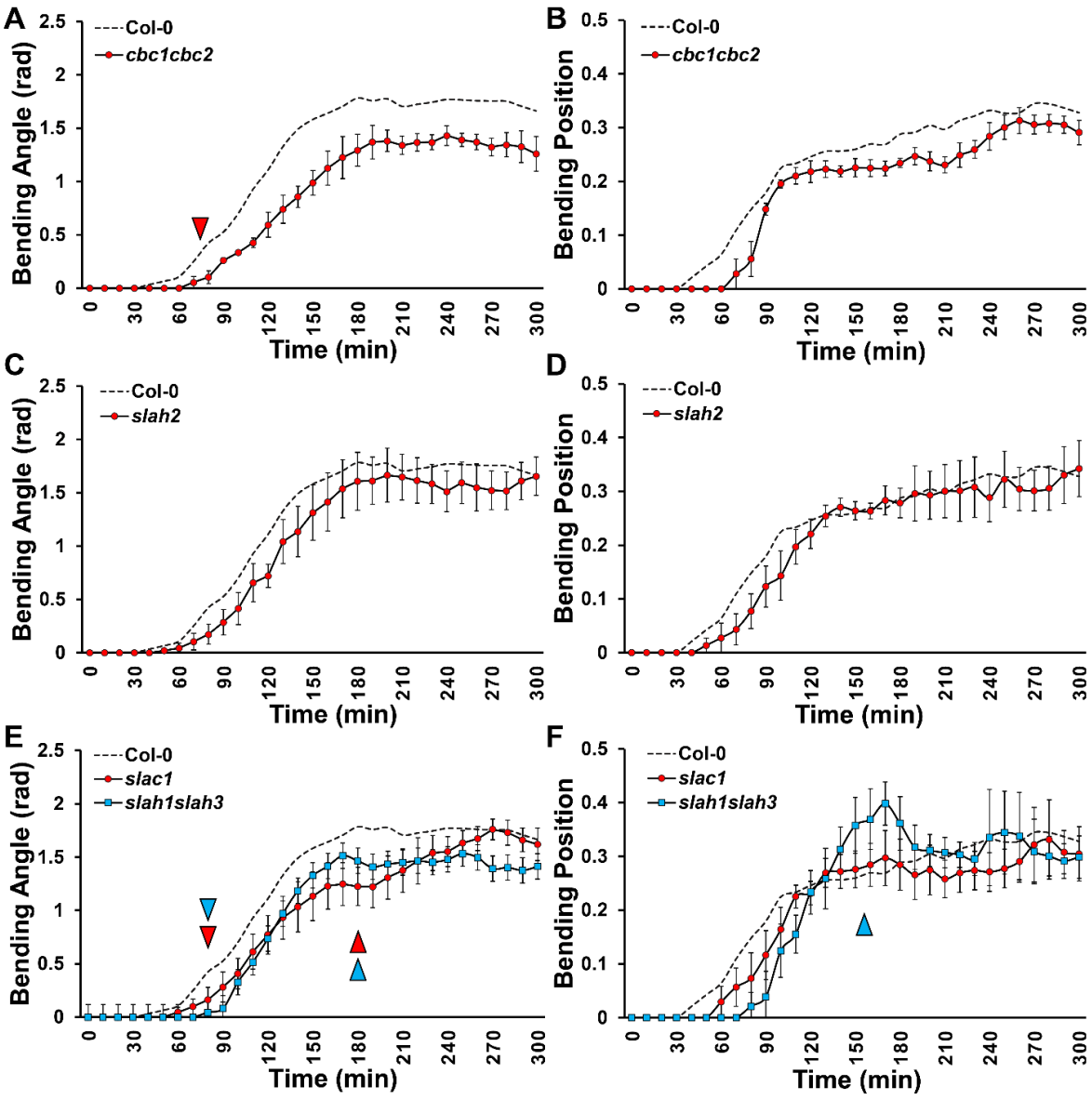

Figure 3.7. Bending kinetics of CBC and anion channel mutants. (A) *cbc1cbc2* double mutants show both early and late defects in phototropic bending, but not (**B**) in bending position. (**C**) The nitrate-specific channel mutant *slah2* shows no defect in bending angle or (**D**) bending position. (**E**) *slac1* and *slah1slah3* mutants show slight delays in initial phototropic bending and overall bending angle. (**F**) Bending position of *slac1* is not significantly different, while *slah1slah3* has a more expansive elongation zone compared to Col-0. Data presented are means ±SE, n ≥ 5 seedlings.

Discussion

The results presented here demonstrate that several complex mechanisms are involved in achievement of phototropic bending. When placed in a spatio-temporal context, events can be separated into discrete stages: perception/signaling, linear phototropic bending, attenuation, and phototropic elongation (**Fig. 2.6**). ABCB19 is the only auxin transporter that has been shown to be a direct target of phot1, and ABCBs in general have not been demonstrated to be involved in rapid dynamic responses. However, the role in phototropism and nature of interaction with phot1 is still not fully understood. The earliest events in this response include perception of blue light by phot1 and interaction with/ phosphorylation of ABCB19 and microtubule reorientation (Motchoulski, 1999; Sakai *et al.*, 2001; Christie *et al.*, 2011; Lindeboom *et al.*, 2013).

The cellular function of ABCBC19, its role seedling development, and the contribution to phototropic bending have been well studied (Noh *et al.*, 2001, 2003; Lin & Wang, 2005a; Blakeslee *et al.*, 2007; Wu *et al.*, 2010a; Christie *et al.*, 2011). Mutant analysis reveals a more rapid initiation of bending compared to wild type. This may be associated with the lack of inhibition of hypocotyl elongation. Since phototropic bending appears to be a differential modification of elongation, this faster initiation of bending may be simply a shift in bending response. Since there is no inhibition of elongation in *abcb19*, no time is needed for elongation to resume in these mutants. This would indicate the mechanisms for bending are still occurring during initial blue light perception, but there may be a truncated lag, resulting in an earlier apparent bending.

Microtubule reorientation from transverse to longitudinal does not appear to occur under phot1 conditions and treatment with microtube inhibitors did not result in a defect in overall phototropic bending (**Fig. S3.2. A-C**). Since microtubule arrays rearrange from transverse to longitudinal rapidly during phototropism, it was hypothesized that pre-treatment with ACC would enhance early phototropic bending, however a decrease in angle was observed (**Fig. S3.2. C**). This suggest that previously observed changes may be phot2-mediated and occurrence of longitudinal microtubule arrays may inhibit phototropism.

Most mutants tested appear to contribute to attenuation of phototropic bending and resumption of elongation when placed in a spatio-temporal context. While ABCB19 has been shown to play a role during initial blue light signaling, the enhancement of maximum bending in *ABCB19* mutants compared to wild type indicates it may play a role during the later stages as well. However, it has been shown that loss of ABCB19 changes global auxin levels and distribution, which may contribute to differences observed during phototropism, including the previously reported "overshoot" phenotype observed in not only phototropism, but gravitropism as well (**Fig. 3.4D**) (Wu *et al.*, 2010a; Christie *et al.*, 2011). Additionally, PIN-mediated auxin efflux is necessary for achievement of a proper maximum bending angle and may be important for integration of gravitropism and phototropic elongation, presumably via rootward transport to the elongation zone during bending and restriction of auxin within the elongation zone (**Fig. 3.3A-D**). However, defects in auxin levels and distribution in these mutants make these results difficult to interpret (**Fig. 3.3. E,F**). The exact role of PINs during phototropism remains to be

determined, as a link between phot1 and PIN activation during phototropism is still not known. However, it is possible that direct regulation of PIN proteins via D6PK could be involved in the early relocalization of auxin, though residual bending seen in these mutants makes this less likely (Willige *et al.*, 2013). It is evident that at this later stage of bending H^+-ATPases promote cell expansion in the elongation zone (**Fig. 3.6. A,B**). Lastly, plasmodesmal gating occurs after phototropism is complete, which may help to maintain bending angle by preventing backflow of auxin (**Fig. S3.1**) (Han *et al.*, 2014).

Direct interaction between CBC1 and CBC2 with phot1 likely occurs in the hypocotyl guard cell meristemoid cells and the severe defects in the double mutant indicate an important role for CBC1 and 2 during phototropism. In guard cells CBC1 an CBC2 are predicted to regulate slow anion channels (Hiyama *et al.*, 2017). Defects observed in the slow anion channel mutants *slac1* and *slah1slah3* suggest a role for chloride channel activity during early stages of bending, and further exploration is needed to reveal specific contribution to phototropism (**Fig. 3.7E,F**). Further investigation into CBC-dependent regulation of plasma membrane targets during phototropism provides a promising avenue to connect early signaling events to late stage phototropic elongation.

Materials and Methods

Plant Material and Growth Conditions. Throughout the study the Col-0 ecotype was used, except where otherwise stated. Lines used include a*bcb19-101* (SALK_033455), *pin3-4* (SALK_038609), *pin4-3* (Friml *et al.*, 2002a), *pin7* (N548791), *pin3-3 pin4-101 pin7-101* (Willige *et al.*, 2013), p*DR5:mRFP1er* (Marin *et al.*, 2010), *pdlp5-1* (SALK_079477), *aha1-6* (SALK_016325), *aha2-4* (SALK-_802786), *pPIN3::PIN3:GFP*, *pPIN4::PIN4:GFP* (Friml *et al.*, 2003; Blilou *et al.*, 2005), and *pB19::B19:GFP* (Mravec *et al.*, 2008). *pin3-4 pin7* (SALK_038609, N548791), DR5:RFP (*pin3-4*), DR5:RFP (*mdr1-101*) were generated via crossing. Seeds were surface sterilized and sown on vertically oriented ¼ MS (pH 5.6; Caisson Labs, Smithfield, UT, USA), 0.5% sucrose, and 0.8% agar (RPI Corp, Mt Prospect, IL, USA) plates. All seeds were stratified at 4 °C for 2-4 days and placed in 80 µmol m^{-2} s^{-1} light (Philips f32t8/tl741; Philips, Andover, MA, USA) at 22°C light for 12 hours to induce germination. For etiolated growth assays, seedlings were removed from light and placed in the dark for 3 days at 22˚C until hypocotyls reached 7-8mm in height. Post-photomorphogenic seedlings were removed from light, placed in dark until the hypocotyls were 3-4 mm in height, then returned to 80 µmol m^{-2} s^{-1} light at 22°C for 8 hours, then returned to dark at least 12 hours, until the hypocotyls were 7-8 mm in height.

Phototropism Assays. For all assays steps performed in dark were carried out under green safe light (Roscolux #2004 Storaro Green, Rosco, Stamford, CT, USA). For kinetic assays three day old etiolated seedlings were transferred in dark from vertical plates to 60 mm petri dishes filled with silicon dioxide (Sigma, St. Louis, MO; Cat

#274739) and water. After a 30-minute acclimation, seedlings were exposed to 0.8 - 0.4 μmol m^{-2} s^{-1} unilateral LED blue light illumination for 8 hours (Rothner Laser Technic). Images were captured every 10 minutes with a USB3 uEYE CP camera (IDS Imaging Development Systems, Woburn, MA, USA) and processed for clarity (brightness, contrast, and exposure adjusted) with Photoshop (Adobe Systems Inc., Cupertino CA). For end-point assays seedlings were grown as described previously, placed in unilateral blue light (BL) treatment for 8 hours, then immediately imaged using a Zeiss Stemi 200-C dissecting microscope (Carl Zeiss, Oberkochen, Germany) equipped with Infinity Capture software (Lumenera Corporation. Ottowa, Ontario, Canada). Phototropic bending angle and bending position were measured as described previously (**Fig. 2.2a)** All phototropic bending and hypocotyl elongation measurements were made using FIJI software (Schindelin *et al.*, 2012; Schneider *et al.*, 2012).

Callose Staining and Imaging. Seedlings were grown under normal bending assay conditions. 5μM NAA was applied as a control directly to the Col-0 seedlings and left to sit 8h. During the assay 0h control was removed prior to blue light illumination, while the rest were taken out at 2, 4, 6, and 8h of BL treatment. Seedlings were immediately fixed in MTSB/4% paraformaldehyde with 5% DMSO solution for 1h and rinsed with plain MTSB solution 3 times, 10 minutes each. The callose staining solution of 0.05% aniline blue in MTSB was applied for 60 minutes, then washed 3 times, 10 minutes each. The seedlings were immediately imaged according to confocal microscopy conditions described below.

Confocal Microscopy. Confocal Laser Scanning Microscope (CLSM) images were collected using a Zeiss 710 Laser Spectral Scanning Microscope (Carl Zeiss, Oberkochen, Germany). For all imaging the detector gain was set to below 800. DR5:RFP images were collected using the 10x objective. Excitation was set at 594-nm with 15% laser strength and emission collected between 599-662-nm. DR5:RFP fluorescence intensity quantitations were carried out using Zeiss Zen 2012 by recording the average intensity. For GFP and aniline blue imaging the 40x water immersion objective was used. GFP excitation was set to 488 and emission collected between 493 and 598 nm. Due to differences in fluorescence intensity *pPIN3::PIN3:GFP* was imaged at 15% laser strength, while *pPIN4::PIN4:GFP* lines were imaged using 20%. All fluorescence intensity quantitations were carried out using Zeiss Zen 2012 by recording the average intensity of equivalent regions of interest on the lit and shaded sides of the hypocotyl and strictly within equivalent cell-types.Aniline blue fluorescence was excited at 405nm and images were collected between 480 and 515 nm. All confocal images were processed to increase brightness and exposure equally for all treatments using Photoshop and Illustrator for ease of visualization in in figures (Adobe Systems Inc., Cupertino, CA, USA).

Statistical Analysis. All statistical analyses were carried out using JMP PRO 14. Statistical significance for kinetic curves was conducted using ANCOVA. Curves were separated according to distinct phases of phototropism defined in Chapter 1: lag/perception, phototropic bending, attenuation, and phototropic elongation (**Fig. 2.6**).

Supplementary Material

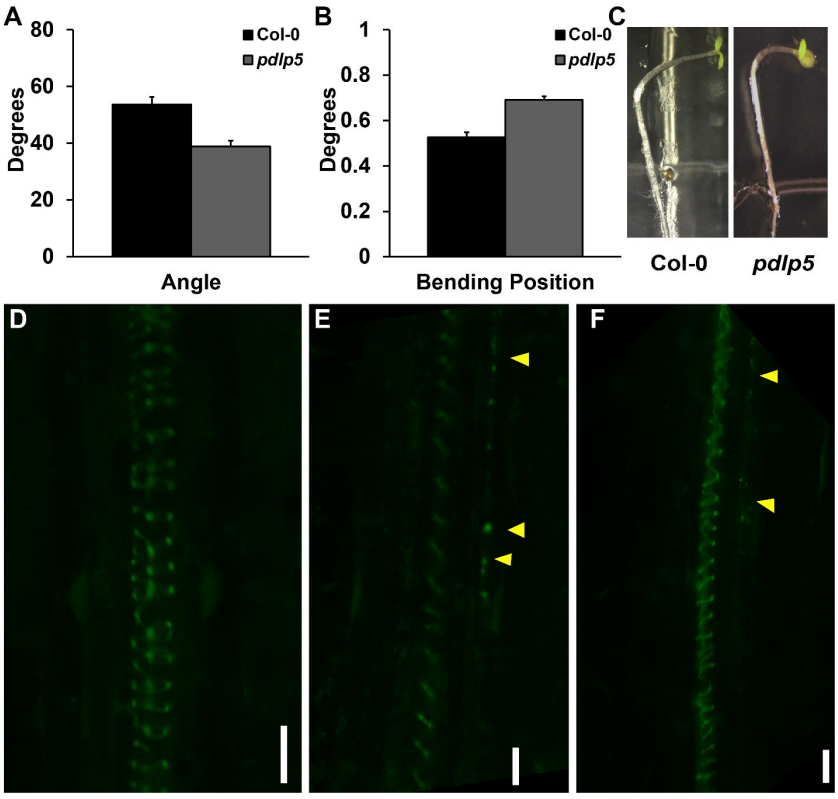

Figure S3.1. Endpoint bending measurement of plasmodesmata mutants and callose deposition during phototropism. (**A**) The decreased overall bending angle, as well as (**B,C**) bending location higher up on the hypocotyl in *pdlp5* mutant indicates the plasmodesmata is involved in the later stages of phototropism. (**D-F**) This is further supported by the callose imaging, which shows that callose deposition begins and continues to increase in the later stages of bending. Callose deposition can be seen in both the 5 µM control (**E**) and the 8h BL treated seedling (**F**), but not in the 0h control (**D**). Bending results are presented from three independent experiments; PDLP5 (n=34), Col-0 (n=39).

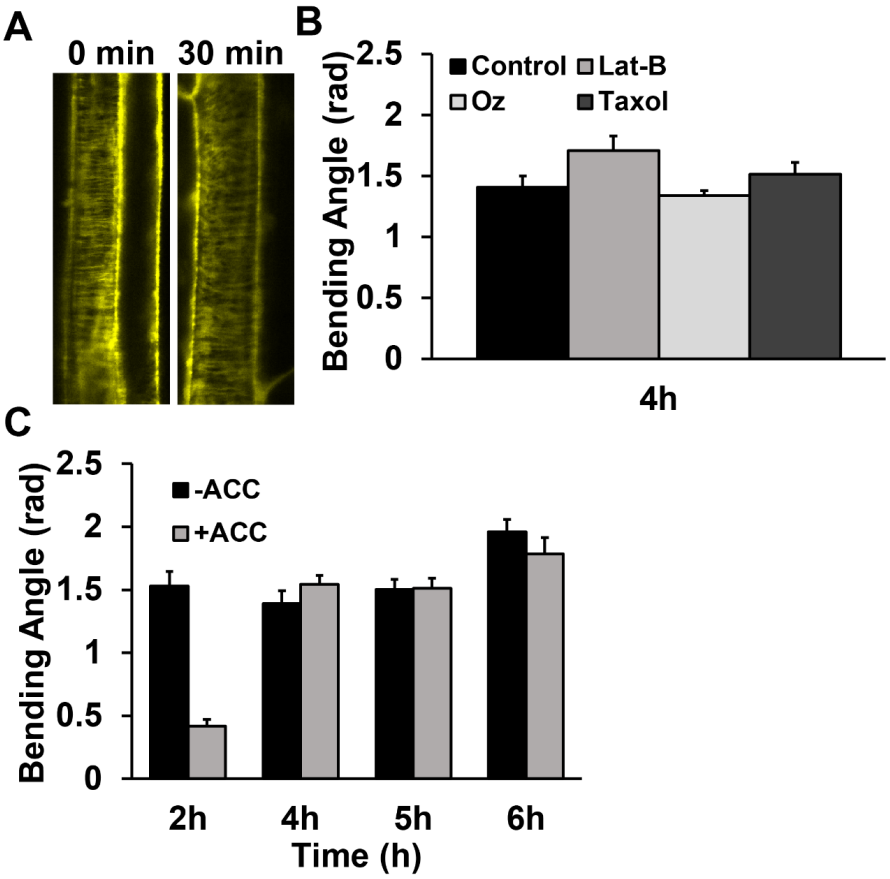

Figure S3.2. Effect of ACC and microtubule inhibitor treatment on phototropic bending. (**A**) Imaging of β-tubulin-GFP in etiolated seedlings and after 30 minutes unilateral BL illumination. (**B**) Seedlings were treated with 5µM Latrunculin-B (Lat-B), 5µM Oryzalin (Oz), or 5µM Taxol 30 minutes prior to unilateral blue light treatment. At 4 hours seedlings were removed and immediately imaged. (**C**) Seedlings were transferred to vertical agar plates with 10 µM with ACC for 30 minutes prior to blue light illumination. Plates were removed and immediately imaged at 2, 4, 5, and 6 hours. All data represent 3 replicates, n≥5 seedlings per replicate.

Chapter 4: Analysis of Auxin Distribution in Arabidopsis Hypocotyls and Roots

Abstract

Apical hook development in dicots is crucial to facilitate emergence from the soil and optimize seedling establishment. Development and maintenance of the hook is controlled by coordination of hormones, including ethylene and auxin. In particular, hook establishment and maintenance have been attributed to asymmetric auxin fluxes that result in accumulation of auxin on the concave side of the hook, resulting in inhibition of elongation within those cells. ABCB19 is expressed on the concave side of the hook and has been proposed to concentrate auxin to maintain inhibitory levels. Here we investigated ABCB transporter contribution to seedling growth using mutant analysis, pharmacological studies, auxin reporters, and direct auxin quantitations. Higher order *ABCB* mutants exhibit exaggerated hook formation. Direct quantiations indicate that auxin levels in the apical hook are low, while auxin conjugate levels are at higher levels. Auxin conjugation in the upper hypocotyl may play a role in asymmetric elongation that helps to establish and maintain the apical hook. Further, enhancement of etiolated hypocotyl elongation by low concentrations of polar auxin transport (PAT) inhibitors suggest a role for ABCB19 channel activity during hypocotyl elongation.

Introduction

Apical hook development and maintenance are tightly controlled mechanisms via a hormonal network, including ethylene and auxin (Schwark & Schierle, 1992;

Lehman *et al.*, 1996). Like phototropism and gravitropism, apical hook development has been attributed to asymmetric auxin accumulation (Zádníková *et al.*, 2010). Ethylene has been demonstrated to positively affect apical hook curvature, as exogenous application leads to an exaggerated hook and several mutants that overproduce ethylene also display exaggerated apical hooks(Guzmán & Ecker, 1990; reviewed in Mazzella *et al.*, 2014). Proper establishment of asymmetric growth has been attributed to ethylene-auxin interactions that establish asymmetric auxin accumulations within a discrete area of the hypocotyl (Vandenbussche *et al.*, 2010; Zádníková *et al.*, 2010; Gallego-Bartolomé *et al.*, 2011).

Imaging of the apical hook with the auxin reporter DR5 shows increased signal on the concave side of the apical hook and these auxin accumulations are proposed to inhibit cell elongation within this discrete region (Benková *et al.*, 2003; Zádníková *et al.*, 2010; Žádníková *et al.*, 2016). PIN polarity has been shown to determine the directionality of auxin fluxes (Friml *et al.*, 2003; Zádníková *et al.*, 2010). The expression pattern of key members of the *PIN* family at the concave side of the apical hook and surrounding cells, together with curvature defects in *pin* mutants, suggest a role for PIN-mediated auxin fluxes in establishment and maintenance of the apical hook (Friml *et al.*, 2002a; Zádníková *et al.*, 2010; Gallego-Bartolomé *et al.*, 2011; Žádníková *et al.*, 2016).

The auxin transporter ABCB19 was shown to be expressed asymmetrically in the hook, favoring the concave versus convex side (Wu *et al.*, 2010a). High ABCB19 expression in this discrete area of DR5 signal maxima and PIN3 expression

(Zádníková *et al.*, 2010; Wu *et al.*, 2010a; Rakusová *et al.*, 2011) are consistent with auxin regulation of PIN and ABCB expression (Noh *et al.*, 2001; Adamowski & Friml, 2015).

Results

Loss of multiple ABCB transporters results in enhancement of apical hook curvature

To determine the contribution of ABCB-mediated auxin transport in the maintenance of the apical hook and hook opening during photomorphogenesis, several higher order mutants were tested. *abcb19* single mutants show no defects in apical hook curvature or hook opening (**Fig. 4.1A**) (Wu *et al.*, 2010a). However, 2-day old etiolated *abcb1abcb19* (*b1b19*) seedlings appeared to have a more exaggerated apical hook, as did *abcb6abcb20* (*b6b20*) seedlings (**Fig. 1A**). As has been previously reported, *b1b19* seedlings responded more slowly during light-induced hook opening (**Fig. 4.1B**) (Wu *et al.*, 2010a). In contrast, *abcb4abcb21* (*b4b21*) seedlings showed no difference compared to Col-0 in apical hook curvature or hook opening (**Fig. 4.1A,B**), which is not surprising since expression of these transporters is not observed in etiolated hypocotyls (Terasaka *et al.*, 2005; Jenness *et al.*, 2019). These results suggest ABCB1/19 and ABCB6/20 regulate auxin levels during early seedling growth. However, loss of these transporters does affect the apparent inhibitory levels of auxin on the concave side of the apical hook.

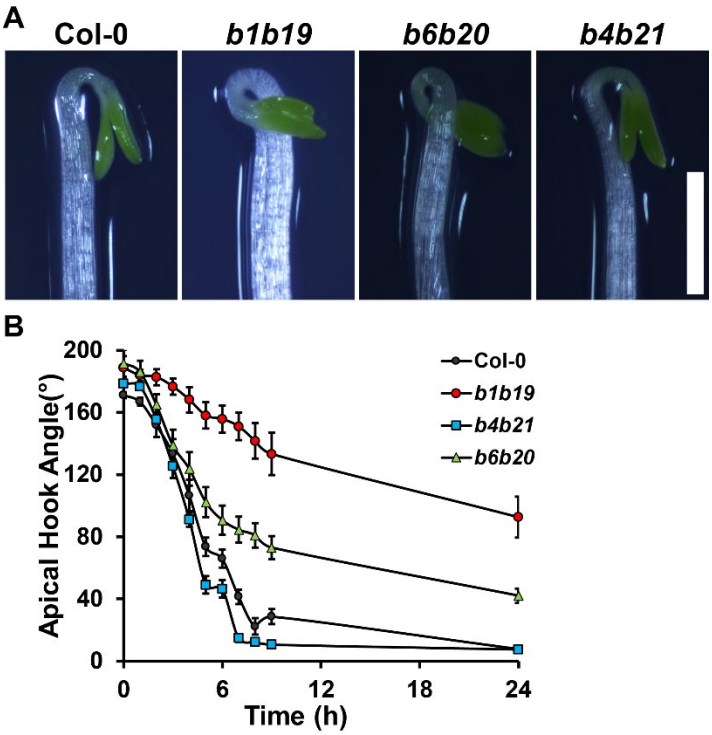

Figure 4.1. Apical hook phenotypes of *abcb* double mutants (**A**) Apical hooks in 2 -day etiolated Col-0, *abcb1abcb19* (*b1b19*), *abcb6abcb20* (*b6b20*) and *abcb4abcb21* (*b4b21*) seedlings. 2-day etiolated *b1b19* and *b6b20* seedlings display an exaggerated apical hook. Scale bar represents 1 mm. (**B**) Apical hook opening. Photomorphogenesis over a 24 hour 90 µmol m^{-2} s^{-1} white light time course indicates reduced hook opening in *b1b19* and *b6b20* seedlings. Data presented are means ±SE, n ≥ 10 seedlings.

Auxin quantitation in etiolated hypocotyls suggest a role for auxin conjugation

To further investigate the contribution of auxin to seedlings phenotypes, etiolated seedlings were treated with auxin and the polar auxin transport inhibitors NPA and CPD. Concentrations of NPA and CPD were used to differentially inhibit ABCBs or global polar auxin transport (PAT). In 2 day old etiolated seedlings, hypocotyl elongation was inhibited by IAA, suggesting that loss of apical hook maintenance was not due to overall cellular elongation in the hook (**Fig. 4.2C**). Treatment with low concentrations of CPD and NPA resulted in enhancement of hypocotyl elongation, while high (>1 μM) levels of CPD, but not NPA, resulted in inhibition of elongation (**Fig. 4.2C**). However, the enhancement of elongation is not observed at 4 days (**Fig. 4.2D**). As has been reported previously, NPA and CPD treatment resulted in hypocotyl and root gravitropic defects (Rashotte *et al.*, 2000); however, a rectification of the gravitropic response occurred and no hypocotyl gravitropism defects were present at 4 days. These data suggest key differences in physiological and hormonal regulation exist during the days following germination and after 4 days of etiolated elongation as the hypocotyl nears maximal elongation and hook opening occurs. Additionally, as has been previously demonstrated, treatment with auxin resulted in loss of apical hook maintenance (**Fig. 4.2B**) (Geisler *et al.*, 2005; Mazzella *et al.*, 2014).

To further study the role of proposed inhibitory levels of auxin at the concave side of the hook, auxin and auxin conjugates levels were measured (**Fig. 4.2A**). Although no free auxin was detected in 4-day etiolated hypocotyls, oxIAA and IAA-Asp were present (**Fig. 4.2A)**. Interestingly, free auxin levels were not detectable in

seedlings, even with continuous 50 μmol m^{-2} s^{-1} white light treatment, although it has been shown that auxin synthesis increases with light intensity (Hornitschek *et al.*, 2012). This suggests that auxin is not actively synthesized in this tissue or that free IAA is not prevalent in dark grown seedlings and that oxIAA and IAA-Asp are the predominant metabolites (**Fig. 4.2A**). This appears contrary to reported IAA levels via the auxin reporter DR5, which indicate high levels of IAA in the hypocotyl hypocotyl (Geisler *et al.*, 2005; Zádníková *et al.*, 2010; Žádníková *et al.*, 2016). Since DR5 is a synthetic promoter from an IAA-amino acid conjugating GH3 enzyme, it possible that the signals observed reflect areas where auxin conjugation activity is high (Peer *et al.*, 2014).

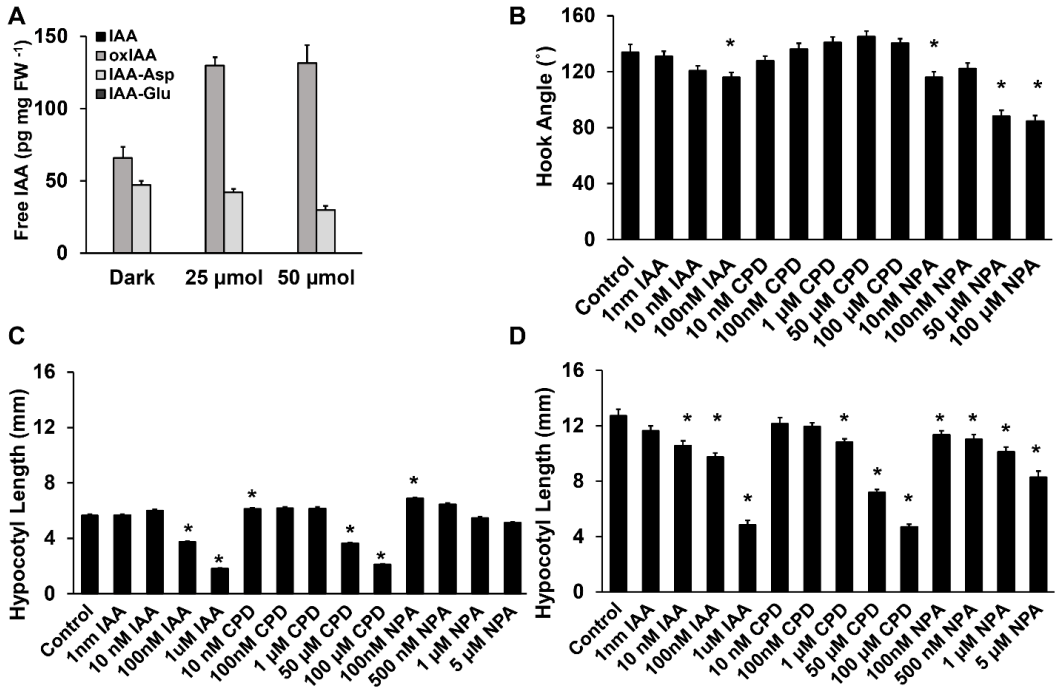

Figure 4.2. Etiolated hypocotyl auxin quantitations and effects of exogenous IAA and PAT inhibitors on hook maintenance and hypocotyl elongation. (**A**) Quantitation of IAA, oxIAA, IAA-Asp, and IAA-Glu in dark, 25 µmol m^{-2} s^{-1}, and 50 µmol m^{-2} s^{-1} white light. (**B**) Effects of exogenous IAA and PAT inhibitors 1-naphthylphthalamic acid (NPA),1-cyclopropyl propane dione (CPD) suggests high levels of IAA and NPA inhibit apical hook maintenance. (**C**) Hypocotyl elongation in etiolated seedlings at 2 days is enhanced with low concentrations of CPD and NPA. Elongation is inhibited by exogenous IAA. (**D**) At 4 days NPA and CPD enhancement of hypocotyl elongation is no longer observed and treatment with IAA, CPD, and NPA inhibits hypocotyl elongation. Data presented are means ±SE, $n \geq 20$ seedlings. Asterisks represent statistical difference by ANOVA $p < 0.001$, Dunnett's post-hoc $p < 0.05$.

Since auxin quantitations did not appear to match the DR5 auxin reporter signals observed and previously reported in hypocotyls, we looked for similar discrepancies in roots using the auxin reporter DII-VENUS (**Fig. 2.3. B**). Unlike DR5, which is transcriptionally activated in the presence of auxin, DII-VENUS is based on auxin signaling-mediated degradation (Brunoud *et al.*, 2012). Therefore, presence of DII-VENUS signals indicates low auxin levels and lack of signal indicate that auxin levels are high. Quantitation of auxin levels in seedling roots showed relatively low IAA levels in 5-day roots, with an increase occurring at 7 days (**Fig. 4.3. A**). This is in agreement with previously published results that showed a pulse of shoot-derived auxin reaches the root at this time (Bhalerao *et al.*, 2002). We proposed that the auxin levels in *b19* and *b1b19* roots would be decreased due to approximately 50% and 75% reductions in rootward auxin transport, respectively (Noh *et al.*, 2001; Blakeslee *et al.*, 2007). However, quantitations show no difference in free IAA levels at 5 days, a slight decrease in 7 days, and a slight increase at 10 days (**Fig. 4.3A**). Imaging of DII-VENUS signals did not show agreement with root auxin quantitations (**Fig. 4.3A,B**). According to DII-VENUS signal there appeared to be more auxin overall in *b19* and *b1b19*, the latter of the two showing the most significant decrease in signal (**Fig. 4.3B**). No DII-VENUS signal was detectable in the lower two-thirds of the root in the double mutant. As was observed with DR5 signal in hypocotyls, auxin levels in the root did not correlate with differences in DII-VENUS signal observed.

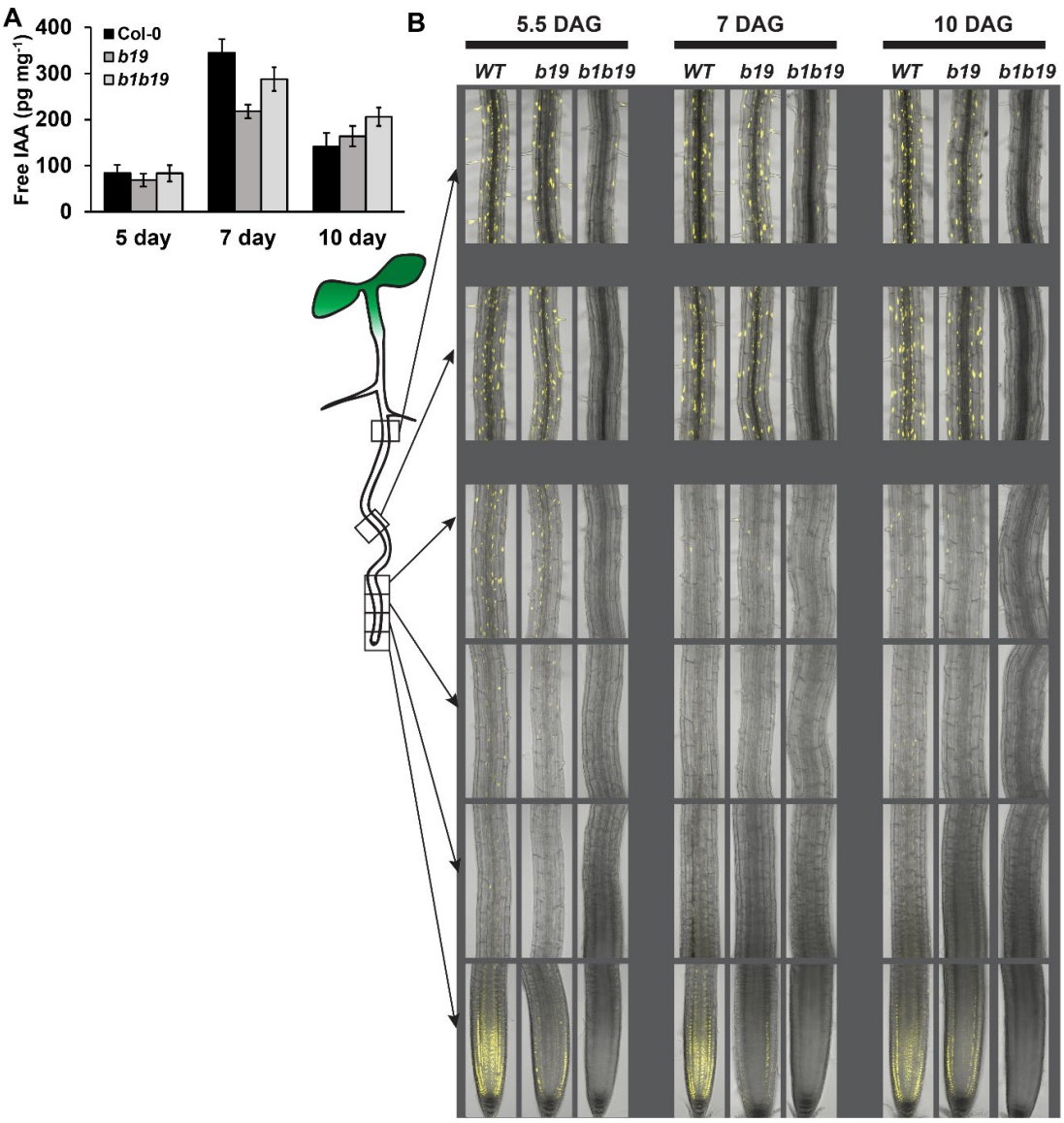

Figure 4.3. Auxin quantitations and DII-VENUS signals in Arabidopsis roots.

(**A**) Quantitation of IAA levels of excised roots at 5,7, and 10 days shows auxin levels are highest at 7 days. At this time auxin levels are lower in *b19* and *b1b19* mutants. (**B**) DII-VENUS signals in WT (Col-0), *abcb19*, and *abcb1abcb19* backgrounds at 5, 7, and 10 days after germination. Seedling diagram boxes indicate regions of the root that images were collected from.

Discussion

Results presented here further support a role for ABCBs during apical hook maintenance and hook opening during photomorphogenesis. Previously, *b19* seedlings were reported to show no defects in apical hook formation or hook opening, but that *b1b19* double mutants have defects in both apical hook curvature and hook opening (Wu *et al.*, 2010a). In this study 2 day etiolated *b1b19* seedlings appeared to have a more exaggerated apical hook (**Fig. 4.1. A**), and hook opening was observed to occur more slowly compared to wild type (**Fig. 4.1. B**). It is possible that this is due to the ecotype-specific auxin levels or age of seedlings measured, as the previously published results were in Wassilewskija (Ws) seedlings and Col-0 seedlings were examined here. Exaggerated apical hook curvature and defects in hook opening in *b6b20* mutants, along with the observed twisted hypocotyl phenotype, indicate these proteins play a role in etiolated growth and photomorphogenesis.

The lack of measurable free auxin in the hypocotyl raises questions about how asymmetric elongation in this discrete region is maintained. The high levels of oxIAA and IAA-Asp in hypocotyls suggest that auxin conjugation on the concave side of the hook area may be high (**Fig. 4.2.A**). Since the DR5 promoter is based on a GH3 aminotransferase, this promoter would be most active where IAA conjugation is necessary (Friml *et al.*, 2003; Peer *et al.*, 2014). It may be that this signal reports where auxin conjugation occurs within the hook. Indeed, application of exogenous IAA was shown to inhibit overall hypocotyl elongation, and the same auxin concentration stimulated apical hook opening (**Fig. 4.2. B,C**).

An interesting result to be explored further is the enhanced hypocotyl elongation observed during growth on low concentrations of CPD and NPA at 2 days (**Fig. 4.2. C**). These inhibitors have been shown to act on ABCB19, which was originally identified via NPA-affinity chromatography (Murphy *et al.*, 2002), and also as having NPPB-sensitive channel activity (Cho & Spalding, 1996). It has been previously shown that NPA disrupts ABCB19 interaction with TWISTED DWARF1 (TWD1), which is required for proper trafficking to and function of ABCB19 on the plasma membrane (Wu *et al.*, 2010b). Additionally, since loss of TWD1 appears to enhance ABCB19 channel activity (Cho & Spalding, 1996), it is possible that treatment with low levels of CPD and NPA could result in enhanced hypocotyl elongation via ABCB19 channel activity.

Materials and Methods

Plant Material and Growth Conditions

Lines used in this study were all in the Col-0 ecotype. Mutants used in this study: *abcb1-100* (Lin & Wang, 2005), *abcb4-1* (Terasaka *et al.*, 2005), *abcb6-1* (Zhang *et al.*, 2018), *abcb19-101* (Lin & Wang, 2005b), *abcb20-2* (Zhang *et al.*, 2018), and *abcb21-2* (Jenness *et al.*, 2019). Surface sterilized seeds were plated on ¼ MS medium (pH 5.6; Caisson Labs, Smithfield, UT, USA) containing 1 g L-1 MES, 0.5% sucrose and 0.8% agar (RPI Corp, Mt Prospect, IL, USA), pH 5.6. Seeds were stratified in the cold/dark for 2 days, place under 90 µmol m-2 s-1 light at 22°C for 12 hours to induce germination, then grown vertically in the dark at 22°C.

Hypocotyl Growth Assays. All dark experiments were carried out under green safe light (Roscolux #2004 Storaro Green, Rosco, Stamford, CT, USA). For etiolated growth assays, plates were placed at 4˚C 48h, moved to light 12h, then placed in dark at 22˚C for the time intervals stated until imaging. For hook opening assays, 2 days etiolated seedlings were moved to 90 μmol m^{-2} s^{-1} light at 22°C to induce hook opening. Plates were scanned at times indicated and hook angles measured using ImageJ (Schneider *et al.*, 2012). 4 day hooks were imaged on a Zeiss Stemi-2000 dissecting microscope. For pharmacological studies seeds were sown directly on plates containing the compounds as stated, including equivalent DMSO solvent controls, with the exception of apical hook maintenance. Pharmacological effects on apical hook maintenance was determined by transferring 3 day etiolated seedlings from standard media described above to media containing Indole-3-acetic acid (IAA), Naphthylphthalamic acid (NPA), 1-cyclopropyl propane dione (CPD), or solvent (DMSO) control plates. After 24 hours plates were removed from dark and imaged. (Roscolux #2004 Storaro Green, Rosco, Stamford, CT, USA).

Auxin and auxin conjugate quantitations. Auxin and auxin conjugate levels were determined according to (Zhang *et al.*, 2016). For root quatitations roots were excised from whole seedlings at 5, 7, and 10 days and quantitated separately from shoots.

Statistical Analysis. All statistical analyses were carried out using JMP PRO 14. Statistical significance was determined by ANOVA $p < 0.001$, Dunnett's post-hoc $p < 0.05$.

Conclusions

Phototropic bending is a fundamental mechanism plants use to optimize light capture, particularly during early seedling growth. Though it has been studied for over 150 years, the specific mechanisms that drive the phototropic response have remained largely unknown. In this dissertation I demonstrate that:

1) Phototropism can be separated into four discrete stages: perception/signaling, phototropic bending, attenuation, and phototropic elongation.

2) Use of an unconstrained open-air system allows for better observation of hypocotyl movement and minimizes the impact of media interaction on phototropic bending and circumnutation. Bending assays conducted on agar can result in a falsely exaggerated bending angle, while bending in open air reduces distortion due to media constraints.

3) Measurement of bending using the central angle can provide spatio-temporal quantitation of bending. The central angle measurement is comparable to traditional measurement of angle of deviation from vertical. However, addition of an arc measurement at the elongation zone provides information about the location of the bending area over time.

4) Circumnutation halts upon unilateral blue light illumination. Additionally, circumnutation is arrested in both etiolated and post-photomorphogenic seedlings, indicating phototropism is not a modification of circumnutation, but a suspension of the mechanism. Following this halt in elongation, phototropic bending is observed in etiolated and post-photomorphogenic seedlings within an hour of unilateral blue light

illumination. Etiolated and post-photomorphogenic seedlings are morphologically distinct, as there are differences in epidermal cell size and overall hypocotyl width and, most notably, differences in the presence of an apical hook (etiolated) and expanded cotyledons (post-photomorphogenic). While there are differences observed in bending response between these two treatments that can likely be attributed to differences in hypocotyl morphology, the stages of bending (perception/signaling, phototropic bending, attenuation, and elongation) appear to be conserved.

5) The lack of observed differential epidermal elongation during the first three hours of phototropism indicates that curvature may be driven by internal endodermal or cortical layers, as has been previously suggested in roots.

6) Analysis of auxin accumulations and bending responses of auxin transporter mutants indicates a role for auxin-mediated elongation during later stages of bending. It is clear that PIN efflux carriers are required for proper phototropic bending, and it is possible that differential regulation of PINs could result in asymmetric auxin fluxes, but there is currently no link to phot1 that would suggest this. No defects were observed in initial phototropic responses and asymmetric localization was not detectable during the approximately 3 hours timeframe in which phototropic bending occurs. However, *PIN* mutants did demonstrate a higher bending position along the hypocotyl, suggesting a role for PIN-mediated auxin transport to the elongation zone. Together, these results indicate it is unlikely that PIN-mediated auxin fluxes drive initiation of phototropism, but that they may participate in establishing pre- and post-bending auxin gradients.

7) As has been previously described, *abcb19* mutants appeared to bend faster compared to wild type. Consistent with observation of bending in *abcb19* and biochemical data, the phot1 inhibition of ABCB19 appears to result in a pooling of auxin. DR5 signal observed in mutants indicates an auxin increase in the upper hypocotyl of *abcb19* compared to wild type. This apparent increase in auxin levels and distribution may contribute to the faster initiation of phototropism observed in *abcb19*.

8) Perhaps the most important observations in this dissertation are the phototropism phenotypes observed in *CBC* and *SLAC*/*SLAH* mutants. The delayed bending observed in *cbc1cbc2*, *slac1*, and *slah1slah3* were the only instances of a delay in initial phototropic bending in any mutants tested. Though the link between early signaling events and late stages of phototropism are still not known, this initial delay in phototropic response suggests CBC signaling and SLAC/SLAH activity may be involved in these intermediate steps. Additionally, the lack of epidermal elongation and asymmetric DR5 signal during the linear stage of phototropic bending further suggests that a rapid mechanism that may precede auxin-induced phototropic elongation. The delay in phototropic bending observed in *CBC* mutants, along with the direct link to phot1 suggests that future research into this mechanism is a promising avenue to link perception with initiation of phototropic bending.

9) Lastly, exploration into the establishment and maintenance of the apical hook remains an interesting avenue of research. Auxin quantitations suggest that the free auxin levels in etiolated seedlings are not detectable. However, the presence of

oxIAA and IAA-Asp indicate that conjugation and oxidation of auxin may be important in establishing or maintaining asymmetric elongation at the apical hook. Hook opening upon application of exogenous auxin, in addition to the lack of detectable free IAA, suggests that DR5 signal in the concave region of the hook may be a better representation of high levels of auxin conjugation activity rather than an indication of high levels of free IAA. Further analysis of DR5 and DII-VENUS paired with direct quantitations suggests auxin reporters may not always reflect auxin levels. Further analysis of the use of and disparities with auxin reporters and auxin quantitations is of significant importance, as these issues have the potential to change our fundamental understanding of auxin transport and response.

Though many aspects of phototropism are well understood, there are still outstanding questions. The phot1-dependent CBC signaling pathway remains promising, as it could provide a link between blue light perception, rapid signaling, and growth events that promote early elongation. Further research into the nature of the interaction between phot1 and CBC in the hypocotyl is needed, particularly if CBC activity could provide a differential response between the lit and shaded sides of the hypocotyl. It is also not known what the downstream signaling targets of CBC may be in the hypocotyl that could alter cell expansion and the contribution of chloride ion channel activity during early phototropism events remains to be elucidated. A more complete understanding of the role of auxin and auxin conjugates in the hypocotyl is needed to understand how phototropic bending is initiated, fully achieved, and maintained in the hypocotyl.

Appendices

Appendix A. Differential epidermal auxin fluxes during root gravitropism.

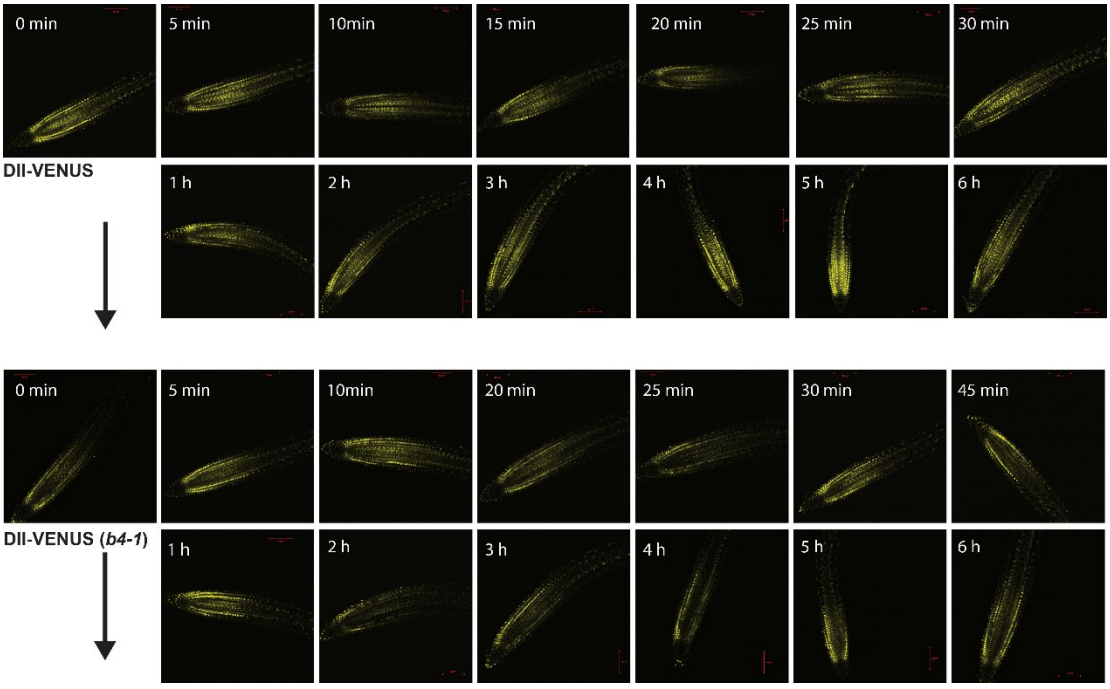

Fig. A1 DII-VENUS expression in 5.5 d seedling roots during gravitropism.

Confocal laser scanning microscopy supports that *abcb4* mutants accumulate auxin on the concave side of the root more quickly than WT. Differential DII-VENUS signals in *abcb4* were seen within 10-30 minutes, as opposed to wild type which occurred between 25-30 minutes of change in gravity vector. However, since *abcb4* root tips show greater waving compared to wild type (Terasaka *et al.*, 2005), more imaging is required establish an early response timeframe. Most interestingly, *abcb4* seedlings show a striking lag in rectification of the DII-VENUS signal in later

stages of gravitropism. Symmetric DII-VENUS signals returned to root tips after 3-4 hours of gravistimulation. However, in *abcb4* attenuation of the response was not observed until 6 hours. Imaging and bending kinetics suggest a role for ABCB4 in attenuation of the gravitropic response. Baseline accumulation of epidermal auxin in *abcb4* may explain the rapid gravitropic response.

This phenotype of faster response and apparent over-shooting is reminiscent of what is observed in *mdr1-101* open-air bending in etiolated and especially in light-treated seedlings (Christie *et al.*, 2011).

Appendix B. Role of ABCB21 during phototropism

The Arabidopsis ATP-BINDING CASSETTE Transporter ABCB21 Regulates Auxin Levels in Cotyledons, the Root Pericycle, and Leaves

Mark Jenness, Nicola Carraro, Candace Pritchard, Angus Murphy

For This publication I contributed phototropism assays for etiolated and light-treated seedlings.

ABCB21 Mobilizes Phototropic Auxin Supply from the Cotyledons

In seedlings, *proABCB21*:GUS signals are high at the base of the cotyledons, the petioles, and the cotyledonary node (Figures 4A–D) suggesting ABCB21 may function in mobilizing auxin from these tissues. To compare auxin transport in *abcb21* to wild type, [^{3}H]IAA was placed at the center of one cotyledon, then the hypocotyl and roots were collected after 2 h (Figure 4E). [3H] IAA transport in abcb21-2 is reduced by >50%. Transport in *abcb21-1* was also reduced, but was highly variable. Auxin transport from the shoot apex to the RSTZ was not different in either *abcb21* mutant (data not shown), which is consistent with the lack of *proABCB21*:GUS expression in the hypocotyl. The defects in mobilization of auxin from the cotyledons leads to a significant increase in cotyledon expansion in 5 d seedlings (Figure 4F), but only small differences in hypocotyl elongation (Figure 4G). Removal of the cotyledons in post-photomorphogenic seedlings reduces phototropic bending, suggesting cotyledon-derived auxin contributes to phototropic bending (Preuten et al., 2013). Similarly, phototropic bending was severely reduced in post-photomorphogenic *abcb21-2* seedlings (Figures 4H,I; Supplementary Movie 1). No difference was observed in etiolated seedlings.

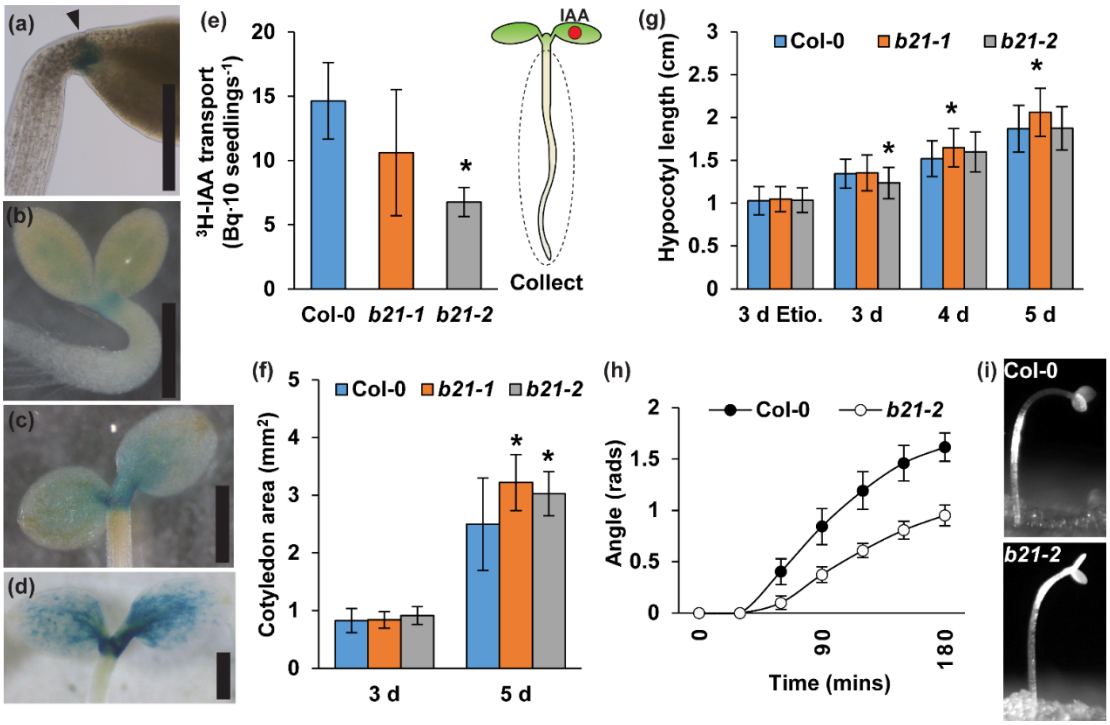

Figure 3. ABCB21 mediates cotyledon-hypocotyl auxin transport. (a) *proABCB21*:GUS expression at the base of petioles in 4d etiolated seedlings. (b-d) *proABCB21*:GUS expression in the petioles and cotyledonary node of (b) 1 d, (c) 3 d, and (d) 5 d light-grown seedlings. (e) Cotyledon-hypocotyl [3H] IAA transport in 5.5 d seedlings. Data shown are means ± SD (n = 3 pools of 12). * indicate statistical difference from Col-0 by Student's t test ($p<0.05$). (f) Hypocotyl length in *abcb21* seedlings. Data shown are means ± SD ($n > 45$ from 3 replicates). * indicate statistical difference from Col-0 by Student's t test ($p < 0.05$). (g) Cotyledon areas of 3 and 5 d light grown seedlings. Data shown are means ± SD ($25 \leq n \leq 32$). * indicate statistical difference from Col-0 by ANOVA $p < 0.001$, Dunnett's post-hoc $p < 0.05$. (h) Second positive Phototropic curvature of light-treated Col-0 and *abcb21-2* seedlings. Data shown are means ± SD (n=8 from 2 replicates). (i) Representative images of Col-0 and *abcb21-2* after phototropic bending for 3 h. Scale bar: (a-d) 500 µm.

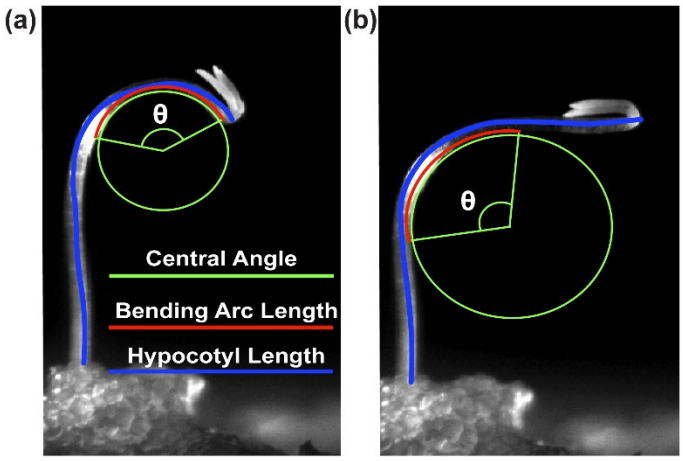

Figure S5. Description of measurement for phototropism assays. (a) Assays conducted in open-air demonstrate that seedlings bend along a circular arc, thus the central angle can be extrapolated from the arc length and area of the circle that fits into the arc (**a**). In this way a central angle is measured separately and elongation zone responses are separated from any events occurring in other areas of the hypocotyl (**b**). This is especially useful for mutants that show hypocotyl elongation differences, since there is no anchoring of the angle measurement to any assumed fixed hypocotyl point not part of the visible bending arc area. Instead the rotation of the seedlings about its own elongation zone can be exploited to isolate bending from elongation. Assuming all seedlings are selected for a uniform height, arc length can be used to describe the scope of the elongation zone along the hypocotyl (**a**). The extent to which this elongation zone migrates down the length of the hypocotyl can be quantitated as the ratio of bending zone to overall hypocotyl length (Arc/Length ratio) (**b,c**).

Works Cited

Abbas M, Alabadí D, Blázquez MA. **2013**. Differential growth at the apical hook: all roads lead to auxin. *Frontiers in plant science* **4**: 441.

Adamowski M, Friml J. **2015**. PIN-Dependent Auxin Transport: Action, Regulation, and Evolution. *The Plant Cell* **27**: 20–32.

Ahmad M. **2016**. Photocycle and signaling mechanisms of plant cryptochromes. *Current Opinion in Plant Biology* **33**: 108–115.

Babourina O, Godfrey L, Voltchanskii K. **2004**. Changes in ion fluxes during phototropic bending of etiolated oat coleoptiles. *Annals of Botany* **94**: 187–194.

Bailly A, Yang H, Martinoia E, Geisler M, Murphy AS. **2011**. Plant Lessons: Exploring ABCB Functionality Through Structural Modeling. *Frontiers in plant science* **2**: 108.

Barbosa IC, Schwechheimer C. **2014**. Dynamic control of auxin transport-dependent growth by AGCVIII protein kinases. *Current Opinion in Plant Biology* **22**: 108–115.

Benková E, Michniewicz M, Sauer M, Teichmann T, Seifertová D, Jürgens G, Friml J. **2003**. Local, Efflux-Dependent Auxin Gradients as a Common Module for Plant Organ Formation. *Cell* **115**: 591–602.

Bessire M, Borel S, Fabre G, Carraça L, Efremova N, Yephremov A, Cao Y, Jetter R, Jacquat A-C, Métraux J-P, *et al.* 2011. A member of the PLEIOTROPIC

DRUG RESISTANCE family of ATP binding cassette transporters is required for the formation of a functional cuticle in Arabidopsis. *The Plant cell* **23**: 1958–70.

Bhalerao RP, Eklöf J, Ljung K, Marchant A, Bennett M, Sandberg G. **2002**. Shoot-derived auxin is essential for early lateral root emergence in Arabidopsis seedlings. *The Plant Journal* **29**: 325–332.

Bielach A, Podlesáková K, Marhavy P, Duclercq J, Cuesta C, Müller B, Grunewald W, Tarkowski P, Benková E. **2012**. Spatiotemporal regulation of lateral root organogenesis in Arabidopsis by cytokinin. *The Plant cell* **24**: 3967–81.

Bisgrove SR. **2008**. The roles of microtubules in tropisms. *Plant Science* **175**: 747–755.

Blakeslee JJ, Bandyopadhyay A, Lee OR, Mravec J, Titapiwatanakun B, Sauer M, Makam SN, Cheng Y, Bouchard R, Adamec J, *et al.* 2007. Interactions among PIN-FORMED and P-glycoprotein auxin transporters in Arabidopsis. *The Plant cell* **19**: 131–47.

Blilou I, Xu J, Wildwater M, Willemsen V, Paponov I, Friml J, Heidstra R, Aida M, Palme K, Scheres B. **2005**. The PIN auxin efflux facilitator network controls growth and patterning in Arabidopsis roots. *Nature* **433**: 39–44.

Briggs WR, Christie JM. **2002**. Phototropins 1 and 2: versatile plant blue-light receptors. *Trends in Plant Science* **7**: 204–210.

Briggs WR, Christie JM, Salomon M. **2001**. Phototropins: a new family of flavin-

binding blue light receptors in plants. *Antioxidants & redox signaling* **3**: 775–88.

Brunoud G, Wells DM, Oliva M, Larrieu A, Mirabet V, Burrow AH, Beeckman T, Kepinski S, Traas J, Bennett MJ, *et al.* 2012. A novel sensor to map auxin response and distribution at high spatio-temporal resolution. *Nature* **482**: 103–6.

Chen M, Chory J. **2011**. Phytochrome signaling mechanisms and the control of plant development. *Trends in Cell Biology* **21**: 664–671.

Cho MH, Spalding EP. **1996**. An anion channel in Arabidopsis hypocotyls activated by blue light. *Proceedings of the National Academy of Sciences of the United States of America* **93**: 8134–8.

Cho H-Y, Tseng T-S, Kaiserli E, Sullivan S, Christie JM, Briggs WR. **2007**. Physiological roles of the light, oxygen, or voltage domains of phototropin 1 and phototropin 2 in Arabidopsis. *Plant physiology* **143**: 517–29.

Christie JM. **2007**. Phototropin Blue-Light Receptors. *Annual Review of Plant Biology* **58**: 21–45.

Christie JM, Murphy AS. **2013**. Shoot phototropism in higher plants: new light through old concepts. *American journal of botany* **100**: 35–46.

Christie JM, Reymond P, Powell GK, Bernasconi P, Raibekas AA, Liscum E, Briggs WR. **1998**. Arabidopsis NPH1: a flavoprotein with the properties of a photoreceptor for phototropism. *Science (New York, N.Y.)* **282**: 1698–701.

Christie JM, Swartz TE, Bogomolni RA, Briggs WR. **2002**. Phototropin LOV

domains exhibit distinct roles in regulating photoreceptor function. *The Plant Journal* **32**: 205–219.

Christie JM, Yang H, Richter GL, Sullivan S, Thomson CE, Lin J, Titapiwatanakun B, Ennis M, Kaiserli E, Lee OR, *et al.* 2011. phot1 inhibition of ABCB19 primes lateral auxin fluxes in the shoot apex required for phototropism. (O Leyser, Ed.). *PLoS biology* **9**: e1001076.

Darwin C, Darwin F. **1880**. *The Power of Movement in Plants*. London: John Murray Publishers.

DeLille JM, Sehnke PC, Ferl RJ. **2001**. The Arabidopsis 14-3-3 Family of Signaling Regulators. *Plant Physiology* **126**: 35–38.

Demarsy E, Schepens I, Okajima K, Hersch M, Bergmann S, Christie J, Shimazaki K, Tokutomi S, Fankhauser C. **2012**. Phytochrome Kinase Substrate 4 is phosphorylated by the phototropin 1 photoreceptor. *The EMBO Journal* **31**: 3457–3467.

DeWitt ND, Hong B, Sussman MR, Harper JF. **1996**. Targeting of two Arabidopsis H(+)-ATPase isoforms to the plasma membrane. *Plant physiology* **112**: 833–44.

Dhonukshe P, Huang F, Galvan-Ampudia CS, Mahonen AP, Kleine-Vehn J, Xu J, Quint A, Prasad K, Friml J, Scheres B, *et al.* 2010. Plasma membrane-bound AGC3 kinases phosphorylate PIN auxin carriers at TPRXS(N/S) motifs to direct apical PIN recycling. *Development* **137**: 3245–3255.

Ding Z, Galván-Ampudia CS, Demarsy E, Łangowski Ł, Kleine-Vehn J, Fan Y, Morita MT, Tasaka M, Fankhauser C, Offringa R, *et al.* 2011. Light-mediated polarization of the PIN3 auxin transporter for the phototropic response in Arabidopsis. *Nature cell biology* **13**: 447–52.

Fankhauser C, Christie JM. **2015a**. Plant Phototropic Growth. *Current Biology* **25**: R384–R389.

Fankhauser C, Christie JM. **2015b**. Plant Phototropic Growth. *Current Biology* **25**: R384–R389.

Feraru E, Feraru MI, Barbez E, Waidmann S, Sun L, Gaidora A, Kleine-Vehn J. **2019**. PILS6 is a temperature-sensitive regulator of nuclear auxin input and organ growth in Arabidopsis thaliana. *Proceedings of the National Academy of Sciences of the United States of America* **116**: 3893–3898.

Folta KM, Lieg EJ, Durham T, Spalding EP. **2003**. Primary Inhibition of Hypocotyl Growth and Phototropism Depend Differently on Phototropin-Mediated Increases in Cytoplasmic Calcium Induced by Blue Light 1.

Franklin KA, Quail PH. **2010**. Phytochrome functions in Arabidopsis development. *Journal of Experimental Botany* **61**: 11–24.

Friml J. **2003**. Auxin transport — shaping the plant. *Current Opinion in Plant Biology* **6**: 7–12.

Friml J, Benková E, Blilou I, Wisniewska J, Hamann T, Ljung K, Woody S,

Sandberg G, Scheres B, Jürgens G, *et al.* 2002a. AtPIN4 Mediates Sink-Driven Auxin Gradients and Root Patterning in Arabidopsis. *Cell* **108**: 661–673.

Friml J, Vieten A, Sauer M, Weijers D, Schwarz H, Hamann T, Offringa R, Jü rgens G. **2003**. *Efflux-dependent auxin gradients establish the apical-basal axis of Arabidopsis*.

Friml J, Wiśniewska J, Benková E, Mendgen K, Palme K. **2002b**. Lateral relocation of auxin efflux regulator PIN3 mediates tropism in Arabidopsis. *Nature* **415**: 806–9.

Fuglsang AT, Guo Y, Cuin TA, Qiu Q, Song C, Kristiansen KA, Bych K, Schulz A, Shabala S, Schumaker KS, *et al.* 2007. *Arabidopsis* Protein Kinase PKS5 Inhibits the Plasma Membrane H^+-ATPase by Preventing Interaction with 14-3-3 Protein. *The Plant Cell* **19**: 1617–1634.

Furutani M, Nakano Y, Tasaka M. **2014**. MAB4-induced auxin sink generates local auxin gradients in Arabidopsis organ formation. *Proceedings of the National Academy of Sciences of the United States of America*: 1316109111-.

Furutani M, Sakamoto N, Yoshida S, Kajiwara T, Robert HS, Friml J, Tasaka M. **2011**. Polar-localized NPH3-like proteins regulate polarity and endocytosis of PIN-FORMED auxin efflux carriers. *Development (Cambridge, England)* **138**: 2069–78.

Furutani I, Watanabe Y, Prieto R, Masukawa M, Suzuki K, Naoi K, Thitamadee S, Shikanai T, Hashimoto T. **2000**. The SPIRAL genes are required for directional

control of cell elongation in Aarabidopsis thaliana. *Development* **127**: 4443–4453.

Gallego-Bartolomé J, Arana M V, Vandenbussche F, Zádníková P, Minguet EG, Guardiola V, Van Der Straeten D, Benkova E, Alabadí D, Blázquez MA. **2011**. Hierarchy of hormone action controlling apical hook development in Arabidopsis. *The Plant journal : for cell and molecular biology* **67**: 622–34.

Gälweiler L. **1998**. Regulation of Polar Auxin Transport by AtPIN1 in Arabidopsis Vascular Tissue. *Science* **282**: 2226–2230.

Geisler M, Blakeslee JJ, Bouchard R, Lee OR, Vincenzetti V, Bandyopadhyay A, Titapiwatanakun B, Peer WA, Bailly A, Richards EL, *et al.* 2005. Cellular efflux of auxin catalyzed by the Arabidopsis MDR/PGP transporter AtPGP1. *The Plant journal : for cell and molecular biology* **44**: 179–94.

Gendreau E, Traas J, Desnos T, Grandjean O, Caboche M, Höfte H. **1997**. Cellular basis of hypocotyl growth in Arabidopsis thaliana. *Plant physiology* **114**: 295–305.

Gjetting KSK, Ytting CK, Schulz A, Fuglsang AT. **2012**. Live imaging of intra- and extracellular pH in plants using pHusion, a novel genetically encoded biosensor. *Journal of experimental botany* **63**: 3207–18.

Goyal A, Karayekov E, Galvão VC, Ren H, Casal JJ, Fankhauser C. **2016**. Shade Promotes Phototropism through Phytochrome B-Controlled Auxin Production. *Current Biology* **26**: 3280–3287.

Goyal A, Szarzynska B, Fankhauser C. **2013**. Phototropism: at the crossroads of light-signaling pathways. *Trends in Plant Science* **18**: 393–401.

Guzmán P, Ecker JR. **1990**. Exploiting the triple response of Arabidopsis to identify ethylene-related mutants. *The Plant cell* **2**: 513–23.

Haga K, Frank L, Kimura T, Schwechheimer C, Sakai T. **2018**. Roles of AGCVIII Kinases in the Hypocotyl Phototropism of Arabidopsis Seedlings. *Plant and Cell Physiology* **59**: 1060–1071.

Haga K, Kimura T. **2019**. Physiological Characterization of Phototropism in Arabidopsis Seedlings. Humana Press, New York, NY, 3–17.

Haga K, Sakai T. **2012**. PIN auxin efflux carriers are necessary for pulse-induced but not continuous light-induced phototropism in Arabidopsis. *Plant physiology* **160**: 763–76.

Haga K, Sakai T. **2013**. Differential roles of auxin efflux carrier PIN proteins in hypocotyl phototropism of etiolated Arabidopsis seedlings depend on the direction of light stimulus. *Plant signaling & behavior* **8**: e22556.

Han X, Hyun TK, Zhang M, Kumar R, Koh E, Kang B-H, Lucas WJ, Kim J-Y. **2014**. Auxin-callose-mediated plasmodesmal gating is essential for tropic auxin gradient formation and signaling. *Developmental cell* **28**: 132–46.

Harada A, Sakai T, Okada K. **2003**. Phot1 and phot2 mediate blue light-induced transient increases in cytosolic Ca2+ differently in Arabidopsis leaves. *Proceedings*

of the National Academy of Sciences of the United States of America **100**: 8583–8.

Haruta M, Burch HL, Nelson RB, Barrett-Wilt G, Kline KG, Mohsin SB, Young JC, Otegui MS, Sussman MR. **2010**. Molecular characterization of mutant Arabidopsis plants with reduced plasma membrane proton pump activity. *The Journal of biological chemistry* **285**: 17918–29.

Heijde M, Ulm R. **2013**. Reversion of the Arabidopsis UV-B photoreceptor UVR8 to the homodimeric ground state. *Proceedings of the National Academy of Sciences of the United States of America* **110**: 1113–8.

Henrichs S, Wang B, Fukao Y, Zhu J, Charrier L, Bailly A, Oehring SC, Linnert M, Weiwad M, Endler A, *et al.* 2012. Regulation of ABCB1/PGP1-catalysed auxin transport by linker phosphorylation. *The EMBO journal* **31**: 2965–80.

Hiyama A, Takemiya A, Munemasa S, Okuma E, Sugiyama N, Tada Y, Murata Y, Shimazaki K. **2017**. Blue light and CO2 signals converge to regulate light-induced stomatal opening. *Nature Communications* **8**: 1284.

Hohm T, Demarsy E, Quan C, Allenbach Petrolati L, Preuten T, Vernoux T, Bergmann S, Fankhauser C. **2014**. Plasma membrane H^+ -ATPase regulation is required for auxin gradient formation preceding phototropic growth. *Molecular systems biology* **10**: 751.

Hohm T, Preuten T, Fankhauser C. **2013**. Phototropism: translating light into directional growth. *American journal of botany* **100**: 47–59.

Hornitschek P, Kohnen M V., Lorrain S, Rougemont J, Ljung K, López-Vidriero I, Franco-Zorrilla JM, Solano R, Trevisan M, Pradervand S, *et al.* 2012. Phytochrome interacting factors 4 and 5 control seedling growth in changing light conditions by directly controlling auxin signaling. *The Plant Journal* **71**: 699–711.

Hu. **1997**. Arabidopsis NPH1: A Protein Kinase with a Putative Redox-Sensing Domain. *Science* **278**: 2120–2123.

Huang F, Zago MK, Abas L, van Marion A, Galván-Ampudia CS, Offringa R. **2010**. Phosphorylation of conserved PIN motifs directs Arabidopsis PIN1 polarity and auxin transport. *The Plant cell* **22**: 1129–42.

Ishida T, Kaneko Y, Iwano M, Hashimoto T. **2007**. Helical microtubule arrays in a collection of twisting tubulin mutants of Arabidopsis thaliana. *Proceedings of the National Academy of Sciences of the United States of America* **104**: 8544–9.

Jacq A, Pernot C, Martinez Y, Domergue F, Payré B, Jamet E, Burlat V, Pacquit VB. **2017**. The Arabidopsis Lipid Transfer Protein 2 (AtLTP2) Is Involved in Cuticle-Cell Wall Interface Integrity and in Etiolated Hypocotyl Permeability. *Frontiers in Plant Science* **8**: 263.

Jang I-C, Henriques R, Seo HS, Nagatani A, Chua N-H. **2010**. Arabidopsis PHYTOCHROME INTERACTING FACTOR proteins promote phytochrome B polyubiquitination by COP1 E3 ligase in the nucleus. *The Plant cell* **22**: 2370–83.

Janoudi A, Poff KL. **1990**. A common fluence threshold for first positive and second

positive phototropism in Arabidopsis thaliana. *Plant physiology* **94**: 1605–8.

Jenness MK, Carraro N, Pritchard CA, Murphy AS. **2019**. The Arabidopsis ATP-BINDING CASSETTE Transporter ABCB21 Regulates Auxin Levels in Cotyledons, the Root Pericycle, and Leaves. *Frontiers in Plant Science* **10**: 806.

Jenness MK, Murphy AS. **2014**. Evolution of Transport Directionality in ABCBs. Springer, Cham, 271–285.

Kaiserli E, Sullivan S, Jones MA, Feeney KA, Christie JM. **2009**. Domain swapping to assess the mechanistic basis of Arabidopsis phototropin 1 receptor kinase activation and endocytosis by blue light. *The Plant cell* **21**: 3226–44.

Kami C, Allenbach L, Zourelidou M, Ljung K, Ed F, Sch€ Utz E, Isono E, Watahiki MK, Yamamoto KT, Schwechheimer C, *et al.* 2013. Reduced phototropism in pks mutants may be due to altered auxin-regulated gene expression or reduced lateral auxin transport.

Kami C, Allenbach L, Zourelidou M, Ljung K, Schütz F, Isono E, Watahiki MK, Yamamoto KT, Schwechheimer C, Fankhauser C. **2014**. Reduced phototropism in *pks* mutants may be due to altered auxin-regulated gene expression or reduced lateral auxin transport. *The Plant Journal* **77**: 393–403.

Kang BG, Burg SP. **1974**. Red light enhancement of the phototropic response of etiolated pea stems. *Plant physiology* **53**: 445–8.

Kasahara M, Swartz TE, Olney MA, Onodera A, Mochizuki N, Fukuzawa H,

Asamizu E, Tabata S, Kanegae H, Takano M, *et al.* 2002. Photochemical properties of the flavin mononucleotide-binding domains of the phototropins from Arabidopsis, rice, and Chlamydomonas reinhardtii. *Plant physiology* **129**: 762–73.

Kim J-I, Park J-E, Zarate X, Song P-S. **2005**. Phytochrome phosphorylation in plant light signaling. *Photochemical & Photobiological Sciences* **4**: 681.

Kinoshita T, Shimazaki K i. **1999**. Blue light activates the plasma membrane H+-ATPase by phosphorylation of the C-terminus in stomatal guard cells. *The EMBO Journal* **18**: 5548–5558.

Kohchi T, Mukougawa K, Frankenberg N, Masuda M, Yokota A, Lagarias JC. **2001**. The Arabidopsis HY2 Gene Encodes Phytochromobilin Synthase, a Ferredoxin-Dependent Biliverdin Reductase. *THE PLANT CELL ONLINE* **13**: 425–436.

Kono A, Umeda-Hara C, Adachi S, Nagata N, Konomi M, Nakagawa T, Uchimiya H, Umeda M. **2007**. The Arabidopsis D-type cyclin CYCD4 controls cell division in the stomatal lineage of the hypocotyl epidermis. *The Plant cell* **19**: 1265–77.

Krecek P, Skupa P, Libus J, Naramoto S, Tejos R, Friml J, Zazímalová E. **2009**. The PIN-FORMED (PIN) protein family of auxin transporters. *Genome biology* **10**: 249.

Le J, Vandenbussche F, Cnodder T, Straeten D, Verbelen J-P. **2005**. Cell Elongation and Microtubule Behavior in the Arabidopsis Hypocotyl: Responses to

Ethylene and Auxin. *Journal of Plant Growth Regulation* **24**: 166–178.

Lee J-Y, Wang X, Cui W, Sager R, Modla S, Czymmek K, Zybaliov B, van Wijk K, Zhang C, Lu H, *et al.* 2011. A plasmodesmata-localized protein mediates crosstalk between cell-to-cell communication and innate immunity in Arabidopsis. *The Plant cell* **23**: 3353–73.

Lehman A, Black R, Ecker JR. **1996**. HOOKLESS1, an ethylene response gene, is required for differential cell elongation in the Arabidopsis hypocotyl. *Cell* **85**: 183–94.

Li Y, Hagen G, Guilfoyle TJ. **1991**. An Auxin-Responsive Promoter Is Differentially Induced by Auxin Gradients during Tropisms. *The Plant Cell* **3**: 1167–1175.

Lin R, Wang H. **2005a**. Two Homologous ATP-Binding Cassette Transporter Proteins, AtMDR1 and AtPGP1, Regulate Arabidopsis Photomorphogenesis and Root Development by Mediating Polar Auxin Transport. *Plant Physiology* **138**: 949–964.

Lin R, Wang H. **2005b**. Two homologous ATP-binding cassette transporter proteins, AtMDR1 and AtPGP1, regulate Arabidopsis photomorphogenesis and root development by mediating polar auxin transport. *Plant physiology* **138**: 949–64.

Lindeboom JJ, Nakamura M, Hibbel A, Gutierrez R, Ketelaar T, Emons AMC, Bela M, Kirik V, Ehrhardt DW. **2013**. A Mechanism for Reorientation of Cortical Microtubule Arrays Driven by Microtubule Severing. *Science*.

Liscum E. **2016**. Blue Light-Induced Intracellular Movement of Phototropins: Functional Relevance or Red Herring? *Frontiers in plant science* **7**: 827.

Liscum E, Briggs WR. **1995**. Mutations in the NPH1 locus of Arabidopsis disrupt the perception of phototropic stimuli. *The Plant cell* **7**: 473–85.

Lloyd C. **2002**. Helical Microtubule Arrays and Spiral Growth. *THE PLANT CELL ONLINE* **14**: 2319–2324.

Luptovčiak I, Komis G, Takáč T, Ovečka M, Šamaj J. **2017**. Katanin: A Sword Cutting Microtubules for Cellular, Developmental, and Physiological Purposes. *Frontiers in Plant Science* **8**: 1982.

Ma Q, Sun J, Mao T. **2016**. Microtubule bundling plays a role in ethylene-mediated cortical microtubule reorientation in etiolated Arabidopsis hypocotyls. *Journal of cell science* **129**: 2043–51.

Ma Q, Wang X, Sun J, Mao T. **2018**. Coordinated Regulation of Hypocotyl Cell Elongation by Light and Ethylene through a Microtubule Destabilizing Protein. *Plant physiology* **176**: 678–690.

Marin E, Jouannet V, Herz A, Lokerse AS, Weijers D, Vaucheret H, Nussaume L, Crespi MD, Maizel A. **2010**. miR390, Arabidopsis TAS3 tasiRNAs, and their AUXIN RESPONSE FACTOR targets define an autoregulatory network quantitatively regulating lateral root growth. *The Plant cell* **22**: 1104–17.

Mazzella MA, Casal JJ, Muschietti JP, Fox AR. **2014**. Hormonal networks

involved in apical hook development in darkness and their response to light. *Frontiers in Plant Science* **5**: 52.

Montgomery BL, Lagarias JC. **2002**. Phytochrome ancestry: sensors of bilins and light. *Trends in plant science* **7**: 357–66.

Motchoulski A. **1999**. Arabidopsis NPH3: A NPH1 Photoreceptor-Interacting Protein Essential for Phototropism. *Science* **286**: 961–964.

Mravec J, Kubes M, Bielach A, Gaykova V, Petrásek J, Skůpa P, Chand S, Benková E, Zazímalová E, Friml J. **2008**. Interaction of PIN and PGP transport mechanisms in auxin distribution-dependent development. *Development (Cambridge, England)* **135**: 3345–54.

Murphy AS, Hoogner KR, Peer WA, Taiz L. **2002**. Identification, Purification, and Molecular Cloning of N-1-Naphthylphthalmic Acid-Binding Plasma Membrane-Associated Aminopeptidases from Arabidopsis. *Plant Physiology* **128**: 935–950.

Nadeau JA, Sack FD. **2002**. Stomatal development in Arabidopsis. *The arabidopsis book* **1**: e0066.

Nakajima K, Furutani I, Tachimoto H, Matsubara H, Hashimoto T. **2004**. SPIRAL1 encodes a plant-specific microtubule-localized protein required for directional control of rapidly expanding Arabidopsis cells. *The Plant cell* **16**: 1178–90.

Neff MM, Van Volkenburgh E. **1994**. Light-Stimulated Cotyledon Expansion in

Arabidopsis Seedl ings' The Role of Phytochrome B. *Plant Physiol*.

Noh B, Bandyopadhyay A, Peer WA, Spalding EP, Murphy AS. **2003**. Enhanced gravi- and phototropism in plant mdr mutants mislocalizing the auxin efflux protein PIN1. *Nature* **423**: 999–1002.

Noh B, Murphy AS, Spalding EP. **2001**. Multidrug Resistance-like Genes of Arabidopsis Required for Auxin Transport and Auxin-Mediated Development. *PLANT CELL* **13**: 2441–2454.

Orbović V, Poff KL. **1997**. Interaction of light and gravitropism with nutation of hypocotyls of Arabidopsis thaliana seedlings. *Plant Growth Regulation* **23**: 141–146.

Parks BM, Quail PH, Hangarter RP. **1996**. Phytochrome A regulates red-light induction of phototropic enhancement in Arabidopsis. *Plant physiology* **110**: 155–62.

Peer WA, Bandyopadhyay A, Blakeslee JJ, Makam SN, Chen RJ, Masson PH, Murphy AS. **2004**. Variation in expression and protein localization of the PIN family of auxin efflux facilitator proteins in flavonoid mutants with altered auxin transport in Arabidopsis thaliana. *The Plant cell* **16**: 1898–911.

Peer WA, Blakeslee JJ, Yang H, Murphy AS. **2011**. Seven things we think we know about auxin transport. *Molecular plant* **4**: 487–504.

Peer WA, Jenness MK, Murphy AS. **2014**. Measure for measure: determining, inferring and guessing auxin gradients at the root tip. *Physiologia Plantarum* **151**: 97–111.

Petrásek J, Friml J. **2009**. Auxin transport routes in plant development. *Development (Cambridge, England)* **136**: 2675–88.

Preuten T, Blackwood L, Christie JM, Fankhauser C. **2015**. Lipid anchoring of Arabidopsis phototropin 1 to assess the functional significance of receptor internalization: should I stay or should I go? *New Phytologist* **206**: 1038–1050.

Preuten T, Hohm T, Bergmann S, Fankhauser C. **2013**. *Defining the Site of Light Perception and Initiation of Phototropism in Arabidopsis*.

Quail PH, Boylan MT, Parks BM, Short TW, Xu Y, Wagner D. **1995**. *Phytochromes: Photosensory Perception and Signal Transduction*.

Rakusová H, Gallego-Bartolomé J, Vanstraelen M, Robert HS, Alabadí D, Blázquez MA, Benková E, Friml J. **2011**. Polarization of PIN3-dependent auxin transport for hypocotyl gravitropic response in Arabidopsis thaliana. *The Plant journal : for cell and molecular biology* **67**: 817–26.

Rashotte AM, Brady SR, Reed RC, Ante SJ, Muday GK. **2000**. Basipetal auxin transport is required for gravitropism in roots of Arabidopsis. *Plant physiology* **122**: 481–90.

Raven JA. **1975**. Transport of Indoleacetic Acid in Plant Cells in Relation to pH and Electrical Potential Gradients, and its Significance for Polar IAA Transport. *New Phytologist* **74**: 163–172.

Ren H, Gray WM. **2015**. SAUR Proteins as Effectors of Hormonal and

Environmental Signals in Plant Growth. *Molecular Plant* **8**: 1153–1164.

Ren H, Park MY, Spartz AK, Wong JH, Gray WM. **2018**. A subset of plasma membrane-localized PP2C.D phosphatases negatively regulate SAUR-mediated cell expansion in Arabidopsis (GK Muday, Ed.). *PLOS Genetics* **14**: e1007455.

Rizzini L, Favory J-J, Cloix C, Faggionato D, O'Hara A, Kaiserli E, Baumeister R, Schäfer E, Nagy F, Jenkins GI, *et al.* 2011. Perception of UV-B by the Arabidopsis UVR8 protein. *Science (New York, N.Y.)* **332**: 103–6.

Rubery PH, Sheldrake AR. **1974**. Carrier-mediated auxin transport. *Planta* **118**: 101–121.

Sakai T. **2019**. Determination of Auxin Flow During Phototropic Responses Using Fluorescent Auxin Analogs. Methods in molecular biology (Clifton, N.J.).157–163.

Sakai T, Kagawa T, Kasahara M, Swartz TE, Christie JM, Briggs WR, Wada M, Okada K. **2001**. Arabidopsis nph1 and npl1: blue light receptors that mediate both phototropism and chloroplast relocation. *Proceedings of the National Academy of Sciences of the United States of America* **98**: 6969–74.

Sakamoto K. **2002**. Cellular and Subcellular Localization of Phototropin 1. *THE PLANT CELL ONLINE* **14**: 1723–1735.

Schindelin J, Arganda-Carreras I, Frise E, Kaynig V, Longair M, Pietzsch T, Preibisch S, Rueden C, Saalfeld S, Schmid B, *et al.* 2012. Fiji: an open-source platform for biological-image analysis. *Nature methods* **9**: 676–82.

Schneider CA, Rasband WS, Eliceiri KW. **2012**. NIH Image to ImageJ: 25 years of image analysis. *Nature Methods* **9**: 671–675.

Schwark A, Schierle J. **1992**. Interaction of Ethylene and Auxin in the Regulation of Hook Growth I The Role of Auxin in Different Growing Regions of the Hypocotyl Hook of Phaseolus vulgaris. *Journal of Plant Physiology* **140**: 562–570.

Simon S, Skůpa P, Viaene T, Zwiewka M, Tejos R, Klíma P, Čarná M, Rolčík J, De Rycke R, Moreno I, *et al.* 2016. PIN6 auxin transporter at endoplasmic reticulum and plasma membrane mediates auxin homeostasis and organogenesis in Arabidopsis. *New Phytologist* **211**: 65–74.

Spalding EP. **2000**. Ion channels and the transduction of light signals. *Plant, Cell and Environment* **23**: 665–674.

Spartz AK, Lee SH, Wenger JP, Gonzalez N, Itoh H, Inzé D, Peer WA, Murphy AS, Overvoorde PJ, Gray WM. **2012**. The SAUR19 subfamily of SMALL AUXIN UP RNA genes promote cell expansion. *The Plant journal : for cell and molecular biology* **70**: 978–90.

Stolarz M. **2009**. Circumnutation as a visible plant action and reaction: physiological, cellular and molecular basis for circumnutations. *Plant signaling & behavior* **4**: 380–7.

Stone BB, Stowe-Evans EL, Harper RM, Celaya RB, Ljung K, Sandberg G, Liscum E. **2008a**. Disruptions in AUX1-Dependent Auxin Influx Alter Hypocotyl Phototropism in Arabidopsis. *Molecular Plant* **1**: 129–144.

Stone BB, Stowe-Evans EL, Harper RM, Celaya RB, Ljung K, Sandberg G, Liscum E. **2008b**. Disruptions in AUX1-dependent auxin influx alter hypocotyl phototropism in Arabidopsis. *Molecular plant* **1**: 129–44.

Suetsugu N, Yamada N, Kagawa T, Yonekura H, Uyeda TQP, Kadota A, Wada M. **2010**. Two kinesin-like proteins mediate actin-based chloroplast movement in Arabidopsis thaliana. *Proceedings of the National Academy of Sciences* **107**: 8860–8865.

Sullivan S, Hart JE, Rasch P, Walker CH, Christie JM. **2016a**. Phytochrome A Mediates Blue-Light Enhancement of Second-Positive Phototropism in Arabidopsis. *Frontiers in Plant Science* **7**: 290.

Sullivan S, Kharshiing E, Laird J, Sakai T, Christie JM. **2019**. Deetiolation Enhances Phototropism by Modulating NON-PHOTOTROPIC HYPOCOTYL3 Phosphorylation Status. *Plant Physiology* **180**: 1119–1131.

Sullivan S, Takemiya A, Kharshiing E, Cloix C, Shimazaki K, Christie JM. **2016b**. Functional characterization of Arabidopsis phototropin 1 in the hypocotyl apex. *The Plant Journal* **88**: 907–920.

Sullivan S, Thomson CE, Kaiserli E, Christie JM. **2009**. Interaction specificity of Arabidopsis 14-3-3 proteins with phototropin receptor kinases. *FEBS letters* **583**: 2187–93.

Swarup R, Péret B. **2012**. AUX/LAX family of auxin influx carriers-an overview. *Frontiers in plant science* **3**: 225.

Takahashi K, Hayashi K, Kinoshita T. **2012**. Auxin Activates the Plasma Membrane H + -ATPase by Phosphorylation during Hypocotyl Elongation in Arabidopsis . *Plant Physiology* **159**: 632–641.

Terasaka K, Blakeslee JJ, Titapiwatanakun B, Peer WA, Bandyopadhyay A, Makam SN, Lee OR, Richards EL, Murphy AS, Sato F, *et al.* 2005. PGP4, an ATP Binding Cassette P-Glycoprotein, Catalyzes Auxin Transport in Arabidopsis thaliana Roots . *The Plant Cell* **17**: 2922–2939.

Thitamadee S, Tuchihara K, Hashimoto T. **2002**. Microtubule basis for left-handed helical growth in Arabidopsis. *Nature* **417**: 193–6.

Tilbrook K, Arongaus AB, Binkert M, Heijde M, Yin R, Ulm R. **2013**. The UVR8 UV-B Photoreceptor: Perception, Signaling and Response. *The arabidopsis book* **11**: e0164.

Titapiwatanakun B, Blakeslee JJ, Bandyopadhyay A, Yang H, Mravec J, Sauer M, Cheng Y, Adamec J, Nagashima A, Geisler M, *et al.* 2009. ABCB19/PGP19 stabilises PIN1 in membrane microdomains in Arabidopsis. *The Plant journal : for cell and molecular biology* **57**: 27–44.

Ugartechea-Chirino Y, Swarup R, Swarup K, Péret B, Whitworth M, Bennett M, Bougourd S. **2010**. The AUX1 LAX family of auxin influx carriers is required for the establishment of embryonic root cell organization in Arabidopsis thaliana. *Annals of botany* **105**: 277–89.

Ulmasov T, Murfett J, Hagen G, Guilfoyle TJ. **1997**. Aux/IAA proteins repress

expression of reporter genes containing natural and highly active synthetic auxin response elements. *The Plant cell* **9**: 1963–71.

Vandenbussche F, Petrásek J, Zádníková P, Hoyerová K, Pesek B, Raz V, Swarup R, Bennett M, Zazímalová E, Benková E, *et al.* 2010. The auxin influx carriers AUX1 and LAX3 are involved in auxin-ethylene interactions during apical hook development in Arabidopsis thaliana seedlings. *Development (Cambridge, England)* **137**: 597–606.

Vandenbussche F, Tilbrook K, Fierro AC, Marchal K, Poelman D, Van Der Straeten D, Ulm R. **2014**. Photoreceptor-Mediated Bending towards UV-B in Arabidopsis. *Molecular Plant* **7**: 1041–1052.

Vanneste S, Friml J. **2009**. Auxin: a trigger for change in plant development. *Cell* **136**: 1005–16.

Vieten A, Vanneste S, Wisniewska J, Benková E, Benjamins R, Beeckman T, Luschnig C, Friml J. **2005**. Functional redundancy of PIN proteins is accompanied by auxin-dependent cross-regulation of PIN expression. *Development (Cambridge, England)* **132**: 4521–31.

Volkov AG, Dunkley TC, Labady AJ, Brown CL. **2005**. Phototropism and electrified interfaces in green plants. *Electrochimica Acta* **50**: 4241–4247.

Wan Y-L, Eisinger W, Ehrhardt D, Kubitscheck U, Baluska F, Briggs W. **2008**. The Subcellular Localization and Blue-Light-Induced Movement of Phototropin 1-GFP in Etiolated Seedlings of Arabidopsis thalianaw. *Molecular Plant* **1**: 103–117.

Wan Y, Jasik J, Wang L, Hao H, Volkmann D, Menzel D, Mancuso S, Baluška F, Lin J. **2012**. The signal transducer NPH3 integrates the phototropin1 photosensor with PIN2-based polar auxin transport in Arabidopsis root phototropism. *The Plant cell* **24**: 551–65.

Wang B, Henrichs S, Geisler M. **2012**. The AGC kinase, PINOID, blocks interactive ABCB/PIN auxin transport. *Plant signaling & behavior* **7**: 1515–7.

Went FW, Thimann K V. 1937. Phytohormones.

Willige BC, Ahlers S, Zourelidou M, Barbosa ICR, Demarsy E, Trevisan M, Davis P a, Roelfsema MRG, Hangarter R, Fankhauser C, *et al.* 2013. D6PK AGCVIII Kinases Are Required for Auxin Transport and Phototropic Hypocotyl Bending in Arabidopsis. *The Plant cell* **25**: 1674–88.

Wu G, Cameron JN, Ljung K, Spalding EP. **2010a**. A role for ABCB19-mediated polar auxin transport in seedling photomorphogenesis mediated by cryptochrome 1 and phytochrome B. *The Plant journal : for cell and molecular biology* **62**: 179–91.

Wu G, Otegui MS, Spalding EP. **2010b**. The ER-localized TWD1 immunophilin is necessary for localization of multidrug resistance-like proteins required for polar auxin transport in Arabidopsis roots. *The Plant cell* **22**: 3295–304.

Yang Z. **2008**. Cell polarity signaling in Arabidopsis. *Annual review of cell and developmental biology* **24**: 551–75.

Yang H, Murphy AS. **2009**. Functional expression and characterization of

Arabidopsis ABCB, AUX 1 and PIN auxin transporters in Schizosaccharomyces pombe. *The Plant journal : for cell and molecular biology* **59**: 179–91.

Zádníková P, Petrásek J, Marhavy P, Raz V, Vandenbussche F, Ding Z, Schwarzerová K, Morita MT, Tasaka M, Hejátko J, *et al.* 2010. Role of PIN-mediated auxin efflux in apical hook development of Arabidopsis thaliana. *Development (Cambridge, England)* **137**: 607–17.

Žádníková P, Wabnik K, Abuzeineh A, Gallemi M, Van Der Straeten D, Smith RS, Inzé D, Friml J, Prusinkiewicz P, Benková E. **2016**. A Model of Differential Growth-Guided Apical Hook Formation in Plants. *The Plant Cell* **28**: 2464–2477.

Zazímalová E, Murphy AS, Yang H, Hoyerová K, Hosek P. **2010**. Auxin transporters--why so many? *Cold Spring Harbor perspectives in biology* **2**: a001552.

Zhang Y, Nasser V, Pisanty O, Omary M, Wulff N, Di Donato M, Tal I, Hauser F, Hao P, Roth O, *et al.* 2018. A transportome-scale amiRNA-based screen identifies redundant roles of Arabidopsis ABCB6 and ABCB20 in auxin transport. *Nature Communications* **9**: 4204.

Zhang J, Nodzynski T, Pencik A, Rolcik J, Friml J. **2009**. PIN phosphorylation is sufficient to mediate PIN polarity and direct auxin transport. *Proceedings of the National Academy of Sciences* **107**: 918–922.

Zhu L, Xin R, Bu Q, Shen H, Dang J, Huq E. **2016**. A Negative Feedback Loop between PHYTOCHROME INTERACTING FACTORs and HECATE Proteins Fine-Tunes Photomorphogenesis in Arabidopsis. *The Plant cell* **28**: 855–74.

Zimmerman BK, Briggs WR. **1963**. Phototropic Dosage-Response Curves for Oat Coleoptiles. *Plant physiology* **38**: 248–53.

Zourelidou M, Müller I, Willige BC, Nill C, Jikumaru Y, Li H, Schwechheimer C. **2009**. The polarly localized D6 PROTEIN KINASE is required for efficient auxin transport in Arabidopsis thaliana. *Development (Cambridge, England)* **136**: 627–36.